Characterization of the cholinergic system and its role in spontaneous neural activity in the spinal cord of zebrafish embryo

Maroun Abi Younes

Sorbonne University Doctoral Thesis

Doctoral Degree in Neuroscience

Cerveau – Cognition – Comportement Doctoral School (ED158)

Presented by

Maroun ABI YOUNES

Characterization of the cholinergic system and its role in spontaneous neural activity in the spinal cord of zebrafish embryo

Thesis Defense on November 6, 2023

Jury Members:

Antonny Czarnecki	Reporter
Muriel Thoby-Brisson	Reporter
Jamilé Hazan	Examiner
Claire Wyart	Examiner
Elim Hong	Thesis Director

A dedication to my near and dear
without whom I wouldn't be here

I never imagined how bittersweet it would be to finish this chapter in my life. Going through the PhD has been an unforgettable experience. A lot of life-changing events happened in these four years, and I emerged from them as a new person. I have all the amazing people who supported me to thank for making it a bit easier and a lot more special.

First, I want to thank my PhD supervisor, Dr Elim Hong for accepting me into her lab. You saw my enthusiasm for learning and for research. I am grateful to you for pushing me towards self-education, autonomy, and independence, both in thinking and in working.

I also want to thank the members of my PhD follow-up committee, Dr Claire Wyart and Dr Coralie Fassier. I remember how nervous I was presenting my work to you for the first time, yet your friendly smiles and positive vibes made the following committee meeting discussions something to look forward to. I hope that one way or another, our paths cross again.

To all the lab members who made and still make the work ambiance a very light one, thank you for helping make this experience a bit easier. To Soumaiya, Nicole, Ninon, and Dania, it's a pleasure to have met all of you and I'm looking forward to your bright futures. To Jean-Pierre and Erika, thank you for the techniques you have taught me and for the laughs we had while working together.

I want to also extend my undying gratitude to Mrs Zeina Karam El-Khoury as well as the Alexis and Anne-Marie Habib foundation for awarding me the scholarship which allowed me to pursue my PhD.

On a more personal note, I want to thank my friends and loved ones, old and new, for being a very positive vibe in my life and a true backbone throughout this journey. To my partner, *mwen malad aw.*

To my family, past and present, I couldn't have made it this far without you. We've been through a lot, but what makes us strong is our resilience and our bond. To my father, mother, and brother … I hope I've made you proud!

List of Abbreviations

ACh – Acetylcholine

AChBP – ACh Binding Protein

AChE – Acetylcholine Esterase

AChRs – Acetylcholine Receptors

Ca^{2+} - Calcium ion

Ch – Choline

chat a - cholineacetyltransferse a

Cl^- - Chloride ions

CNS – Central Nervous System

Cys-loop – Cysteine loop

DHBE – Dihydro Beta Erythroidine

dpf – days post fertilization

dTC – d Tubocurarine

FISH – Fluorescent in situ hybridozation

GABA – Gamma amino butyric acid

GAD – Glutamic Acid Decarboxylase

HACT – High Affinity Choline Transporter

hpf – hours post fertilization

IN – interneuron

ISH – immunohistochemistry

ISH – in situ hybridization

LGIC – Ligand gated ion channel

LGN – Lateral Geniculate Nucleus

mAChR – muscarinic acetylcholine receptor

MN – motoneuron

nAChR - nicotinic acetylcholine receptor

NMJ – Neuromuscular junction

OPC – Oligodendrocyte Precursor

PNS – Peripheral Nervous System

RGC – Retinal Ganglion Cells

SC - Superior Colliculus

SNA – Spontaneous Neural Activity

VAChT – Vesicular Acetylcholine Transporter

WT – wildtype

Abstract

Cholinergic signaling plays a critical role in numerous biological processes throughout development. In rodents and chick, cholinergic signaling is involved in the initiation and maintenance of spontaneous neural activity, which refers to the coordinated activation of large groups of neurons without external input. Spontaneous neural activity is observed in many areas in the vertebrate nervous system, including the spinal cord. Multiple studies have demonstrated that the disruption of cholinergic signaling during development leads to neural tube defects, developmental delays, cognitive deficits, and behavioral abnormalities. Maternal exposure to smoking causes nicotine to enter the fetal circulation and interact with nicotinic acetylcholine receptors, which leads to disturbances in cholinergic signaling to impact the development and function of the nervous system. While studies have shown the adverse effects of nicotine in the peripheral nervous system and in muscles, how it and other disruptors of cholinergic signaling affect the spinal central nervous system development is less understood.

We characterized the spatio-temporal regulation of the cholinergic system in early zebrafish spinal cord using in situ hybridization and immunohistochemistry. We found that genes that encode pre- and post-synaptic elements are expressed as early as 20 hours post fertilization. Surprisingly, the expression of presynaptic components decreases after 3 days suggesting that cholinergic signaling plays an important role during early embryonic development.

By carrying out calcium imaging on large groups of neurons in the 1 day old embryonic spinal cord, we discovered that neurons display different patterns of synchronized activity, consisting of high or low frequency activity. We utilized a transgenic line to label motoneurons and found that groups of neurons displaying high or low frequency activity contain both moto- and interneurons. In addition, we found that neurons that display low frequency activity contain earlier born primary motoneurons, whereas

those with high frequency activity contain later born secondary motoneurons. These results suggest that neurons that are born together form microcircuits that first exhibit high frequency activity, which then transitions to low frequency activity. To investigate the role of cholinergic signaling during spontaneous neural activity, we performed calcium imaging in the mutant for *cholineacetyltransferse a* (*chata*), which encodes an enzyme for acetylcholine synthesis. We found that the emergence of correlated activity is altered in mutants. The highly rhythmic events observed in WT siblings are not found in the *chata* mutants as they display higher interval variability between calcium transients. Application of nicotine increased neural activity, suggesting a role of nicotinic acetylcholine receptors in regulating high frequency activity. The results attribute a yet undescribed role for cholinergic signaling through the nicotinic acetylcholine receptors in modulating highly rhythmic activity during early spontaneous activity. Taken together, we show that both genetic and environmental factors that modify cholinergic signaling alter early spontaneous neural activity, suggesting that the cholinergic system plays a critical role in the recruitment of neural circuits in the developing zebrafish spinal cord. This work establishes the zebrafish embryo as a model system to study the relationship between cholinergic signaling-mediated neural activity and the cellular processes underlying the establishment of neural circuits and its long-term implications in behavior.

Table of Contents

Chapter 1: Introduction

1. Cholinergic Transmission

1.1 **Acetylcholine**

Acetylcholine (ACh) was the first neurotransmitter to be discovered in the first quarter of the 20th century (Valenstein, 2002). ACh is found in a multitude of species including bacteria, fungi, plants and animals (Horiuchi *et al.*, 2003). This discovery came from the works of Henry Hallet Dale and Otto Loewi. Dale accidentally discovered the molecule due to a contamination in the ergot he was working on caused by the bacterium *Bacillus acetylcholini* (Dale, 1914). It was later shown that it is synthesized in and acts on the nervous system due to the works of Loewi on the vagus nerve (Loewi, 1921). He showed that electrical communication between cells of the nervous system can be induced by chemical substances.

Cholinergic signaling has been historically studied at the neuromuscular junction (NMJ). The skeletal neuromuscular junction is composed of 3 main elements: the presynaptic component, which is the motoneuron terminal end, the postsynaptic component which is the muscle end plate, and the synaptic cleft which is between the pre and post synaptic components (Slater, 2017). At the NMJ, ACh functions as a neurotransmitter to mediate fast synaptic transmission. However, there is less evidence that ACh has a similar function in the CNS. ACh appears to be a neuromodulator in the brain; it changes neuronal excitability, neurotransmitter release and neuronal firing (Picciotto, Higley and Mineur, 2012).

Cholinergic signaling is mediated by the action of pre- and post-synaptic components found in the pre- and post-synaptic cells, respectively (**Figure 1)**. The presynaptic cells are cholinergic and release ACh, while the pre- and post-synaptic cells express either nicotinic or muscarinic ACh receptors, respectively named after the agonists that bind to and activate them (Dale, 1914). In presynaptic neurons, Choline Acetyl Transferase (ChAT) mediates the synthesis of ACh from Choline and AcetylCoA. Vesicular Acetylcholine Transporter (VAChT) then packages the ACh into vesicles, which are transported to the synaptic membrane to await release. After

release, ACh binds to cholinergic receptors expressed on the membranes of the pre- and postsynaptic cells. ACh then gets degraded into acetate and choline by Acetylcholine Esterase (AChE). 50% of the choline is then recycled and its reuptake into the presynaptic neuron is achieved by the High Affinity Choline Transporter (HACT) (Taylor and Brown, 1999; Abreu-Villaça, Filgueiras and Manhães, 2011).

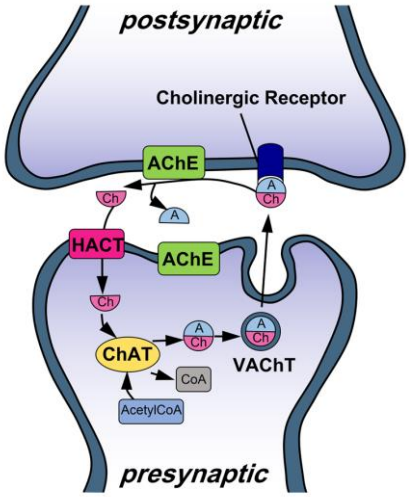

Figure 1. Synthesis, storage, and release of Acetylcholine. Acetylcholine (ACh) is synthesized in cholinergic neurons from choline and AcetylCoA, catalyzed by the enzyme choline acetyl transferase (ChAT). It is then packaged into vesicles by the Vesicular Acetylcholine Transporter (VAChT). After its release, it binds to cholinergic receptors on the postsynaptic neurons, where it degraded by Acetylcholine Esterase (AChE) shortly after. This results in two byproducts: acetate and choline – where choline is taken back into the presynaptic cell by the High Affinity Choline Transporter (HACT). Adapted from Rima *et al.,* 2020. From Rima M., Lattouf Y.*, **Abi Younes M.*** et al, 2020.

1.2 **The cholinergic system**

Achieving proper chemical neurotransmission in the nervous system requires the precise expression of genes coding for the synthesis, packaging, release, and reception of the neurotransmitter. Cholinergic cells are distributed throughout the central and peripheral nervous systems, and components of cholinergic signaling are present during pre- and postnatal stages. During development, transcripts of ChAT, VAChT, AChE and AChRs are found in tissues of flies, insects, echinoderms, fish, birds, and mammals (Bataillé *et al.*, 1998; Enjin *et al.*, 2010; Cho *et al.*, 2014).

Presynaptic components

Transcripts for *chat* and *ache* were detected in gastrulating sea urchin and in E3 chick embryos (Gustafson and Toneby, 1970; Smith *et al.*, 1979; Reich, Drews and Caesar, 1983; Schmidt *et al.*, 1984). In the developing chick spinal cord, genes that specify

motoneuron identity and regulate the expression of cholinergic genes are expressed as early as E3 (Cho *et al.*, 2014). In the spinal cords of developing mice, the expression of ChAT, ACh and AChE is detected as early as E14 (Enjin *et al.*, 2010), and in rat spinal cords as early as E15 (Bataillé *et al.*, 1998). While ChAT expressing cells are found in the brain and spinal cord of the developing zebrafish (Seredick et al., 2012; Arenzana et al., 2005), the emergence of the cholinergic system was not systemically studied.

Nicotinic acetylcholine receptors: Structure and conformational changes

Cholinergic receptors are found both on pre- and post-synaptic cells (Rima *et al.*, 2020). There are two families of AChRs: nicotinic (nAChR) and muscarinic (mAChR) acetylcholine receptors. The nicotinic receptors are ionotropic ligand gated proteins while the muscarinic receptors are G-coupled proteins (Wess, 1996; Changeux and Edelstein, 2001). Here, I will focus on the nAChRs.

Understanding the function, structure and allostery of the nAChRs largely came from the accumulation of works in the neuromuscular junction of the *Torpedo* ray electric organ, and the ACh binding protein (AChBP) secreted by glial cells of snails (Karlin and Akabas, 1995; Smit *et al.*, 2001). nAChRs are part of the Ligand Gated Ion Channels (LGIC), a superfamily of *Cys-loop* receptors (Changeux, 2010). This family of receptors has a characteristic extracellular domain, four or five transmembrane domains that line the channel and an intracellular domain (Karlin, 2002). The receptor is composed of five subunits positioned pseudo-symmetrically around an axis that forms the water filled channel (**Figure 2**) (Toyoshima and Unwin, 1988). There are two types of nAChRs: the muscle N1 located at the NMJs and the neuronal N2.

There are 5 muscle nAChR subunits (α1, β1, γ, δ, ε) (Lindstrom, 1997). Prenatal and fetal muscle nAChRs have a $(\alpha1)_2\beta1\gamma\delta$ subunit assembly, then they undergo a switch in subunit expression where the γ subunit is substituted with ε, where adult muscle nAChRs have the $(\alpha1)_2\beta1\varepsilon\delta$ subunit assembly. Both the γ/ε and δ subunits play crucial roles, in conjunction with the α1 subunits, in determining the configuration of the ligand-binding sites and maintaining cooperative interactions among the α1

subunits (Kalamida *et al.*, 2007). Without the binding of a ligand, the nAChR is in a resting state where the channel is closed. At low concentrations of ligand, the nAChR is in an active state where the channel is open and conducting ions. This state of the nAChR is short-lived; if the ligands are at a high concentration in the medium and occupy the binding site for a long time, the receptor becomes desensitized and non-conducting (Katz and Thesleff, 1957).

Neuronal nAChRs are distributed throughout numerous regions of the CNS. Their structure is also pentameric whereby the heteropentamers consist of two α- β units (α2- α10, β2- β4) forming ligand binding domains, and the fifth subunit composed of either an α or β, while the only exception is the α7 homopentamer (Zoli, Pistillo and Gotti, 2015). Pentameric combinations constitute a wide variety of receptor subtypes with different affinities to binding ligands, calcium permeability and distinct activation and desensitization kinetics (Disney and Higley, 2020) (**Figure 3**). For example, the α7 homopentamers in the CNS have rapid activation and desensitization kinetics and have the highest permeability for calcium (Albuquerque *et al.*, 1997). Heteropentamers have lower desensitization kinetics than α7 receptors, but their sensitivity to ACh and nicotine is higher (Albuquerque *et al.*, 1997). ACh in the brain has been implicated in the release of other neurotransmitters from presynaptic cells, lending more to its role as a neuromodulator (Picciotto, Higley and Mineur, 2012). In the CNS, ACh release

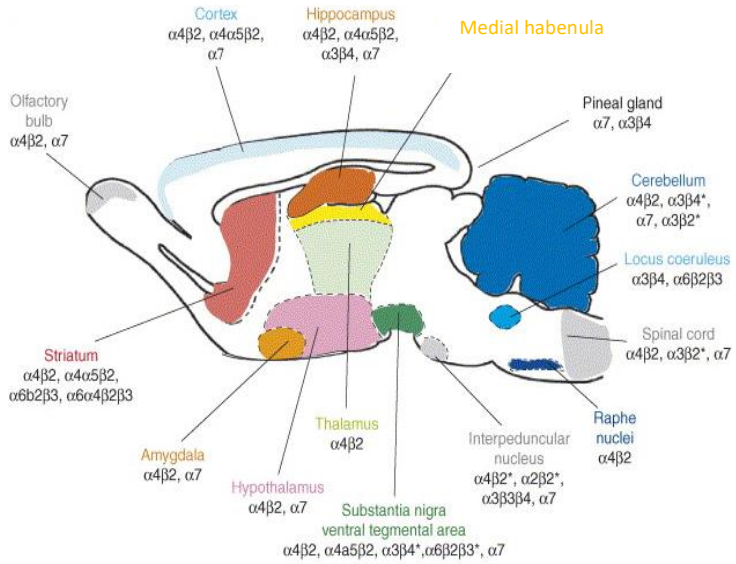

Figure 3. Distribution of diverse nAChRs in the mouse CNS. Regional distribution of the main nAChR subtypes in the rodent CNS. The subtypes were identified either through immunoprecicpitation, immunopurification, in situ hybridization, or receptor subunit knockout. Gotti *et al.*, 2006.

occurs via both synaptic and volumetric release, and nAChRs were located on neurons that are not directly adjacent (post-synaptic) to ACh releasing neurons (Picciotto, Higley and Mineur, 2012; Disney and Higley, 2020).

All receptor subunits expressed in mammals such as rats and humans have also been cloned in zebrafish and display high degree of homology with mammalian nAChRs (Zirger *et al.*, 2003; Papke *et al.*, 2012). In situ hybridization experiments have revealed that β subunits (β1a and β1b) are expressed in zebrafish brain and spinal cord in 1 dpf embryos (Papke *et al.*, 2012).

1.3 Functional role of the cholinergic system during neural network formation

I will focus on the role of ACh in the formation of neural networks by mediating axonal projection, synaptogenesis, and spontaneous neural activity (Dahm and Landmesser, 1988; Behra *et al.*, 2002; Misgeld *et al.*, 2002; Myers, 2005).

Axonal Projection

In chick embryos, the use of nAChRs antagonists to block cholinergic activity showed an increase in the number of axonal projections from spinal motoneurons (MNs) to muscle targets (Hanson and Landmesser, 2004). *Cholineacetyltransferase (chat)* mutant mice embryos also showed similar results (**Figure 4**) (Dahm and Landmesser, 1988; Brandon *et al.*, 2003). Two day old zebrafish embryos with a loss of function mutation in *acetylcholinesterase (ache)* show defective motoneuron projections and nAChR clustering on muscle cells (Behra *et al.*, 2002). These studies suggest a role for cholinergic signaling in axonal projection and pathfinding in locomotor circuits.

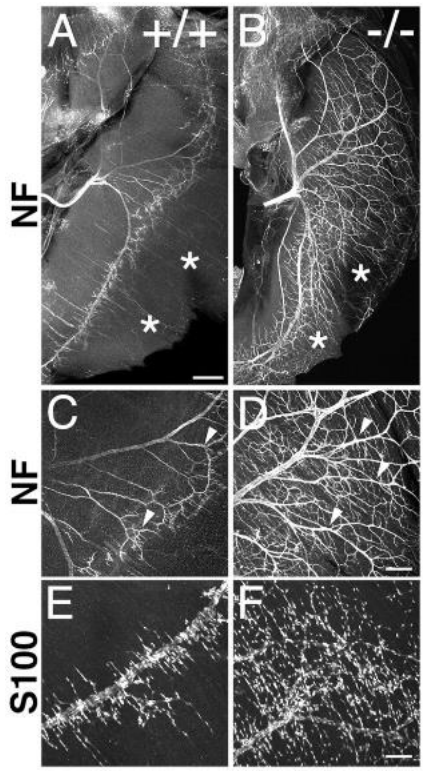

Figure 4. Hyperinnervation of *chat* mutant muscle. Diaphragm muscle samples from WT (A) and *chat* mutant (B) where the mutant is showing increased axonal branching (D) compared to WT (C) shown by neurofilament (NF) labeling. S100, a marker to label Schwann cells, is increased in the mutant (F) compared with WT (E). Adapted from Brandon *et al.,* 2003.

The role of cholinergic signaling in axonal projections was also shown in other circuits during development. Exposing rat and mice amacrine retinal ganglion cells to ACh free medium or to nAChR antagonists significantly increased axonal growth in these cells (Lipton *et al.*, 1988). This is consistent with experiments on E15 dissociated rat retinal ganglion cells exposed to AChE inhibitors, where they saw increased outgrowth of neurites from the cells (Bigbee *et al.*, 1999).

Synaptogenesis

Cholinergic signaling also influences synaptogenesis; the formation of synapses between cells which allows for chemical neurotransmission. In mice, axons targeting muscles form synapses on a distinct area rich in nAChRs known as the endplate band. In *chat* mutant mice, the area of the endplate band is almost twice that of the control embryos suggesting that axons reaching their target sites extend more terminals than in WT (Brandon *et al.*, 2003). Analysis of Bcl2-associated X protein (*BAX)* in mice mutants that lack proapoptotic proteins and have more axonal projections to muscles showed no increase in size of the endplate band between wildtype and *BAX* mutants. Taken together, these studies suggest that perturbing cholinergic signaling also increases the number of synapses in the endplate band area (Misgeld *et al.*, 2002; Brandon *et al.*, 2003).

Spontaneous Neural Activity

Spontaneous neural activity (SNA) is the activation of groups of neurons independently of external stimuli (Hamburger, Wenger and Oppenheim, 1966). In several vertebrate species like chicks and rodents, the main neurotransmitter mediating SNA during early stages of development is ACh (Kirkby *et al.*, 2013).

Briefly, pharmacological and genetic manipulations of the cholinergic system have underscored the significance of ACh in either initiating or sustaining SNA in diverse developing circuits. For instance, in the developing motor system of chick embryos, administration of Dihydro Beta Erythroidine (DHβE) and d-Tubocurarine (dTC), antagonists for nAChRs, led to the cessation of activity, which suggested that non-α7 receptor subunits are involved in modulating SNA (Milner and Landmesser, 1999). In *chat*$^{-/-}$ mutant mouse embryos, where the rate limiting enzyme for ACh synthesis is nonfunctional, spontaneous activity emerges a day later (E13.5) compared to control mice (E12.5) and is mediated by glutamatergic instead of cholinergic signaling (Myers, 2005) (**Figure 5**).

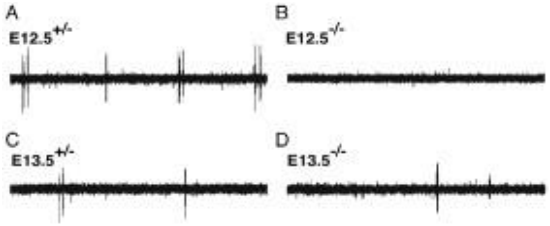

Figure 5*. chat*$^{-/-}$ mutants activity emergence is delayed compared to their WT siblings. Electrophysiological recordings from WT (A) and *chat* mutant (B) embryonic mouse spinal cords at E12.5. Recordings show rhythmic activity in the WT (A), while activity is not detected in the *chat* mutants (B) at the same developmental stage under similar conditions. (C) shows a recording from an E13.5 WT mouse embryo and (D) from a *chat* mutant. Although there is activity in the mutant, it is less frequent than in WT. Adapted from Myers *et al.,* 2005.

In the following section, I will discuss spontaneous neural activity in detail, focusing on its emergence and functional roles in the spinal cord.

2 Spontaneous Neural Activity

2.1 History of Spontaneous Neural Activity

A conserved phenomenon seen across terrestrial and aquatic vertebrate embryos is that they exhibit spontaneous movements that are generated in the spinal cord or trunk. This movement is seen in embryos even before the complete formation of the central and peripheral nervous systems. In the 1800s, William T. Preyer described these movements in several developing organisms and particularly in the chick. It wasn't until later in 1965 that Victor Hamburger and his colleagues demonstrated for the first time that there is motility in the developing chick embryo without sensory stimulation. They removed spinal segments 23 up to 27 of the developing chick spinal cord, and for the segments caudal to 27, they completely removed the dorsal part of the developing segments ensuring that no sensory ganglia could reach the segments that innervate the legs. The embryos with the removed thoracic segments and sensory ganglia showed similar activity in their limbs compared to the controls. From these studies, it was concluded that embryonic motility at early stages is not solely due to sensory stimulation (Hamburger, 1963; Hamburger, Wenger and Oppenheim, 1966). Based on the results, they coined the term non-reflexogenic or spontaneous neural activity (SNA) referring to the firing of a group of nervous system cells prior to the input of external stimuli. These early studies inferred that this type of activity is restricted to a short period of time during development and that it is comprised of bouts of activity separated by periods of inactivity. Major characteristics of this activity are its rhythmicity, pattern, and propagation across large groups of cells (Momose-Sato and Sato, 2013).

SNA is conserved and found in many species including rodents, ferrets, fish, birds and primates (Hamburger, Wenger and Oppenheim, 1966; Hubel and Wiesel, 1970; Galli and Maffei, 1988; Nishimaru *et al.*, 1996; Saint-Amant and Drapeau, 2000) and occurs in various parts of the nervous system including but not limited to the visual

system, auditory system, motor system, and the hippocampus (Feller, 1999; Kirkby *et al.*, 2013).

2.2 **Functional role of SNA in spinal cord formation**

Formation of neural networks was thought to occur in two stages: in the early stage, genetic and molecular cues would dictate the differentiation of neurons as well as their projection and synapse formation, while in later stages the network would be refined based on sensory input. This view was first challenged by Hubel and Wiesel who studied the effect of activity during critical periods on the formation of proper neural circuits (Hubel and Wiesel, 1970). Pharmacological, genetic and optogenetic approaches were used to understand the role of SNA in building a functional neural network (Kirkby *et al.*, 2013).

Differentiation

Activity dependent cell differentiation has been demonstrated in different areas of the nervous system. In the chick spinal cord, blockade of early spontaneous activity with picrotoxin resulted in differentiation defects seen after motoneuron axons projected to the wrong muscles (Hanson and Landmesser, 2004). Briefly, activity disruption resulted in the misexpression of the homeodomain transcription factor LIM, leading to the differentiation of neurons in incorrect sections of the spine that resulted in improper axonal projections. Another study demonstrated that mRNA transcripts of GAD67 are not expressed in the absence of calcium transients, negatively affecting the release of GABA in GABAergic neurons (Watt *et al.*, 2000). Activity may also influence cellular differentiation by increasing the time it spends in the cell cycle designed for progenitor cell proliferation. Oligodendrocyte precursor cells (OPC) express purinergic receptors that are activated by Adenosine released from presynaptic cells. Inhibition of activity in the presynaptic cells negatively affects the differentiation of OPC which is marked by lower levels of myelination of axons (Stevens *et al.*, 2002).

Neurotransmitter specification

Cell excitability and neurotransmitter specification are also influenced by SNA. Cultured *Xenopus* cells show GABA immunoreactivity when cultured in Ca^{2+} containing medium and in Ca^{2+} -free medium where cells were stimulated to the frequency seen in their soma, whereas unstimulated cells cultured in Ca^{2+}-free medium showed less GABA immunoreactivity (Gu and Spitzer, 1995). In another study, Borodisnky et al. studied the effect of disrupting neural activity on neurotransmitter phenotypes in *Xenopus* neural tube. Enhancing frequency of the activity by overexpression of Na^{+} channels or insertion of veratridine beads into the neural tube resulted in a decrease in excitatory neurons and an increase in inhibitory neurons. Conversely, inhibiting the activity in spinal neurons by overexpressing K^{+} rectifier channels or inserting calcium blocker containing beads into the neural tube resulted in an increased number of excitatory synapses (Borodinsky *et al.*, 2004).

Axon pathfinding

In the E4 chick embryo, blockade of early synchronized activity with picrotoxin resulted in motoneuron axons projecting to the wrong target muscle. Immunohistochemistry experiments revealed that the axons targeted the wrong muscles due to incorrectly positioned soma and the inability to properly defasciculate (Hanson and Landmesser, 2004). Alternatively, enhancing the frequency of activity resulted in motoneurons of the same segment innervating only one type of muscle (Hanson and Landmesser, 2006). Conversely, restoration of the normal frequency of activity using optogenetic stimulation under picrotoxin application resulted in proper motoneuron axon extension **(Figure 6)** (Kastanenka and Landmesser, 2010).

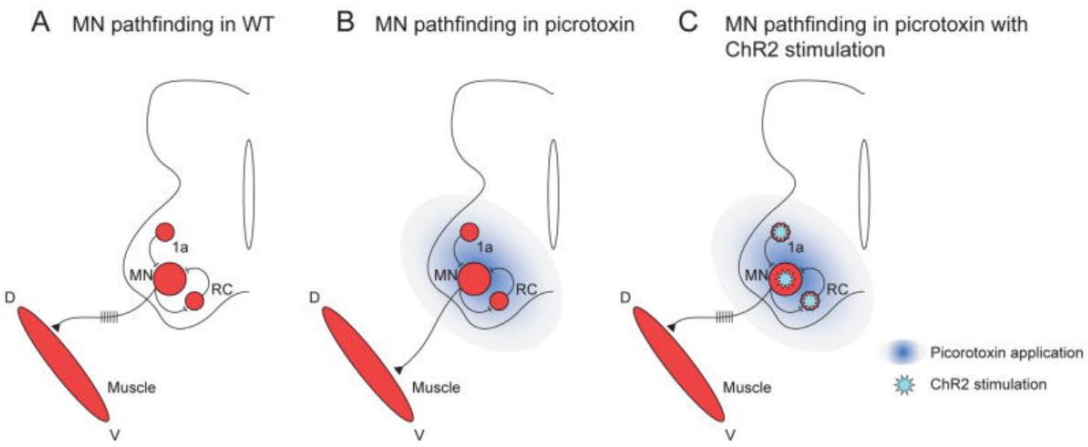

Figure 6. Motoneuron pathfinding in the developing spinal cord under different activity conditions. Illustration of motoneuron pathfinding under undisturbed activity conditions in developing spinal cord (A), in the presence of activity disruption in (B) leading to aberrant axon pathfinding. (C) is under the same activity disruption conditions as in (B) but with the proper activity frequency restored via optogenetics leading to proper axon pathfinding. V: ventral, D: dorsal, MN: motoneuron, RC: Renshaw cell, 1a: 1a inhibitory interneuron; ChR2: channelrhodopsin-2. Adapted from Kastanenka and Landmesser, 2010.

2.3 Common features of SNA across vertebrates with emphasis on the motor system

Spontaneous movements of embryos were described to a great extent by William T Preyer (Preyer, 1885) but it wasn't until almost a century later that scientists were able to identify the molecular mechanisms underlying spontaneous activity. The output of spinal SNA can be seen as movements of the trunk of the body across many developing vertebrates. Several common features of SNA are also present in other central nervous system regions, but I will focus on the motor system below.

Chick and rodents

The emergence of SNA occurs in a rostral to caudal direction, likely reflecting the developmental progression of the rostral to caudal axis of the spinal cord (Ensini *et al.*,

1998). Recordings of population activity in the spinal cords of several terrestrial vertebrates have shown that SNA is first initiated at the rostral spinal cord that propagates in a wavelike pattern to the caudal axis (Kirkby *et al.*, 2013). As the embryos develop, the activity is mostly initiated and detected in the caudal segments of the spinal cord. Later, SNA is rarely detected in the caudal spinal cord and activity is observed only in response to sensory stimulation (Yvert, Branchereau and Meyrand, 2004; Ren *et al.*, 2006). SNA emerges prior to the motoneurons contacting their muscle targets. Electrophysiological recordings showed the emergence of rostral spinal activity in chick embryos at E3.5, in mice at E11.5, and in rats at E12.5 (O'Donovan and Landmesser, 1987; Hanson and Landmesser, 2003; Ren *et al.*, 2006). SNA is also observed in other developing nervous system regions, including the retinal ganglion cells (birds, ferrets, rodents, cats) (Feller, 1999; Kirkby *et al.*, 2013) and in the inner hair cells and spiral ganglion cells of the developing cochlea (Kandler, Clause and Noh, 2009; Tritsch *et al.*, 2010).

As the embryos develop, the frequency of SNA gradually decreases and is then replaced by sensory stimulation, while the duration of the episode increases. Chick, mouse, and rat embryo spinal recordings showed a frequency of 1 episode every 1, 1-2, and 2-3 minutes, respectively (Nishimaru *et al.*,996; Milner and Landmesser, 1999; Hanson and Landmesser, 2003).

In chicks and rodents, the activity is initially driven by excitatory cholinergic transmission, and to a lesser extent GABAergic and glycinergic transmission (Chub and O'Donovan, 1998; Myers, 2005; Gonzalez-Islas and Wenner, 2006; Ren *et al.*, 2006; Czarnecki *et al.*, 2014). In these studies, blockade of nAChRs resulted in abolishing the activity. Additionally, the blockade of glycinergic and GABAergic receptors decreased the frequency of activity. During early embryonic stages, the activity of GABA and glycine is excitatory because the chloride equilibrium potential is more positive than the resting membrane potential of neurons, leading to an efflux of Cl^- ions through the ionotropic glycine and GABA receptors and resulting in depolarization of neurons (Ben-Ari, 2002; Vinay and Jean-Xavier, 2008). Gap junctions also play a role in activity progression, whereby they mediate activity from descending inputs and their blockade resulted in a decrease of activity frequency

(Momose-Sato and Sato, 2013). Pharmacological experiments have shown that as development progresses in chicks and rodents, the major excitatory drive switches from ACh to glutamate in the spinal cord (Momose-Sato and Sato, 2013). This switch between acetylcholine to glutamatergic signaling mediating SNA is also observed in the developing visual system (Catsicas *et al.*, 1998; McLaughlin *et al.*, 2003; Wosniack *et al.*, 2021).

The activity is synchronized between both sides of the spinal cord at the onset of SNA, and then transitions to alternating between the left and right sides (Momose-Sato and Sato, 2013). This seems to be attributed to the switch of glycine and GABA from being excitatory neurotransmitters to becoming inhibitory neurotransmitters. It also happens in parallel to the switch in the main excitatory drive from cholinergic signaling to glutamatergic signaling.

Zebrafish

Spontaneous activity in the zebrafish spinal cord emerges at around 17 hours post fertilization (hpf) and is composed of depolarizing potentials and synaptic bursts. A depolarizing potential is a short-lived increase in the voltage of a neuron lasting about half a second giving rise to the tail coils, while a synaptic burst is a similar increase in the activity of a neuron but doesn't cause the spiking of motoneurons and in turn doesn't lead to contractions (Saint-Amant and Drapeau, 2000, 2001). These two activity types are sequential, and periodic depolarizations on one side of the spinal cord occur simultaneously with the synaptic bursts on the contralateral side. In zebrafish embryos, the early born motoneurons and interneurons are the active cells at the emergence of spontaneous activity. The frequency of episodes decreases with time from 0.4 Hz at 19 hpf to 0.1 Hz at 24 hpf, while the number of spikes within the episode increases between 19 hpf and 24 hpf (Saint-Amant and Drapeau, 2000). Transection of the zebrafish spinal cord at the edge of the hindbrain did not abolish the activity, suggesting that it is independent of descending inputs from supraspinal regions (Saint-Amant and Drapeau, 2001; Wan *et al.*, 2019). Additionally, transection of the spinal cord between segments 5 and 7 at the emergence of correlated activity

results in correlated population activity in both anterior and posterior segments, yet the transection at other sites only yields population activity in the section containing segments 5 to 7 (Wan *et al.*, 2019). These results further validate that the activity is independent of descending inputs, and suggests the presence of either: 1. Pacemaker cells within these rostral segments such as the IC neurons that contain sodium channels implicated in having pacemaker properties in other systems, and their blockade resulted in a non-sustained motor output (Tong and McDearmid, 2012), or 2. The activation of enough cells to reach threshold giving rise to population activity as seen in the spinal cords of developing mice where the activation of enough local circuits triggers a propagating wave of activity along the spinal cord (Hanson and Landmesser, 2003).

Pharmacological agents aimed at blocking chemical neurotransmission did not abolish spontaneous activity. Electrophysiological recordings while applying specific and non-specific nAChR blockers did not inhibit SNA (Saint-Amant and Drapeau, 2001), unlike in other vertebrates (Momose-Sato and Sato, 2020). Only strychnine application led to the abolishment of synaptic bursts that were shown to not trigger action potentials in the recorded neurons. These glycinergic inputs are hypothesized to be descending inputs from the rostral spinal cord of the developing zebrafish (Higashijima, Mandel and Fetcho, 2004). On the other hand, gap junction uncouplers abolished spontaneous activity in the zebrafish spinal cord **(Figure 7)** (Saint-Amant

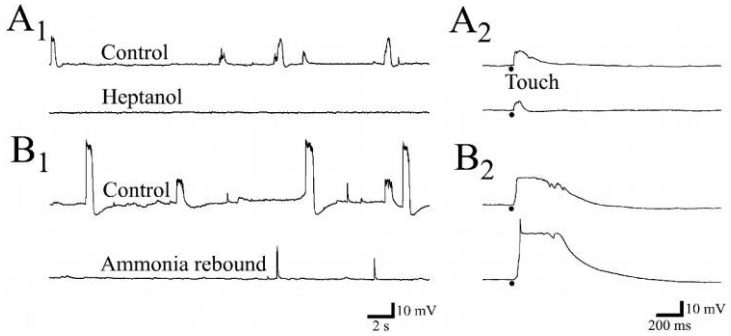

Figure 7. Rhythmic Activity Is Abolished by Gap Junction Blockers. Electrophysiological recordings showing the normal spontaneous activity (A1, B1) and a touch-evoked response (A2, B2) in an embryonic zebrafish interneuron before the application of a gap junction blocker (heptanol(A) & ammonia rebound (B)). Application of heptanol(A) & ammonia (B) (bottom traces of A1 & B1) show that spontaneous activity is abolished, while sensory stimulation remains (A2 & B2). From Saint Amant and Drapeau, 2001.

and Drapeau, 2001). Calcium conductance appears to be driving the synaptic bursts while calcium driven potassium conductance terminates them.

At the onset of SNA at 17 hpf, there is no correlation between the active groups of neighboring cells on the ipsilateral side nor between the two sides of the spinal cord (Warp *et al.*, 2012). At around 20 hpf, the activity becomes ipsilaterally correlated and contralaterally anticorrelated (**Figure 8**) (Saint-Amant and Drapeau, 2001; Warp et al., 2012). Conversely to other animal models, SNA in the zebrafish spinal cord does not disappear at the onset of sensory stimulation since touch-evoked movement

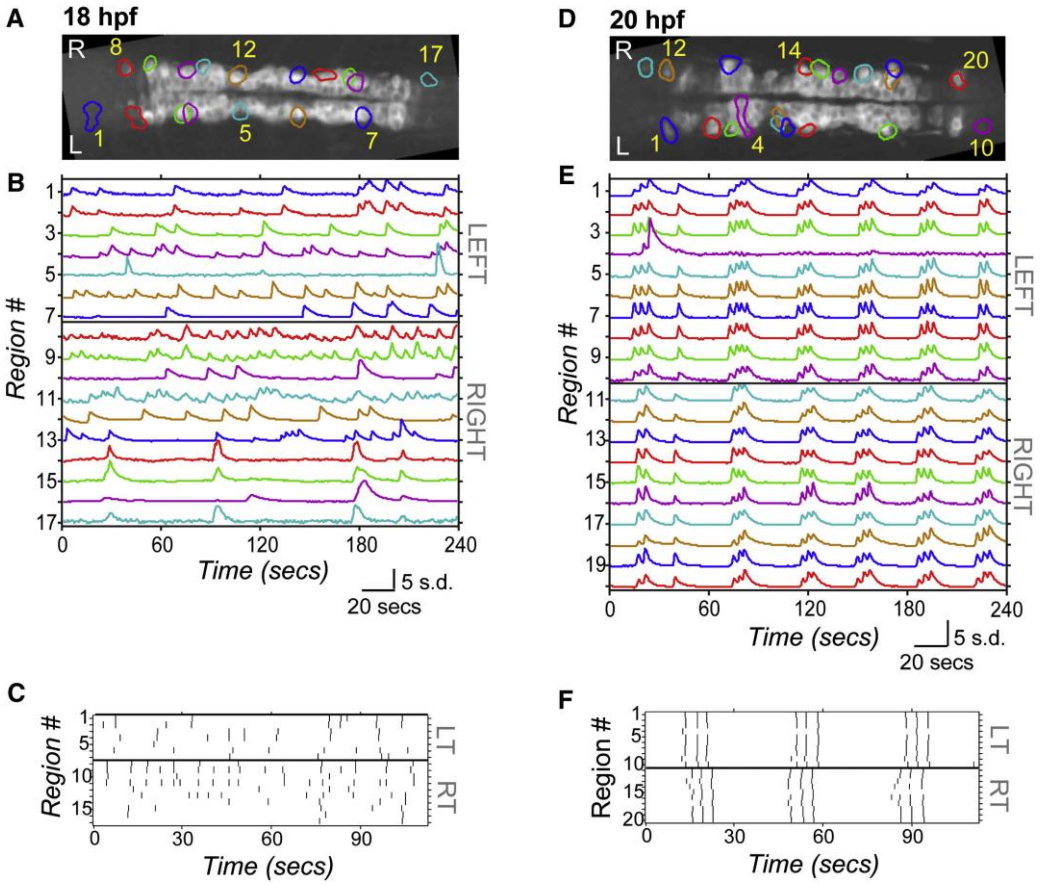

Figure 8. GCaMP3 activity in single neurons in one representative embryo at 18 hpf (left) and 20 hpf (right). (A, D) show calcium imaging recording from a dorsal view-point of an embryonic zebrafish spinal cord. (B) shows the emergence of activity at 18 hpf, whereby it is not correlated among neighboring groups of cells (C) and does not follow a specific pattern. (E) shows the start of correlated activity around 20 hpf, demonstrating that cells on the same side of the spinal cord display correlated activity at this developmental stage, and the two sides of the spinal cord firing pattern is anti-correlated (F). From Warp et al., 2012.

responses have been characterized as early as 21 hpf when SNA is still well detected (Saint-Amant and Drapeau, 2001).

Although there may appear to be many differences in SNA between zebrafish and terrestrial vertebrates, it is important to note that there are also differences between terrestrial animals that are not discussed at length here. Distinct animal models display different pros and cons and the advantages of using the zebrafish as a model system to study neural circuits will be described in the following chapter.

3 Zebrafish as a model for the study of motor circuits

Zebrafish, *Danio* rerio, is a small freshwater species native to south Asia. They have become a popular model organism in scientific and medical research due to their small size, fast reproduction, and genetic similarities to humans (Weber *et al.*, 2005). Zebrafish development is characterized by rapid embryonic growth and early organogenesis, which occurs within the first 5 days post fertilization (dpf). The transparency of the embryos allows for non-invasive observation of internal structures, and genetic tools enable the manipulation of gene expression and cell behavior during development (Long *et al.*, 1997). Zebrafish development is a valuable model for studying fundamental processes of vertebrate development, including organogenesis, morphogenesis, and neural development. I will discuss general aspects of zebrafish nervous system development while focusing on the development of the embryonic spinal neural circuit.

3.1 Development of the spinal neural network

Early zebrafish neural development is a highly dynamic process that involves the formation of the neural plate, which then folds to form the neural tube. This process is tightly regulated by a complex interplay of signaling pathways, transcription factors, and morphogens. The neural tube ultimately gives rise to the brain and spinal cord (Lewis and Eisen, 2003). After neural tissue specification, the spinal cord is segmented into different domains that are occupied by specific neuronal cell types and glial cells (Park *et al.*, 2002; Shirasaki and Pfaff, 2002; Appel, 2004). Floor plate cells at the base of the spinal cord releasing sonic hedgehog (shh) and roof plate cells at the top of the spinal cord releasing bone morphogenic protein (bmp) are crucial for patterning and differentiation of adjacent neural cells (Jessell, 2000; Odenthal *et al.*, 2000; Etheridge *et al.*, 2001). Different concentrations of these morphogens along the dorsal-ventral

(DV) axis leads to the expression of different transcription factors, and the interplay between these two groups of molecules divides the ventral spinal cord into V0, V1, V2, MN, and V3 domains which will be discussed in more detail below.

3.2 **Organization of the zebrafish neural spinal circuit**

Genome sequencing of various animals has supported the idea that the transcription factor code remains similar across the vertebrate lineage during the developmental stages of the spinal cord (Grillner and Jessell, 2009). The transcription factor code is responsible for determining the different cardinal domains within the spinal cord that gives rise to distinct cell populations **(Figure 9)**. Studies in chick, mouse, zebrafish, and other vertebrate spinal cords have shown that the ventral spinal cord is patterned into 11 progenitor cardinal domains where the five ventral (pMN, p0, p1, p2, & p3) give rise to MNs in the MN domain, in addition to distinct classes of INs in the V0, V1, V2, and V3 domains (Corral and Storey, 2001). Within each domain there are several classes of interneurons with varying functions (Wilson and Sweeney,

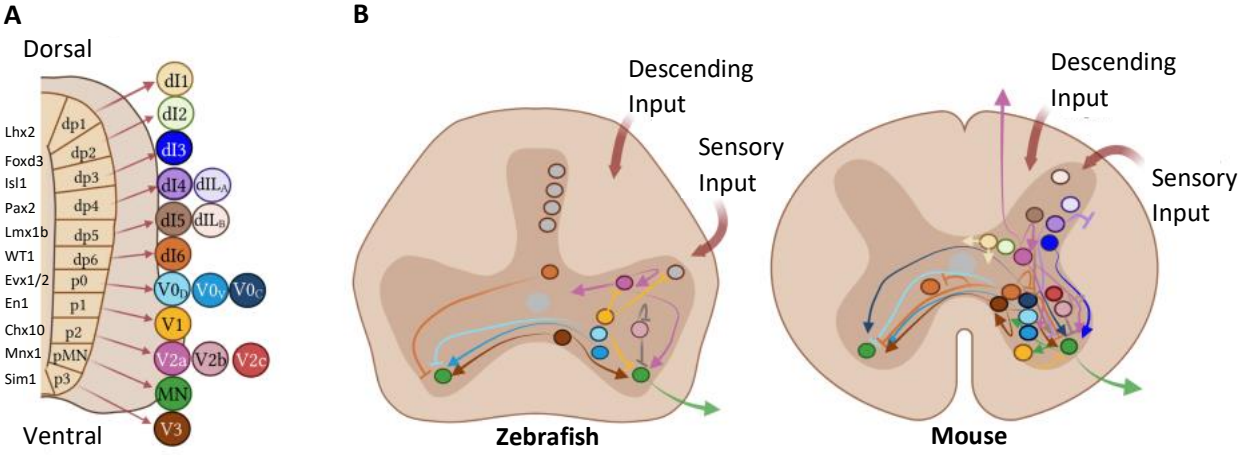

Figure 9. Homology between cardinal neuron domains and neuronal classes across vertebrates. A: Cross section of a developing mouse spinal cord displaying the 11 cardinal progenitor domains in the embryonic spinal cord. dI1-dI5 neurons occupying the dorsal spinal cord participate in sensory transduction, whiledI6, MN, and V0–V3 neurons, arising from intermediate/ventral progenitors, are crucial for locomotor circuitry. Certain postmitotic transcription factors that help identify these eleven early neuron populations in various vertebrates are to the left. B: Comparison of homologous interneuron subtypes and projection patterns in the spinal cord of zebrafish versus mice. Colors represent different neuron classes; gray represents neurons without a clear cardinal class. Adapted from Wilson and Sweeny, 2023.

2023). Conservation of cell types among vertebrates has also been shown in several studies, where neurons in specific domains share the same set of transcription factors. Although the species are different from one another, the neurons in the same domains expressing the same set of transcription factors adopt the same neurotransmitter phenotype and are implicated in similar functions in locomotion (Goulding, 2009). The homology among different classes of spinal neurons could provide the link between shared vertebrate movements and their underlying circuits from early development until adult stages.

Motoneurons

The zebrafish spinal circuit is stereotypically divided into different domains along the dorsoventral axis and becomes active early in development. Most ventrally above the floor plate cells are the motoneurons. There are two classes of motoneurons in zebrafish, known as primary (PMN) and secondary (SMN) motoneurons, distinguished by their differentiation timing, axonal projection, soma and axon sizes (Myers, 1985). Primary motoneurons that innervate axial muscles are born around 14 hours post-fertilization (hpf), while secondary motoneurons that innervate both axial muscles and pectoral fins, are born after 22-24 hpf (Eisen, 1991; Kimmel, Warga and Kane, 1994). The differentiation of primary motoneurons is regulated by hedgehog (hh) signaling and the expression of olig2 (Park *et al.*, 2002). An important feature of the zebrafish motor circuit is the conservation of primary motoneuron number and position along the anteroposterior axis. Specifically, every hemisegment of the spinal cord contains three primary motoneurons, which are arranged in a consistent pattern from rostral to caudal: the rostral (RoP), middle (MiP), and caudal (CaP) primary motoneurons (**Figure 10**).

The primary motoneurons in zebrafish exhibit a precise pattern of myotomal innervation and have been shown to exhibit different electrical properties (Moreno and Ribera, 2009). Specifically, the RoP MN innervates the middle part of the myotome, the MiP MN innervates the dorsal myotome, and the CaP MN innervates the ventral

myotome. A fourth primary motoneuron, known as the variable primary motoneuron (VaP), adjacent to the CaP, often fails to extend an axon and dies at 2-3 days post-fertilization (dpf) as it competes with the CaP for innervation of the ventral myotome (Eisen, 1992).

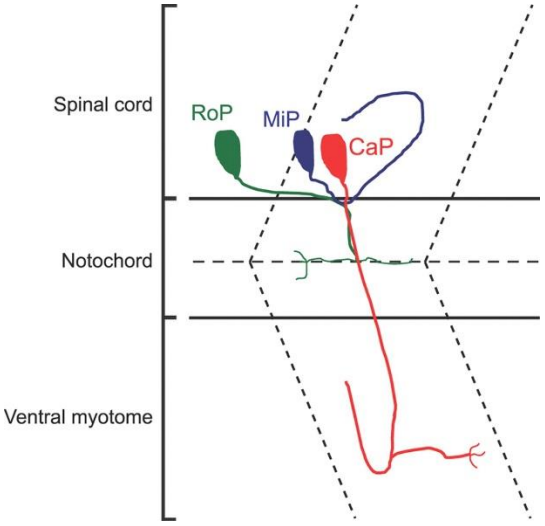

Figure 10. Development of primary motoneurons (PMNs) in zebrafish spinal cord. PMNs CaP, MiP, RoP, and sometimes VaP are born at around 14 hours post fertilization (hpf). By 17-19 hpf, all three PMNs have started extending their axons. The axons pause momentarily at the ventral midline marked by the horizontal line beneath the MN soma. The CaP axon travels ventrally to innervate the ventral myotome, the MiP axon bends upwards and innervates the dorsal myotome while the RoP extends laterally at the ventral midline. By 24 hpf, the axons are at their target sites innervating muscles. From Seredick et al., 2012.

The CaP is the first primary motoneuron to extend its axon at around 17 hpf, followed by the MiP and RoP at around 19 hpf. Additionally, up to twenty-two secondary motoneurons (SMNs) are present per hemisegment, and they project their axons and innervate the same parts of the myotome as the adjacent primary motoneurons (Pike, Melancon and Eisen, 1992). Interestingly, rodents and zebrafish express a conserved transcription factor, *mnx1*, in MNs (as well as one class of ventral INs), which can be used to identify and label them (Goulding, 2009).

Interneurons

Adjacent and dorsal to the MNs are the interneurons (IN) and sensory (SN) neurons. INs are adjacent or dorsal to the MNs depending on their class, while SNs occupy the dorsal most domain of the spinal cord. INs are named based on their axonal trajectories, side of the spinal cord they innervate, and soma positions. Longitudinal

axons project directly from their soma to the target, unlike the circumferential and commissural INs, which first project to the ventral midline (Bernhardt *et al.*, 1990).

Dorsal interneurons process sensory information, while more ventral interneurons control motor output. Commissural interneurons connect the two sides of the spinal cord and are involved in coordinating bilateral movements. Longitudinal interneurons are involved in coordinating the movements of different segments of the body. Inhibitory interneurons regulate the activity of other neurons, while excitatory interneurons initiate and amplify signals (**Table 1)**.

IN type	Soma position	Neurotransmitter	Homologue in mice
Kolmer Aghdur neurons (KA)	Ventral SC	GABA	-
Ventral Longitudinal Descending (VeLD)	Ventral SC	GABA/Glycine	V2b INs (Al-Mosawie, Wilson and Brownstone, 2007)
Circumferential Ascending (CiA)	Medial SC	Glycine	V1 INs (Wilson and Sweeney, 2023)
Circumferential Descending (CiD)	Medial SC	Glutamate	V2a INs (Al-Mosawie, Wilson and Brownstone, 2007)
Commissural Bifurcating (CoB)	Dorsomedial SC	Glycine	dI6 INs (Goulding, 2009)
Commissural Secondary Ascending (CoSA)	Dorsomedial SC	Glycine/Glutamate	V0 INs (Menelaou, Kishore and McLean, 2019)
Commissural Primary Ascending (CoPA)	Dorsal SC	Glutamate	dI1 INs (Wilson and Sweeney, 2023)
Dorsal Longitudinal Ascending (DoLA)	Dorsal SC	GABA	-

Table 1. Zebrafish embryonic spinal interneurons.

The first primary interneurons to project axons are the DoLA, CoPA, CiD, and VeLD at around 16-17 hpf. Their axons traverse several segments and the DoLA and CoPA axons reach the hindbrain at around 26 hpf (Kuwada, Bernhardt and Nguyen,

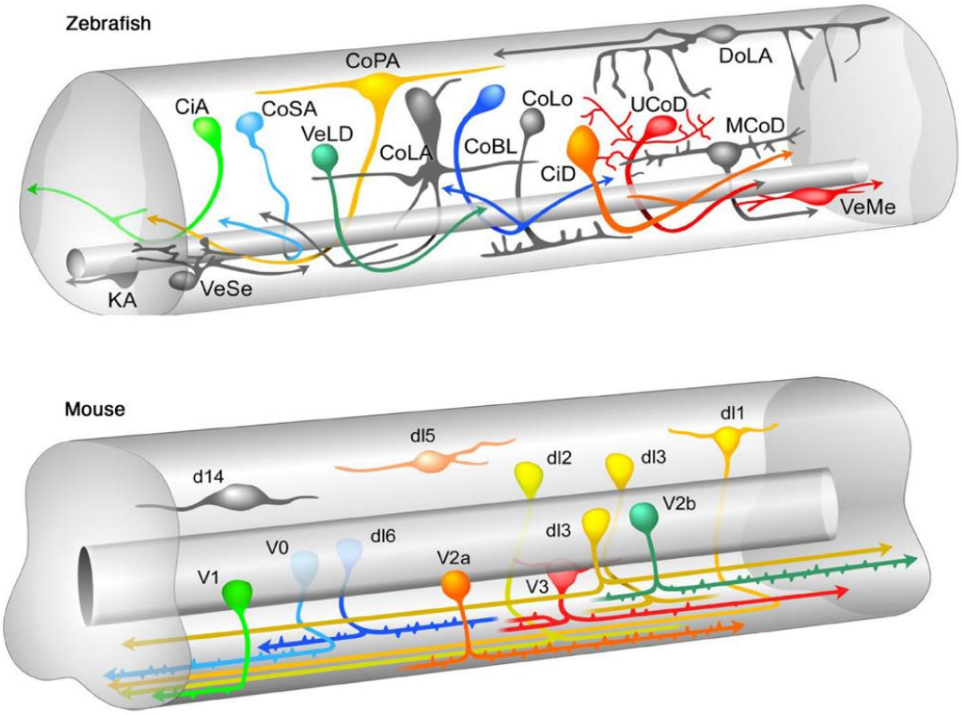

Figure 11. Similar neuronal cell types are present in the embryonic spinal cords of aquatic and terrestrial vertebrates. Illustration of larval zebrafish and embryonic mouse spinal cord showing homologous interneurons (same color) arising in the V3, V2,V1,MN, and V0 domains. From Goulding, 2009

1990) **(Figure 11)**. Of all the embryonic primary INs, DoLA is the only one that is inactive at 1 dpf after extending their axons (Saint-Amant and Drapeau, 2001).

Neurotransmitter phenotypes were characterized in zebrafish embryos and larvae through in situ hybridization and immunohistochemistry. Cholineacetyltransferase immunoreactivity was found in motoneurons, *GAD65/67* transcripts were found in KA, DoLA, and VeLD, *VGLUT* transcripts were found in CiD, CoPA, and a subset of CoSA, and *GLYT2* transcripts were found in CoB, CiA, and another subset of CoSA (Bernhardt *et al.*, 1992; Clemente *et al.*, 2004; Higashijima, Mandel and Fetcho, 2004; Higashijima, Schaefer and Fetcho, 2004).

Sensory neurons are not implicated in spontaneous activity, so I will just briefly mention them. The mechanosensory Rohon-Beard neurons play a crucial role in detecting touch and proprioception, and their axons extend both rostrally and caudally along the spinal cord. They persist until larval stages and are important for the swimming behavior and response to tactile stimuli (Williams and Ribera, 2020).

The motor circuit is involved in zebrafish trunk movement and small bouts of locomotion, and at early stages of development is active independently of descending inputs from the hindbrain or higher regions (Saint-Amant and Drapeau, 2001; Wan *et al.*, 2019). After selective ablation of segments along the AP axis of the spinal cord, it was hypothesized that population activity is either triggered by segments in the middle of the spinal cord capable of generating rhythm, or it is dependent on a sufficient number of active cells to allow its propagation (Hanson and Landmesser, 2003; Tong and McDearmid, 2012; Wan *et al.*, 2019). Indeed, ipsilateral caudal (IC) cells in the rostral zebrafish spinal cord display pacemaker properties (Tong and McDearmid, 2012). Additionally, the theory proposing that a sufficient number of active cells trigger population activity can also hold true since it was shown that in mice, the activation of enough local circuits elicits the propagating wave of activity sweeping the spinal cord (Hanson and Landmesser, 2003).

The first movements observed in zebrafish embryos arise around 17hpf, and from that time until larval stages (around 3 dpf), three types of movement are recorded: spontaneous contractions, touch evoked responses and swimming (Saint-Amant and Drapeau, 1998). Spontaneous contractions arise at 17hpf at 0.5Hz and peak at 1Hz at 19hpf, touch evoked responses appear around 21 hpf while the spontaneous contractions persist but at a lower frequency, and swimming behavior appears around the time they hatch out of the chorion at 3 dpf (Pike, Melancon and Eisen, 1992; Saint-Amant and Drapeau, 1998). The spinal motor circuit undergoes changes in the neuronal populations from embryonic to larval stages. At these stages, new cell types are added to the spinal cord such as UCoD, MCoD, CoLA, CoLo, VeSe and VeMe (Hale, Ritter and Fetcho, 2001; Goulding, 2009; Satou *et al.*, 2009). UCoD, MCoD, and VeMe are glutamatergic while CoLA and CoLo are glycinergic (Higashijima, Schaefer and Fetcho, 2004; Satou *et al.*, 2009).

3.3 Advancements in research tools for the study of neural circuit development in vivo

The nervous system is made up of a meshwork of connected neurons underlying the ability of animals to maintain homeostasis, move around, and discover their environment. At the basis of these complex behaviors are specialized cells with finely tuned connections that excite and inhibit one another to achieve the proper behavioral outcome. Understanding the proper organization of the brain or spinal circuit depends on understanding the interactions and connections of the tens of billions of neurons. To this end, we need methods to record the activity in the neuron or neural circuit of interest, process the electrical and chemical activities of each cell, identify which other neurons it connects to, and locate every synapse it makes with the cells it projects onto. We now have access to methods to probe neural circuits including transgenic lines to express specific genes to record neural population dynamics by calcium imaging or activate specific neurons by optogenetics (Antinucci *et al.*, 2020). Other than having certain IN types that are homologous to other vertebrates in a simple nervous system, the zebrafish embryo offers several other advantages. Zebrafish are easier to maintain than mammalian animal models in the lab, and a single female can lay up to 100 eggs per week. The embryos are accessible to live imaging from the moment of fertilization since they are transparent and are concealed in a transparent chorion. The embryos remain relatively transparent until they reach 3 days old. This makes them a perfect candidate for the analysis of developing circuits through different live imaging techniques. I will focus on two techniques that are widely used in the developing zebrafish to dissect neural circuits: Gal4-UAS system and the genetically encoded calcium indicators.

Gal4-UAS system allows for cell type specific identification

Methods have been developed to target specific cell types to modify its activity and/or gene expression, including the cre/lox system, viral injections, and the GAL4-UAS

system. The Gal4-UAS system is a means to express reporter proteins in a cell-type specific manner. Gal4 is a regulatory protein identified in yeast and binds to short DNA strands termed Upstream Activating Sequences (UAS) located upstream of target genes (Halpern *et al.*, 2008; Kawakami *et al.*, 2016). The Gal4 protein contains a DNA-binding domain at its N-terminus and a transcription activation domain at its C-terminus that recruits transcriptional machinery after binding to the UAS on target genes. The Gal4-UAS system emerged as a prominent tool in *Drosophila* and is currently being widely used also in zebrafish. The advantage is that any gene can be expressed in a Gal4-UAS containing cell. Briefly, the Gal4 sequence inserted downstream of a cell- or tissue- specific transcription factor will be transcribed and translated at the same time. Then, the Gal4 protein enters the nucleus and in turn binds to the UAS upstream of the reporter gene, thereby recruiting the transcriptional machinery to that site, leading to the expression of the reporter gene in the cell or tissue of interest. Despite the popularity and ease of use of the Gal4-UAS system, scientists have reported variegated expression of their genes of interest (Brand and Perrimon, 1993). Mosaic expression of the gene is due to DNA methylation on the UAS sequences, inhibiting the Gal4 protein from binding to it and recruiting transcriptional machinery. Although there may be mosaic expression of the gene the creation of stable Gal4-UAS lines offers a non-invasive and accurate method to locate and track specific cells or tissues of interest. Another advantage is that different transgenic lines can be created by simply crossing a tissue or cell specific Gal4-containing line with a reporter gene UAS- containing line, resulting in the generation of a transgenic line that reports the expression of a different gene of interest.

This technique facilitates the study of different biological processes and different organ systems throughout development. Of interest to us are several lines that label specific cells in the zebrafish spinal cord and hindbrain allowing us to study the premotor and locomotor circuits. A few of these lines are summarized in the table below.

The expression of reporter genes in cells of interest can be used to track cellular differentiation and cell lineages but could also be used to locate specific cell types to measure their activities, or express opsins to specifically activate cell types (Antinucci

et al., 2020). I will focus on calcium sensors since it was the major tool used in our study on SNA.

Line name	Expression Pattern	Reference
Hb9:Gal4 (mnx1:gal4)	Spinal motoneurons and VeLD interneurons	(Flanagan-Steet *et al.*, 2005)
Gad1b:Gal4	GABAergic interneurons	Filosa *et al.*, 2016
SAGFF31B	spinal cord motor- and interneurons	Asakawa et al 2008
SAGFF36B	RB sensory neurons	Asakawa et al 2008
Elavl3:GCaMP6f	Pan-neuronal expression of calcium sensor GCaMP6f	Wolf *et al.*, 2017
mnGFF7	Ventral spinal cord	Asakawa et al 2013
SAIGFF213A	Ventral spinal neurons	Muto et al 2012

Table 2. Gal4-UAS transgenic lines labelling specific cell types located in the zebrafish spinal cord and hindbrain

Calcium sensors to study circuit activity

While electrophysiology is an extremely powerful method to analyze neural activity, it is invasive and difficult to carry out in vivo recordings. Furthermore, despite the development of multi-electrode arrays to analyze activity in a large group of neurons, the spatial resolution is poor (Spira and Hai, 2013). Synthetic calcium sensors emerged as a tool for measuring neural activity by detecting changes in intracellular calcium concentrations during an action potential. However, the technique is invasive because synthetic calcium sensors have to be injected, running the risk of diffusing away from the injection site (Whitaker, 2010).

To overcome these limitations, it was necessary to develop a tool with high spatial resolution that is also non-invasive. In 2001, Junichi Nakai developed a genetically encoded calcium indicator (GECI), more specifically the GCaMP family of calcium indicators to track intracellular changes in Ca^{2+} concentrations (Nakai, Ohkura and Imoto, 2001). GCaMP is a multicomplex protein composed of circularly permuted

Green Fluorescent Protein (cpGFP), Calmodulin (CaM), and the CaM-interacting myosin light chain 13 peptide (M13). Conformational change in the protein complex caused by the binding of calcium ions increases the fluorescence of the cpGFP (**Figure 12**) (Zhang *et al.*, 2023). The transgenic calcium sensor GCaMP offers the advantage of being inserted under a promoter region coding for a transcription factor that is expressed solely in the cell population of interest. As with other technologies, the GCaMP family of calcium sensors has undergone modifications to improve their sensitivity, kinetics, and the signal to noise ratio (Chen *et al.*, 2013).

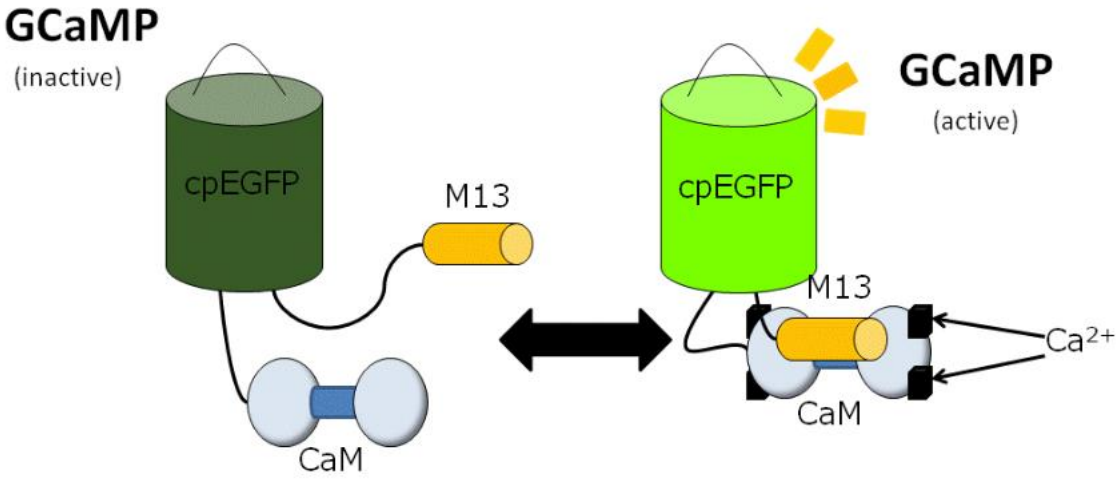

Figure 12. Mechanism of GCaMP activation. GCaMP is composed of improved GFP, Calmodulin (CaM, calcium-binding protein) and M13 peptide. Upon the binding of calcium ions, a conformational change in GCaMP leads to an increase in fluorescence. When the ions are no longer bound, fluorescence goes back down to baselines levels. (*Visualization and analysis of neural activity|I Laboratory*)

The ease of transgenesis to express cell-type specific calcium sensors and reporter genes, combined with its transparency and external development make the embryonic zebrafish the ideal animal model system to study the formation and function of neural circuits using live in vivo imaging.

Aims of the thesis

Cholinergic signaling plays a role in several biological processes like axon pathfinding, synaptogenesis, cell survival, and spontaneous neural activity. Spontaneous neural activity (SNA) is involved in the formation of functional neural networks in many species and its disruption leads to aberrant network formation. Additionally, cholinergic signaling is the main excitatory drive behind SNA in different vertebrate species such as the chick and mouse embryos.

SNA was detected in the zebrafish spinal cord around 17 hours post fertilization (hpf). Pharmacological studies suggest that SNA is mainly dependent on gap junctions and glycinergic transmission. Interestingly, cholineacetyltransferase immunoreactivity was detected in the primary and secondary spinal motoneurons as early as 20hpf zebrafish embryos. However, the cholinergic signaling system and its contribution to spontaneous neural activity in the zebrafish spinal cord remain unclear. For my thesis, I wanted to re-explore the role of cholinergic signaling during SNA in the zebrafish spinal cord.

In this thesis I aimed to:

- Characterize the spatio-temporal expression of cholinergic signaling components in the spinal cord of 1 to 6 dpf zebrafish using immunohistochemistry and in situ hybridization.
- Study the progression of SNA in the zebrafish spinal cord at a population level down to a single cell resolution using calcium imaging.
- Study the contribution of cholinergic signaling to SNA by using pharmacological and genetic manipulations.

Overall, this work will contribute to the broader understanding of the role of cholinergic signaling during SNA in the zebrafish embryo.

References

Abreu-Villaça, Y., Filgueiras, C.C. and Manhães, A.C. (2011) 'Developmental aspects of the cholinergic system', *Behavioural Brain Research*, 221(2), pp. 367–378. Available at: https://doi.org/10.1016/j.bbr.2009.12.049.

Albuquerque, E.X. *et al.* (1997) 'Properties of neuronal nicotinic acetylcholine receptors: pharmacological characterization and modulation of synaptic function', *The Journal of Pharmacology and Experimental Therapeutics*, 280(3), pp. 1117–1136.

Al-Mosawie, A., Wilson, J.M. and Brownstone, R.M. (2007) 'Heterogeneity of V2-derived interneurons in the adult mouse spinal cord', *European Journal of Neuroscience*, 26(11), pp. 3003–3015. Available at: https://doi.org/10.1111/j.1460-9568.2007.05907.x.

Antinucci, P. *et al.* (2020) 'A calibrated optogenetic toolbox of stable zebrafish opsin lines', *eLife*. Edited by H. Burgess et al., 9, p. e54937. Available at: https://doi.org/10.7554/eLife.54937.

Appel, B. (2004) *Spatial and temporal regulation of ventral spinal cord precursor specification by Hedgehog signaling | Development | The Company of Biologists*. Available at: https://journals.biologists.com/dev/article/131/23/5959/42667/Spatial-and-temporal-regulation-of-ventral-spinal (Accessed: 15 March 2023).

Bataillé, S. *et al.* (1998) 'Influence of acetylcholinesterase on embryonic spinal rat motoneurones growth in culture: a quantitative morphometric study', *European Journal of Neuroscience*, 10(2), pp. 560–572. Available at: https://doi.org/10.1046/j.1460-9568.1998.00065.x.

Behra, M. *et al.* (2002) 'Acetylcholinesterase is required for neuronal and muscular development in the zebrafish embryo', *Nature Neuroscience*, 5(2), pp. 111–118. Available at: https://doi.org/10.1038/nn788.

Ben-Ari, Y. (2002) 'Excitatory actions of gaba during development: the nature of the nurture', *Nature Reviews. Neuroscience*, 3(9), pp. 728–739. Available at: https://doi.org/10.1038/nrn920.

Bernhardt, R.R. *et al.* (1990) 'Identification of spinal neurons in the embryonic and larval zebrafish', *The Journal of Comparative Neurology*, 302(3), pp. 603–616. Available at: https://doi.org/10.1002/cne.903020315.

Bernhardt, R.R. *et al.* (1992) 'Axonal trajectories and distribution of GABAergic spinal neurons in wildtype and mutant zebrafish lacking floor plate cells', *Journal of Comparative Neurology*, 326(2), pp. 263–272. Available at: https://doi.org/10.1002/cne.903260208.

Bigbee, J.W. *et al.* (1999) 'Morphogenic role for acetylcholinesterase in axonal outgrowth during neural development', *Environmental Health Perspectives*, 107 Suppl 1(Suppl 1), pp. 81–87. Available at: https://doi.org/10.1289/ehp.99107s181.

Borodinsky, L.N. *et al.* (2004) 'Activity-dependent homeostatic specification of transmitter expression in embryonic neurons', *Nature*, 429(6991), pp. 523–530. Available at: https://doi.org/10.1038/nature02518.

Brand, A.H. and Perrimon, N. (1993) 'Targeted gene expression as a means of altering cell fates and generating dominant phenotypes', *Development (Cambridge, England)*, 118(2), pp. 401–415. Available at: https://doi.org/10.1242/dev.118.2.401.

Brandon, E.P. *et al.* (2003) 'Aberrant Patterning of Neuromuscular Synapses in Choline Acetyltransferase-Deficient Mice', *Journal of Neuroscience*, 23(2), pp. 539–549. Available at: https://doi.org/10.1523/JNEUROSCI.23-02-00539.2003.

Catsicas, M. *et al.* (1998) 'Spontaneous Ca2+ transients and their transmission in the developing chick retina', *Current biology*, 8(5), pp. 283–286. Available at: https://doi.org/10.1016/s0960-9822(98)70110-1.

Changeux, J. and Edelstein, S.J. (2001) 'Allosteric mechanisms in normal and pathological nicotinic acetylcholine receptors', *Current Opinion in Neurobiology*, 11(3), pp. 369–377. Available at: https://doi.org/10.1016/s0959-4388(00)00221-x.

Changeux, J.-P. (2010) 'Nicotine addiction and nicotinic receptors: lessons from genetically modified mice', *Nature Reviews Neuroscience*, 11(6), pp. 389–401. Available at: https://doi.org/10.1038/nrn2849.

Chen, T.-W. *et al.* (2013) 'Ultrasensitive fluorescent proteins for imaging neuronal activity', *Nature*, 499(7458), pp. 295–300. Available at: https://doi.org/10.1038/nature12354.

Cho, H.-H. *et al.* (2014) 'Isl1 directly controls a cholinergic neuronal identity in the developing forebrain and spinal cord by forming cell type-specific complexes', *PLoS genetics*, 10(4), p. e1004280. Available at: https://doi.org/10.1371/journal.pgen.1004280.

Chub, N. and O'Donovan, M.J. (1998) 'Blockade and Recovery of Spontaneous Rhythmic Activity after Application of Neurotransmitter Antagonists to Spinal Networks of the Chick Embryo', *Journal of Neuroscience*, 18(1), pp. 294–306. Available at: https://doi.org/10.1523/JNEUROSCI.18-01-00294.1998.

Clemente, D. *et al.* (2004) 'Cholinergic elements in the zebrafish central nervous system: Histochemical and immunohistochemical analysis', *Journal of Comparative Neurology*, 474(1), pp. 75–107. Available at: https://doi.org/10.1002/cne.20111.

Corral, R.D. del and Storey, K.G. (2001) 'Markers in vertebrate neurogenesis', *Nature Reviews Neuroscience*, 2(11), pp. 835–839. Available at: https://doi.org/10.1038/35097587.

Dahm, L.M. and Landmesser, L.T. (1988) 'The regulation of intramuscular nerve branching during normal development and following activity blockade', *Developmental Biology*, 130(2), pp. 621–644. Available at: https://doi.org/10.1016/0012-1606(88)90357-0.

Dale, H.H. (1914) 'The Action of Certain Esters and Ethers of Choline, and Their Relation to Muscarine', *Journal of Pharmacology and Experimental Therapeutics*, 6(2), pp. 147–190.

Disney, A.A. and Higley, M.J. (2020) 'Diverse Spatiotemporal Scales of Cholinergic Signaling in the Neocortex', *Journal of Neuroscience*, 40(4), pp. 720–725. Available at: https://doi.org/10.1523/JNEUROSCI.1306-19.2019.

Eisen, J. (1991) *Determination of Primary Motoneuron Identity in Developing Zebrafish Embryos*. Available at: https://doi.org/10.1126/science.1708527.

Eisen, J.S. (1992) 'The role of interactions in determining cell fate of two identified motoneurons in the embryonic zebrafish', *Neuron*, 8(2), pp. 231–240. Available at: https://doi.org/10.1016/0896-6273(92)90290-t.

Enjin, A. *et al.* (2010) 'Identification of novel spinal cholinergic genetic subtypes disclose Chodl and Pitx2 as markers for fast motor neurons and partition cells', *The Journal of Comparative Neurology*, 518(12), pp. 2284–2304. Available at: https://doi.org/10.1002/cne.22332.

Ensini, M. *et al.* (1998) 'The control of rostrocaudal pattern in the developing spinal cord: specification of motor neuron subtype identity is initiated by signals from paraxial mesoderm', *Development (Cambridge, England)*, 125(6), pp. 969–982. Available at: https://doi.org/10.1242/dev.125.6.969.

Etheridge, L.A. *et al.* (2001) 'Floor plate develops upon depletion of tiggy-winkle and sonic hedgehog', *genesis*, 30(3), pp. 164–169. Available at: https://doi.org/10.1002/gene.1056.

Feller, M.B. (1999) 'Spontaneous Correlated Activity in Developing Neural Circuits', *Neuron*, 22(4), pp. 653–656. Available at: https://doi.org/10.1016/S0896-6273(00)80724-2.

Filosa, A. *et al.* (2016) 'Feeding State Modulates Behavioral Choice and Processing of Prey Stimuli in the Zebrafish Tectum', *Neuron*, 90(3), pp. 596–608. Available at: https://doi.org/10.1016/j.neuron.2016.03.014.

Flanagan-Steet, H. *et al.* (2005) 'Neuromuscular synapses can form in vivo by incorporation of initially aneural postsynaptic specializations', *Development*, 132(20), pp. 4471–4481. Available at: https://doi.org/10.1242/dev.02044.

Galli, L. and Maffei, L. (1988) 'Spontaneous Impulse Activity of Rat Retinal Ganglion Cells in Prenatal Life', *Science*, 242(4875), pp. 90–91. Available at: https://doi.org/10.1126/science.3175637.

Gonzalez-Islas, C. and Wenner, P. (2006) 'Spontaneous Network Activity in the Embryonic Spinal Cord Regulates AMPAergic and GABAergic Synaptic Strength', *Neuron*, 49(4), pp. 563–575. Available at: https://doi.org/10.1016/j.neuron.2006.01.017.

Goulding, M. (2009) 'Circuits controlling vertebrate locomotion: moving in a new direction', *Nature Reviews Neuroscience*, 10(7), pp. 507–518. Available at: https://doi.org/10.1038/nrn2608.

Grillner, S. and Jessell, T.M. (2009) 'Measured motion: searching for simplicity in spinal locomotor networks', *Current Opinion in Neurobiology*, 19(6), pp. 572–586. Available at: https://doi.org/10.1016/j.conb.2009.10.011.

Gu, X. and Spitzer, N.C. (1995) 'Distinct aspects of neuronal differentiation encoded by frequency of spontaneous Ca2+ transients', *Nature*, 375(6534), pp. 784–787. Available at: https://doi.org/10.1038/375784a0.

Gustafson, T. and Toneby, M. (1970) 'On the role of serotonin and acetylcholine in sea urchin morphogenesis', *Experimental Cell Research*, 62(1), pp. 102–117. Available at: https://doi.org/10.1016/0014-4827(79)90512-3.

Hale, M.E., Ritter, D.A. and Fetcho, J.R. (2001) 'A confocal study of spinal interneurons in living larval zebrafish', *The Journal of Comparative Neurology*, 437(1), pp. 1–16. Available at: https://doi.org/10.1002/cne.1266.

Halpern, M.E. *et al.* (2008) 'Gal4/UAS transgenic tools and their application to zebrafish', *Zebrafish*, 5(2), pp. 97–110. Available at: https://doi.org/10.1089/zeb.2008.0530.

Hamburger, V. (1963) 'Some Aspects of the Embryology of Behavior', *The Quarterly Review of Biology*, 38(4), pp. 342–365.

Hamburger, V., Wenger, E. and Oppenheim, R. (1966) 'Motility in the chick embryo in the absence of sensory input', *Journal of Experimental Zoology*, 162(2), pp. 133–159. Available at: https://doi.org/10.1002/jez.1401620202.

Hanson, M.G. and Landmesser, L.T. (2003) 'Characterization of the Circuits That Generate Spontaneous Episodes of Activity in the Early Embryonic Mouse Spinal Cord', *The Journal of Neuroscience*, 23(2), pp. 587–600. Available at: https://doi.org/10.1523/JNEUROSCI.23-02-00587.2003.

Hanson, M.G. and Landmesser, L.T. (2004) 'Normal patterns of spontaneous activity are required for correct motor axon guidance and the expression of specific guidance molecules', *Neuron*, 43(5), pp. 687–701. Available at: https://doi.org/10.1016/j.neuron.2004.08.018.

Hanson, M.G. and Landmesser, L.T. (2006) 'Increasing the frequency of spontaneous rhythmic activity disrupts pool-specific axon fasciculation and pathfinding of embryonic spinal motoneurons', *The Journal of Neuroscience: The Official Journal of the Society for Neuroscience*, 26(49), pp. 12769–12780. Available at: https://doi.org/10.1523/JNEUROSCI.4170-06.2006.

Higashijima, S.-I., Mandel, G. and Fetcho, J.R. (2004) 'Distribution of prospective glutamatergic, glycinergic, and GABAergic neurons in embryonic and larval zebrafish', *Journal of Comparative Neurology*, 480(1), pp. 1–18. Available at: https://doi.org/10.1002/cne.20278.

Higashijima, S.-I., Schaefer, M. and Fetcho, J.R. (2004) 'Neurotransmitter properties of spinal interneurons in embryonic and larval zebrafish', *The Journal of Comparative Neurology*, 480(1), pp. 19–37. Available at: https://doi.org/10.1002/cne.20279.

Horiuchi, Y. *et al.* (2003) 'Evolutional study on acetylcholine expression', *Life Sciences*, 72(15), pp. 1745–1756. Available at: https://doi.org/10.1016/S0024-3205(02)02478-5.

Hubel, D.H. and Wiesel, T.N. (1970) 'The period of susceptibility to the physiological effects of unilateral eye closure in kittens', *The Journal of Physiology*, 206(2), pp. 419–436. Available at: https://doi.org/10.1113/jphysiol.1970.sp009022.

Jessell, T.M. (2000) 'Neuronal specification in the spinal cord: inductive signals and transcriptional codes', *Nature Reviews Genetics*, 1(1), pp. 20–29. Available at: https://doi.org/10.1038/35049541.

Kalamida, D. *et al.* (2007) 'Muscle and neuronal nicotinic acetylcholine receptors. Structure, function and pathogenicity', *The FEBS journal*, 274(15), pp. 3799–3845. Available at: https://doi.org/10.1111/j.1742-4658.2007.05935.x.

Kandler, K., Clause, A. and Noh, J. (2009) 'Tonotopic reorganization of developing auditory brainstem circuits', *Nature Neuroscience*, 12(6), pp. 711–717. Available at: https://doi.org/10.1038/nn.2332.

Karlin, A. (2002) 'Emerging structure of the Nicotinic Acetylcholine receptors', *Nature Reviews Neuroscience*, 3(2), pp. 102–114. Available at: https://doi.org/10.1038/nrn731.

Karlin, A. and Akabas, M.H. (1995) 'Toward a structural basis for the function of nicotinic acetylcholine receptors and their cousins', *Neuron*, 15(6), pp. 1231–1244. Available at: https://doi.org/10.1016/0896-6273(95)90004-7.

Kastanenka, K.V. and Landmesser, L.T. (2010) 'In vivo activation of channelrhodopsin-2 reveals that normal patterns of spontaneous activity are required for motoneuron guidance and maintenance of guidance molecules', *The Journal of Neuroscience: The Official Journal of the Society for Neuroscience*, 30(31), pp. 10575–10585. Available at: https://doi.org/10.1523/JNEUROSCI.2773-10.2010.

Katz, B. and Thesleff, S. (1957) 'A study of the desensitization produced by acetylcholine at the motor end-plate', *The Journal of Physiology*, 138(1), pp. 63–80. Available at: https://doi.org/10.1113/jphysiol.1957.sp005838.

Kawakami, K. *et al.* (2016) 'Chapter Three - Gal4 Driver Transgenic Zebrafish: Powerful Tools to Study Developmental Biology, Organogenesis, and Neuroscience', in N.S. Foulkes (ed.) *Advances in Genetics*. Academic Press (Genetics, Genomics and Fish Phenomics), pp. 65–87. Available at: https://doi.org/10.1016/bs.adgen.2016.04.002.

Kimmel, C.B., Warga, R.M. and Kane, D.A. (1994) 'Cell cycles and clonal strings during formation of the zebrafish central nervous system', *Development*, 120(2), pp. 265–276. Available at: https://doi.org/10.1242/dev.120.2.265.

Kirkby, L. *et al.* (2013) 'A role for correlated spontaneous activity in the assembly of neural circuits', *Neuron*, 80(5), pp. 1129–1144. Available at: https://doi.org/10.1016/j.neuron.2013.10.030.

Kuwada, J.Y., Bernhardt, R.R. and Nguyen, N. (1990) 'Development of spinal neurons and tracts in the zebrafish embryo', *Journal of Comparative Neurology*, 302(3), pp. 617–628. Available at: https://doi.org/10.1002/cne.903020316.

Lewis, K.E. and Eisen, J.S. (2003) 'From cells to circuits: development of the zebrafish spinal cord', *Progress in Neurobiology*, 69(6), pp. 419–449. Available at: https://doi.org/10.1016/S0301-0082(03)00052-2.

Lindstrom, J. (1997) 'Nicotinic acetylcholine receptors in health and disease', *Molecular Neurobiology*, 15(2), pp. 193–222. Available at: https://doi.org/10.1007/BF02740634.

Lipton, S.A. *et al.* (1988) 'Nicotinic Antagonists Enhance Process Outgrowth by Rat Retinal Ganglion Cells in Culture', *Science*, 239(4845), pp. 1293–1296. Available at: https://doi.org/10.1126/science.3344435.

Loewi, O. (1921) *Loewi: Über humorale übertragbarkeit der Herznervenwirkung - Google Scholar*. Available at: https://scholar.google.com/scholar_lookup?title=%C3%9Cber%20humorale%20%C3%9Cbertragbarkeit%20der%20Herznervenwirkung.%20X.%20Mitteilung%3A%20%C3%9Cber%20das%20Schicksal%20des%20Vagusstoffs&publication_year=1926&author=O.%20Loewi&author=E.%20Navratil (Accessed: 2 March 2023).

Long, Q. *et al.* (1997) 'GATA-1 expression pattern can be recapitulated in living transgenic zebrafish using GFP reporter gene', *Development*, 124(20), pp. 4105–4111. Available at: https://doi.org/10.1242/dev.124.20.4105.

McLaughlin, T. *et al.* (2003) 'Retinotopic map refinement requires spontaneous retinal waves during a brief critical period of development', *Neuron*, 40(6), pp. 1147–1160. Available at: https://doi.org/10.1016/s0896-6273(03)00790-6.

Menelaou, E., Kishore, S. and McLean, D.L. (2019) 'Distinct Spinal V2a and V0d Microcircuits Distribute Locomotor Control in Larval Zebrafish'. bioRxiv, p. 559799. Available at: https://doi.org/10.1101/559799.

Milner, L.D. and Landmesser, L.T. (1999) 'Cholinergic and GABAergic Inputs Drive Patterned Spontaneous Motoneuron Activity before Target Contact', *Journal of Neuroscience*, 19(8), pp. 3007–3022. Available at: https://doi.org/10.1523/JNEUROSCI.19-08-03007.1999.

Misgeld, T. *et al.* (2002) 'Roles of Neurotransmitter in Synapse Formation: Development of Neuromuscular Junctions Lacking Choline Acetyltransferase', *Neuron*, 36(4), pp. 635–648. Available at: https://doi.org/10.1016/S0896-6273(02)01020-6.

Momose-Sato, Y. and Sato, K. (2013) 'Large-scale synchronized activity in the embryonic brainstem and spinal cord', *Frontiers in Cellular Neuroscience*, 7. Available at: https://www.frontiersin.org/articles/10.3389/fncel.2013.00036 (Accessed: 28 August 2023).

Momose-Sato, Y. and Sato, K. (2020) 'Prenatal exposure to nicotine disrupts synaptic network formation by inhibiting spontaneous correlated wave activity', *IBRO reports*, 9, pp. 14–23. Available at: https://doi.org/10.1016/j.ibror.2020.06.003.

Moreno, R.L. and Ribera, A.B. (2009) 'Zebrafish Motor Neuron Subtypes Differ Electrically Prior to Axonal Outgrowth', *Journal of Neurophysiology*, 102(4), pp. 2477–2484. Available at: https://doi.org/10.1152/jn.00446.2009.

Myers, C. (2005) 'Cholinergic Input Is Required during Embryonic Development to Mediate Proper Assembly of Spinal Locomotor Circuits'. Available at: https://core.ac.uk/reader/82664400 (Accessed: 13 March 2023).

Myers, P.Z. (1985) 'Spinal motoneurons of the larval zebrafish', *The Journal of Comparative Neurology*, 236(4), pp. 555–561. Available at: https://doi.org/10.1002/cne.902360411.

Nakai, J., Ohkura, M. and Imoto, K. (2001) 'A high signal-to-noise Ca2+ probe composed of a single green fluorescent protein', *Nature Biotechnology*, 19(2), pp. 137–141. Available at: https://doi.org/10.1038/84397.

Nishimaru, H. *et al.* (1996) 'Spontaneous motoneuronal activity mediated by glycine and GABA in the spinal cord of rat fetuses in vitro.', *The Journal of Physiology*, 497(1), pp. 131–143. Available at: https://doi.org/10.1113/jphysiol.1996.sp021755.

Odenthal, J. *et al.* (2000) 'Two Distinct Cell Populations in the Floor Plate of the Zebrafish Are Induced by Different Pathways', *Developmental Biology*, 219(2), pp. 350–363. Available at: https://doi.org/10.1006/dbio.1999.9589.

O'Donovan, M.J. and Landmesser, L. (1987) 'The development of hindlimb motor activity studied in the isolated spinal cord of the chick embryo', *Journal of Neuroscience*, 7(10), pp. 3256–3264. Available at: https://doi.org/10.1523/JNEUROSCI.07-10-03256.1987.

Papke, R.L. *et al.* (2012) 'The nicotinic acetylcholine receptors of zebrafish and an evaluation of pharmacological tools used for their study', *Biochemical Pharmacology*, 84(3), pp. 352–365. Available at: https://doi.org/10.1016/j.bcp.2012.04.022.

Park, H.-C. *et al.* (2002) 'olig2 Is Required for Zebrafish Primary Motor Neuron and Oligodendrocyte Development', *Developmental Biology*, 248(2), pp. 356–368. Available at: https://doi.org/10.1006/dbio.2002.0738.

Picciotto, M.R., Higley, M.J. and Mineur, Y.S. (2012) 'Acetylcholine as a neuromodulator: cholinergic signaling shapes nervous system function and behavior', *Neuron*, 76(1), pp. 116–129. Available at: https://doi.org/10.1016/j.neuron.2012.08.036.

Pike, S.H., Melancon, E.F. and Eisen, J.S. (1992) 'Pathfinding by zebrafish motoneurons in the absence of normal pioneer axons', *Development (Cambridge, England)*, 114(4), pp. 825–831. Available at: https://doi.org/10.1242/dev.114.4.825.

Preyer, W.T. (1885) 'Special Physiology of the Embryo'.

Reich, A., Drews, U. and Caesar, S. (1983) 'Choline acetyltransferase in the chick limb bud', *Histochemistry*, 78(3), pp. 383–389. Available at: https://doi.org/10.1007/BF00496624.

Ren, J. *et al.* (2006) 'Rhythmic Neuronal Discharge in the Medulla and Spinal Cord of Fetal Rats in the Absence of Synaptic Transmission', *Journal of Neurophysiology*, 95(1), pp. 527–534. Available at: https://doi.org/10.1152/jn.00735.2005.

Rima, M. *et al.* (2020) 'Dynamic regulation of the cholinergic system in the spinal central nervous system', *Scientific Reports*, 10(1), p. 15338. Available at: https://doi.org/10.1038/s41598-020-72524-3.

Saint-Amant, L. and Drapeau, P. (1998) 'Time course of the development of motor behaviors in the zebrafish embryo', *Journal of Neurobiology*, 37(4), pp. 622–632. Available at: https://doi.org/10.1002/(SICI)1097-4695(199812)37:4<622::AID-NEU10>3.0.CO;2-S.

Saint-Amant, L. and Drapeau, P. (2000) 'Motoneuron Activity Patterns Related to the Earliest Behavior of the Zebrafish Embryo', *The Journal of Neuroscience*, 20(11), pp. 3964–3972. Available at: https://doi.org/10.1523/JNEUROSCI.20-11-03964.2000.

Saint-Amant, L. and Drapeau, P. (2001) 'Synchronization of an Embryonic Network of Identified Spinal Interneurons Solely by Electrical Coupling', *Neuron*, 31(6), pp. 1035–1046. Available at: https://doi.org/10.1016/S0896-6273(01)00416-0.

Satou, C. *et al.* (2009) 'Functional Role of a Specialized Class of Spinal Commissural Inhibitory Neurons during Fast Escapes in Zebrafish', *The Journal of Neuroscience*, 29(21), pp. 6780–6793. Available at: https://doi.org/10.1523/JNEUROSCI.0801-09.2009.

Schmidt, H. *et al.* (1984) 'Intracellular calcium mobilization on stimulation of the muscarinic cholinergic receptor in chick limb bud cells', *Wilhelm Roux's Archives of Developmental Biology*, 194(1), pp. 44–49. Available at: https://doi.org/10.1007/BF00848953.

Shirasaki, R. and Pfaff, S.L. (2002) 'Transcriptional codes and the control of neuronal identity', *Annual Review of Neuroscience*, 25, pp. 251–281. Available at: https://doi.org/10.1146/annurev.neuro.25.112701.142916.

Slater, C.R. (2017) 'The Structure of Human Neuromuscular Junctions: Some Unanswered Molecular Questions', *International Journal of Molecular Sciences*, 18(10), p. 2183. Available at: https://doi.org/10.3390/ijms18102183.

Smit, A.B. *et al.* (2001) 'A glia-derived acetylcholine-binding protein that modulates synaptic transmission', *Nature*, 411(6835), pp. 261–268. Available at: https://doi.org/10.1038/35077000.

Smith, J. *et al.* (1979) 'Acetylcholine synthesis by mesencephalic neural crest cells in the process of migration in vivo', *Nature*, 282(5741), pp. 853–855. Available at: https://doi.org/10.1038/282853a0.

Spira, M.E. and Hai, A. (2013) 'Multi-electrode array technologies for neuroscience and cardiology', *Nature Nanotechnology*, 8(2), pp. 83–94. Available at: https://doi.org/10.1038/nnano.2012.265.

Stevens, B. *et al.* (2002) 'Adenosine: A Neuron-Glial Transmitter Promoting Myelination in the CNS in Response to Action Potentials', *Neuron*, 36(5), pp. 855–868. Available at: https://doi.org/10.1016/S0896-6273(02)01067-X.

Taylor, P. and Brown, J.H. (1999) 'Synthesis, Storage and Release of Acetylcholine', *Basic Neurochemistry: Molecular, Cellular and Medical Aspects. 6th edition* [Preprint]. Available at: https://www.ncbi.nlm.nih.gov/books/NBK28051/ (Accessed: 2 March 2023).

Tong, H. and McDearmid, J.R. (2012) 'Pacemaker and Plateau Potentials Shape Output of a Developing Locomotor Network', *Current Biology*, 22(24), pp. 2285–2293. Available at: https://doi.org/10.1016/j.cub.2012.10.025.

Toyoshima, C. and Unwin, N. (1988) 'Ion channel of acetylcholine receptor reconstructed from images of postsynaptic membranes', *Nature*, 336(6196), pp. 247–250. Available at: https://doi.org/10.1038/336247a0.

Tritsch, N.X. *et al.* (2010) 'Calcium action potentials in hair cells pattern auditory neuron activity before hearing onset', *Nature neuroscience*, 13(9), pp. 1050–1052. Available at: https://doi.org/10.1038/nn.2604.

Valenstein, E.S. (2002) 'The Discovery of Chemical Neurotransmitters', *Brain and Cognition*, 49(1), pp. 73–95. Available at: https://doi.org/10.1006/brcg.2001.1487.

Vinay, L. and Jean-Xavier, C. (2008) 'Plasticity of spinal cord locomotor networks and contribution of cation–chloride cotransporters', *Brain Research Reviews*, 57(1), pp. 103–110. Available at: https://doi.org/10.1016/j.brainresrev.2007.09.003.

Wan, Y. *et al.* (2019) 'Single-Cell Reconstruction of Emerging Population Activity in an Entire Developing Circuit', *Cell*, 179(2), pp. 355-372.e23. Available at: https://doi.org/10.1016/j.cell.2019.08.039.

Warp, E. *et al.* (2012) 'Emergence of patterned activity in the developing zebrafish spinal cord', *Current biology: CB*, 22(2), pp. 93–102. Available at: https://doi.org/10.1016/j.cub.2011.12.002.

Watt, S.D. *et al.* (2000) 'Specific Frequencies of Spontaneous Ca2+ Transients Upregulate GAD 67 Transcripts in Embryonic Spinal Neurons', *Molecular and Cellular Neuroscience*, 16(4), pp. 376–387. Available at: https://doi.org/10.1006/mcne.2000.0871.

Weber, G.J. *et al.* (2005) 'Mutant-specific gene programs in the zebrafish', *Blood*, 106(2), pp. 521–530. Available at: https://doi.org/10.1182/blood-2004-11-4541.

Wess, J. (1996) 'Molecular biology of muscarinic acetylcholine receptors', *Critical Reviews in Neurobiology*, 10(1), pp. 69–99. Available at: https://doi.org/10.1615/critrevneurobiol.v10.i1.40.

Whitaker, M. (2010) 'Genetically-encoded probes for measurement of intracellular calcium', *Methods in cell biology*, 99, pp. 153–182. Available at: https://doi.org/10.1016/B978-0-12-374841-6.00006-2.

Williams, K. and Ribera, A.B. (2020) 'Long-lived zebrafish Rohon-Beard cells', *Developmental Biology*, 464(1), pp. 45–52. Available at: https://doi.org/10.1016/j.ydbio.2020.05.003.

Wilson, A.C. and Sweeney, L.B. (2023) 'Spinal cords: Symphonies of interneurons across species', *Frontiers in Neural Circuits*, 17. Available at: https://www.frontiersin.org/articles/10.3389/fncir.2023.1146449 (Accessed: 27 August 2023).

Wolf, S. *et al.* (2017) 'Sensorimotor computation underlying phototaxis in zebrafish', *Nature Communications*, 8(1), p. 651. Available at: https://doi.org/10.1038/s41467-017-00310-3.

Wosniack, M.E. *et al.* (2021) 'Adaptation of spontaneous activity in the developing visual cortex', *eLife*, 10, p. e61619. Available at: https://doi.org/10.7554/eLife.61619.

Yvert, B., Branchereau, P. and Meyrand, P. (2004) 'Multiple Spontaneous Rhythmic Activity Patterns Generated by the Embryonic Mouse Spinal Cord Occur Within a Specific Developmental Time Window', *Journal of Neurophysiology*, 91(5), pp. 2101–2109. Available at: https://doi.org/10.1152/jn.01095.2003.

Zhang, Y. *et al.* (2023) 'Fast and sensitive GCaMP calcium indicators for imaging neural populations', *Nature*, 615(7954), pp. 884–891. Available at: https://doi.org/10.1038/s41586-023-05828-9.

Zirger, J.M. *et al.* (2003) 'Cloning and expression of zebrafish neuronal nicotinic acetylcholine receptors', *Gene expression patterns: GEP*, 3(6), pp. 747–754. Available at: https://doi.org/10.1016/s1567-133x(03)00126-1.

Zoli, M., Pistillo, F. and Gotti, C. (2015) 'Diversity of native nicotinic receptor subtypes in mammalian brain', *Neuropharmacology*, 96, pp. 302–311. Available at: https://doi.org/10.1016/j.neuropharm.2014.11.003.

Chapter 2:

Dynamic regulation of the cholinergic system in the spinal central nervous system

For the first aim of my PhD, we sought to characterize the spatiotemporal expression of cholinergic signaling genes in the embryonic and larval zebrafish spinal cord. To achieve this goal, we employed various techniques such as immunohistochemistry, colorimetric and fluorescent in situ hybridization on both whole-mount and spinal cord sections of zebrafish aged 1 to 6 days post fertilization. In situ hybridization results showed that pre- and postsynaptic cholinergic signaling transcripts are expressed in the zebrafish spinal cord starting 20hpf. We then confirmed that presynaptic transcripts are expressed in motoneurons while postsynaptic transcripts are expressed in interneurons. Interestingly, we saw that presynaptic mRNA transcripts and protein levels started to decrease at 3dpf in a rostrocaudal manner, while the expression level of postsynaptic transcripts remained constant.

For this publication, I carried out bacterial transformation to increase the copy number of the plasmids of interest. I then performed probe extraction, linearization, and synthesis to obtain the mRNA probes. Subsequently, I performed colorimetric in situ hybridization on whole-mount zebrafish aged 1-, 3-, and 6-days post fertilization (dpf) to determine the expression of *cholineacetyltransferase a, vesicular acetylcholine transporter b*, *nicotinic acetylcholine receptor α3*, *nicotinic acetylcholine receptor α2B* and *nicotinic acetylcholine receptor α7* mRNA transcripts (Figures 1-2, S1, S4-5 in Rima *et al.*, 2020). Following the observation of downregulation in presynaptic components at 3 dpf, I carried out immunohistochemistry using ChAT and VAChT antibodies in 6 dpf larvae and larval spinal cord sections to determine whether the downregulation in mRNA concentration was reflected in proteins. I found that protein levels of ChAT and VaChT are consistent with the decrease in mRNA levels (Rima *et al.*, 2020). Subsequently, I conducted fluorescent in situ hybridization using the nAChRa3 probe coupled with immunohistochemistry using the HuC (pan-neuronal marker) antibody to check whether postsynaptic components were expressed in neural or glial cells. I found that postsynaptic cholinergic signaling components are

expressed in HuC-positive cells in the ventromedial spinal cord, indicating that nAChR subunits are expressed primarily in interneurons (Rima *et al.*, 2020). I subsequently checked for the reason we see a decrease in cholinergic signaling components by crossing the mnx1:GFP line with the vgluT:DsRed to check if there is colocalization between ACh synthesizing machinery and glutamatergic synthesizing machinery (S7).

OPEN

Dynamic regulation of the cholinergic system in the spinal central nervous system

Mohamad Rima[1,2], Yara Lattouf[1,3], Maroun Abi Younes[1,3], Erika Bullier[1], Pascal Legendre[1], Jean-Marie Mangin[1] & Elim Hong[1]✉

While the role of cholinergic neurotransmission from motoneurons is well established during neuromuscular development, whether it regulates central nervous system development in the spinal cord is unclear. Zebrafish presents a powerful model to investigate how the cholinergic system is set up and evolves during neural circuit formation. In this study, we carried out a detailed spatiotemporal analysis of the cholinergic system in embryonic and larval zebrafish. In 1-day-old embryos, we show that spinal motoneurons express presynaptic cholinergic genes including *choline acetyltransferase* (*chata*), *vesicular acetylcholine transporters* (*vachta*, *vachtb*), *high-afinity choline transporter* (*hacta*) and acetylcholinesterase (*ache*), while nicotinic acetylcholine receptor (nAChR) subunits are mainly expressed in interneurons. However, in 3-day-old embryos, we found an unexpected decrease in presynaptic cholinergic transcript expression in a rostral to caudal gradient in the spinal cord, which continued during development. On the contrary, nAChR subunits remained highly expressed throughout the spinal cord. We found that protein and enzymatic activities of presynaptic cholinergic genes were also reduced in the rostral spinal cord. Our work demonstrating that cholinergic genes are initially expressed in the embryonic spinal cord, which is dynamically downregulated during development suggests that cholinergic signaling may play a pivotal role during the formation of intraspinal locomotor circuit.

Acetylcholine (ACh) is an ancient molecule found throughout most life forms including bacteria, fungi, plants and animals[1]. In vertebrates, cholinergic neurons, which release ACh during neurotransmission, are found in both the spinal cord and also in distinct areas of the brain, including the basal forebrain, brainstem and the habenula[2]. Brain cholinergic systems regulate many cognitive processes including learning, memory, attention and sleep and as such, has been targeted to treat various diseases including Alzheimer's, Huntington's and Parkinson's diseases[2–5]. During development, cholinergic signaling, the binding of ACh to its receptors, is essential for physiological processes necessary for the formation of the peripheral and central nervous systems (CNS), including spontaneous neuronal activity, axon pathfinding and synaptogenesis[6]. As nicotine binds with high affinity to the endogenous nicotinic ACh receptors (nAChRs) and is able to cross the placenta and the blood brain barrier, many studies have described the detrimental impact of early nicotine exposure on fetal development in humans and animal models resulting in neurobehavioral and locomotion defects[7,8].

In the nervous system, cholinergic signaling generally occurs by the coordinated action of the ACh-releasing pre-synaptic and ACh-receiving postsynaptic cells (Fig. 1A). Cholinergic neurons are characterized by the presence of Choline AcetylTransferase (ChAT), which mediates ACh synthesis and the Vesicular AcetylCholine Transporter (VAChT), which loads ACh into vesicles. Presynaptic vesicular release of ACh into the synaptic cleft binds to and activates ACh receptors before being degraded by Acetylcholinesterase (AChE) into acetate and choline. The latter is carried into the presynaptic neurons by the High-Affinity Choline Transporter (HACT). In vertebrates, the effects of ACh is mediated by two pharmacologically-distinct families of receptors; namely, nicotinic and muscarinic ACh receptors (nAChR and mAChR, respectively). Cholinergic signaling has also been

shown to occur prior to synapse formation. For example, ACh-release was detected at the growth cone of growing spinal neurons[9], and ACh somatic exocytosis has also been reported[10]. These findings suggest a functional role of ACh even before the onset of synaptogenesis. As such, it has been shown that cholinergic signaling mediates the emergence of spontaneous neuronal activity during embryonic development of many animal models, and regulates circuit formation in the spinal cord[11–13]. However, how the cholinergic system develops during the early phases of neuronal circuit formation is still poorly understood.

Previous studies have shown that both pre- and postsynaptic cholinergic genes are expressed in the spinal CNS during development. Presynaptic cholinergic genes start being expressed at early embryonic stages in chick (stage 26) and mouse (E10.5)[14,15] spinal cord. In parallel, nAChRs are also expressed in different regions of the embryonic spinal cord in human, mouse and chick[16–18]. However, a systemic study to investigate whether there are any changes in the cholinergic system throughout spinal CNS development has not been carried out.

The embryonic zebrafish has emerged as an attractive vertebrate model system to study the development and function of neural circuits[19–22]. It is easy to observe and manipulate the embryos during development as they are externally fertilized. In addition, the small size and transparency of the embryo allows the observation of various experimental techniques without the need to dissect the embryo. Therefore, the embryonic zebrafish presents an ideal model system to probe the development of the cholinergic system in the whole organism during early development. Furthermore, the spinal neuronal circuit is well characterized and specific neuronal populations express transcription factors that are conserved in vertebrates[23,24]. In the embryonic zebrafish, motoneurons start expressing *chat* transcript from 16 hours post fertilization (hpf)[25] and ChAT protein is found in 2-day- old embryos[26]. In addition, *ache* and various nAChR subunit transcripts are present in the spinal cord during early development[27–29]. However, the precise spatial and temporal resolution of many cholinergic genes are still unknown. Therefore, we carried out a detailed analysis on the spatiotemporal expression of the pre- and post-synaptic cholinergic system during early development.

We found high levels of presynaptic cholinergic gene expression in motoneurons and nAChR subunits in interneurons in the embryonic spinal cord, suggesting cholinergic transmission between motoneurons and interneurons in the CNS. During development into larval stages, the cholinergic phenotype in spinal motoneurons is downregulated and gradually becomes restricted to the tail tip, while interneurons continuously express nAChRs throughout the spinal cord. In addition, we found that ChAT-expressing neurons, VAChT puncta on muscles and AChE activity were all decreased in the rostral compared with the caudal spinal cord. Our findings show an unexpected transition of the cholinergic system during development and suggests a pivotal role for cholinergic signaling in the formation of the intra-spinal locomotor circuit.

Results

Pre- and postsynaptic cholinergic genes are expressed in the embryonic spinal cord. To understand the spatiotemporal relationship of the different cholinergic genes during early development, we firstly carried out whole mount *in-situ* hybridization (ISH) in 22–24 h post fertilization (hpf) embryos. We found that presynaptic cholinergic genes *chata*, *hacta*, *vachta* and *vachtb* are expressed in the spinal cord of 22–24 hpf embryos (Fig. 1A, C, Supplementary Fig. 1A–C). The presynaptic cholinergic genes *chatb* (Supplementary Fig. 1E) and *hactb* (data not shown) are not expressed in the spinal cord at this stage. nAChR α3 subunit (*chrna3*), α7 subunit (*chrna7*) and α2 subunit (*chrna2a*) transcripts are also expressed in the 22–24 hpf spinal cord (Fig. 1E, F, Supplementary Fig. 1D). *ache* was present in the spinal cord, and ubiquitously expressed in the muscles (Fig. 1D). In the spinal cord, all cholinergic genes show a rostral (high) to caudal (low) expression pattern that coincides with the rostral to caudal sequential development of zebrafish spinal cord[30].

In the zebrafish embryo, the spinal cord shows a ventral to dorsal organization consisting of motoneurons, interneurons and sensory neurons (Fig. 1B). The expression pattern of presynaptic genes *chata*, *hacta*, *vachta* and *vachtb* appeared different from that of *chrna3* and *chrna2a*. Presynaptic genes, *chrna7* and *ache* were located more ventrally compared to *chrna3* and *chrna2a* (Fig. 2A). We carried out transverse sections of embryos and found *hacta*, *ache* and *chrna7* expression in the ventral area, while *chrna3* was found in the medial area of the spinal cord (Fig. 2A). These results suggest that the presynaptic cholinergic genes, *ache*, and *chrna7* are expressed in motoneurons while *chrna3* and *chrna2a* are expressed in interneurons. This was confirmed by carrying out fluorescence in situ hybridization (FISH) in a transgenic line that expresses the green fluorescent protein (GFP) under the promoter for the Motor Neuron and Pancreas Homeobox 1 (*mnx1*) gene [*Tg*(*mnx1:GFP*)], which is commonly used to identify motoneurons[31]. We found that *hacta*, *ache* and *chrna7* expressing cells co-express *mnx1:*GFP, indicating that they are indeed expressed in motoneurons. Interestingly, less than half of *mnx1:*GFP neurons co-express *chrna7*, suggesting that while most motoneurons express *hacta* and *ache*, *chrna7* is found only in a subpopulation of motoneurons (Fig. 2D). Conversely, most *chrna3* expressing cells did not co-express *mnx1:*GFP, suggesting that they are expressed mainly in interneurons (Fig. 2B–D). To confirm that *chrna3* is expressed in neurons and not in neural progenitor cells, we carried out FISH and labeled neurons using anti-Hu antibody, a marker for differentiated neurons in zebrafish[32,33]. We found that all *chrna3*-expressing cells were also positive for anti-Hu labeling (Supplementary Fig. 2). Based on the medial location of *chrna3*-expressing neurons along the dorsal–ventral spinal cord (Fig. 2A), we conclude that *chrna3* is indeed expressed in interneurons in the embryo.

In adult zebrafish and rats, there is no evidence for cholinergic descending projections from the brain to the spinal cord but only intraspinal cholinergic innervation[34–36]. However, to test for the possibility of transient cholinergic neurons from the brain that project to the nAChR-expressing interneurons in the spinal cord, we also examined the expression of cholinergic genes in the brain. We found faint ubiquitous expression of *vachtb*, *ache*, *chrna3* and *chrna7* transcripts at 22–24 hpf in the embryonic brain (Fig. 1D, F, Supplementary Fig. 1B, D), suggesting that they were not specific to cholinergic neurons. Only *chatb* was expressed in distinct nuclei adjacent

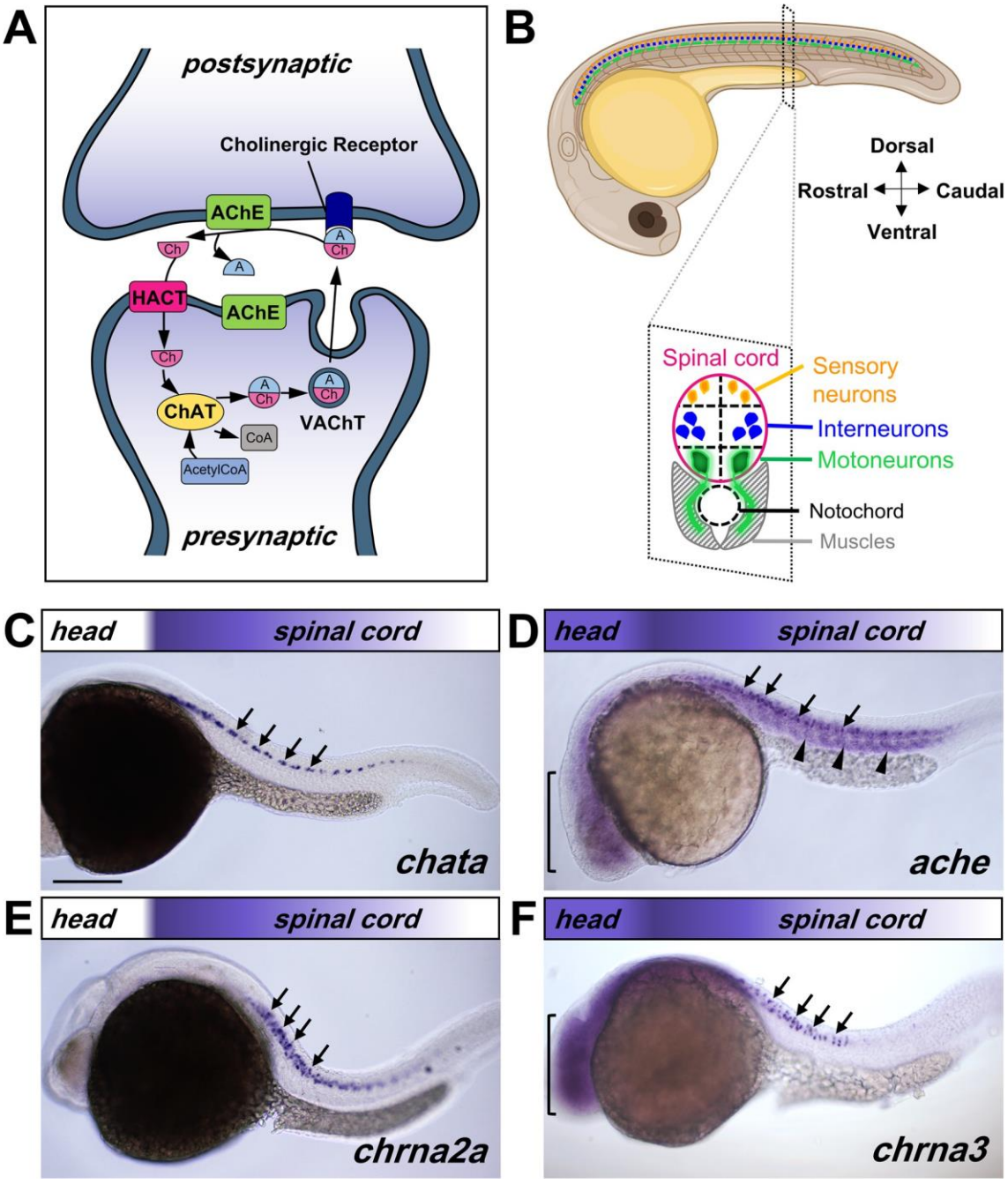

Figure 1. Transcript map of cholinergic genes in the 22–24 hpf embryo. (**A**) Simplified illustration of ACh signaling between pre- and postsynaptic neurons. Choline Acetyltransferase (ChAT), Vesicular Acetylcholine Transporter (VAChT), Acetylcholinesterase (AChE), High Affinity Choline Transporter (HACT), acetyl (A), Choline (Ch), Acetyl Coenzyme A (AcetylCoA). (**B**) Schematic representation of embryonic zebrafish spinal cord organization, showing lateral view of a 24 hpf zebrafish embryo (top), and an illustration of transverse section of the spinal cord (bottom). (**C**–**F**) Lateral view of 22–24 hpf embryos processed by in situ hybridization showing expression for *chata* (**C**) in the spinal cord (arrows), *ache* (**D**) in the spinal cord (arrows), muscles (arrowheads) and the brain (bracket), *chrna2a* (**E**) in the spinal cord (arrows), *chrna3* (**F**) in the spinal cord (arrows) and brain (bracket). The rostro-caudal expression pattern of the transcript is represented by the colored gradient bar on top of each image. Magnification is the same for all images in (**C**–**F**). Scale bar: 200 µm. Cartoon from (**B**) was modified from Biorender.

to the eyes (Supplementary Fig. 1E), suggesting the presence of the putative oculomotor cholinergic neurons. These results showing a lack of clear presynaptic gene expression in the brain combined with the strong expression

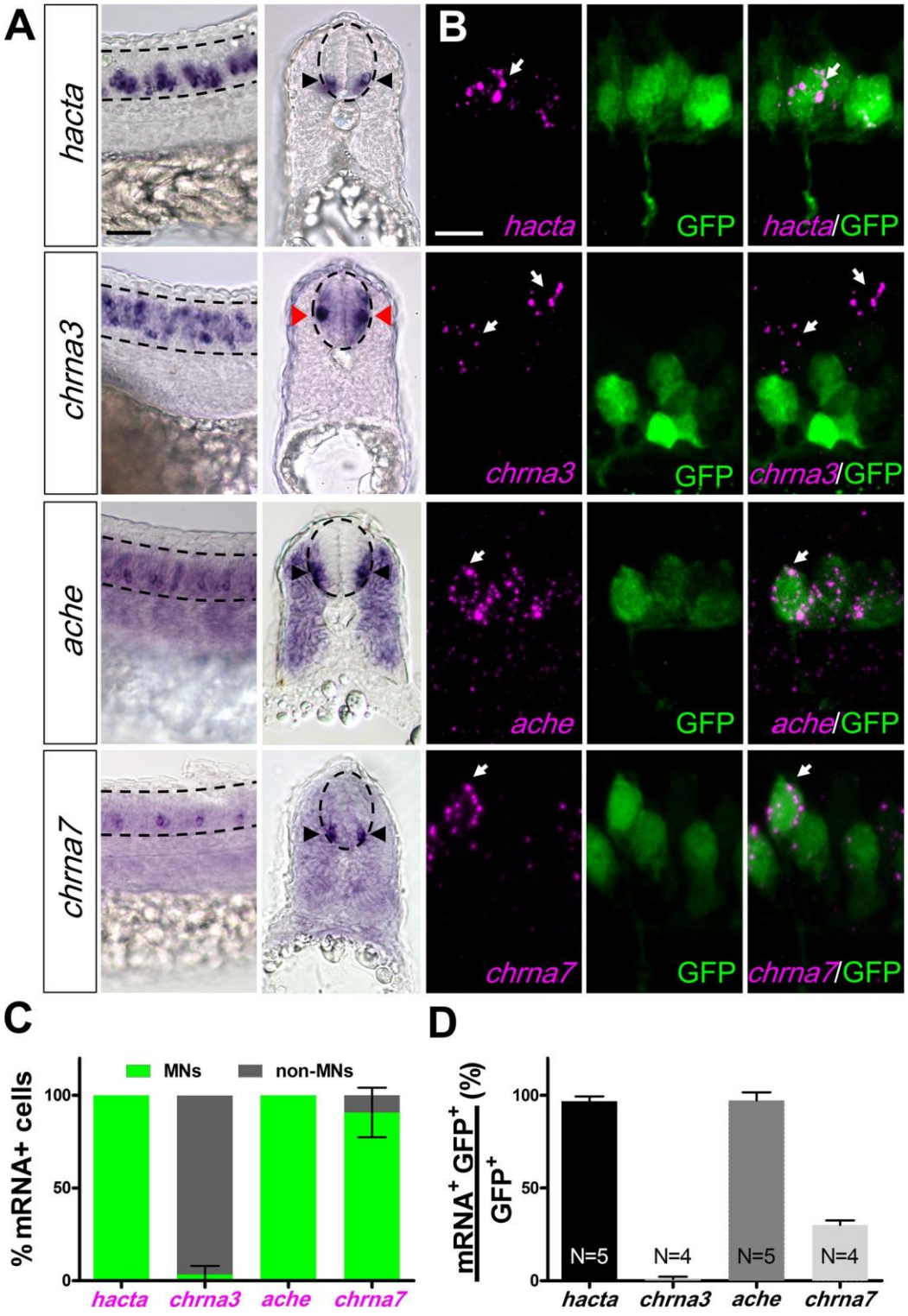

Figure 2. Spatial expression pattern of cholinergic genes in spinal inter- and motoneurons at 24 hpf. (**A**) Lateral view (left) and cross sections (right) of embryos processed by in situ hybridization showing *hacta*, *chrna3*, *ache*, and *chrna7* transcripts in the spinal cord. While *hacta*, *ache*, and *chrna7* transcripts are expressed in the ventral spinal cord (black arrowheads) that contains motoneurons (MNs), *chrna3* is expressed in intermediate spinal cord (red arrowheads) consistent with location of interneurons (INs). The spinal cord is outlined by dashed lines. Scale bar: 30 µm. (**B**) Representative confocal images of fluorescent in situ hybridization of 24 hpf *Tg*(*mnx1:GFP*) embryos showing MNs in green (GFP) and *hacta* (first row), *chrna3* (second row), *ache* (third row), and *chrna7* (fourth row) transcript in magenta (white arrows). Scale bar: 15 µm. (**C**) Classification of *hacta*, *chrna3*, *ache*, and *chrna7* expression in MNs (green) or non-MNs (grey). (**D**) Percentage of *hacta*, *chrna3*, *ache*, and *chrna7* expressing *mnx1:*GFP neurons. *hacta:* N=5 embryos (176 *mnx1:*GFP$^+$ neurons, 171 *hacta*$^+$ neurons). *chrna3:* N = 4 embryos (214 *mnx1:*GFP$^+$ neurons, 77 *chrna3*$^+$ neurons). *ache*: N = 5 (132 *mnx1:*GFP$^+$ neurons, 128 *ache*$^+$ neurons). *chrna7:* N=8 embryos (223 *mnx1:*GFP$^+$ neurons, 59 *chrna7*$^+$ neurons).

of both presynaptic and nAChR subunits in the spinal cord suggest that the nAChRs in the interneurons may detect ACh released from motoneurons during early embryonic development.

Presynaptic cholinergic genes and *ache* transcripts are decreased in the spinal cord from 3 days. We found that *chata*, *hacta* and *vachtb* are expressed in the brain of 2-day-old embryos (Supplementary Fig. 3). *chata* was expressed in oculomotor (asterisk), secondary gustatory (arrowhead), trigeminal motor nuclei (arrow) and cluster of hindbrain neurons. *hacta* and *vachtb* transcripts were found in midbrain nuclei (brackets). Additionally, *vachtb* transcripts were detected in the habenula (white arrowhead). The expression ofcholinergic genes did not differ greatly in 2-day-old spinal cord compared with that in 24 hpf embryos (data not shown).

In 3- and 4-day old embryos more areas in the brain start expressing *chata*, *hacta* and *ache*. However, ISH staining for these genes start to become fainter at the rostral spinal cord (arrowhead) (Fig. 3A, Supplementary Fig. 4A, B). In addition, while *chatb* transcript remained absent in the spinal cord, *vachtb* expression decreased drastically and is barely detectable in the spinal cord by 3 days (Supplementary Fig. 4C, D). By contrast, nAChR subunits α_3 and α_7 transcripts remain uniformly highly expressed throughout the spinal cord (Fig. 3B, Supplementary Fig. 4E). These results suggest that from 3 days, there is a decrease of presynaptic cholinergic transcripts and *ache* in a rostral to caudal gradient.

In 6-day-old larvae, ISH staining for *chata*, *vachta*, *hacta* and *ache* in the spinal cord is mainly expressed in the caudal spinal cord (Fig. 3C, Supplementary Fig. 5A–C). Conversely, nAChR subunits α_3 and α_7 transcripts remain expressed along the spinal cord (Fig. 3D, Supplementary Fig. 5D). *chata* transcript expression continues to decrease in the rostral spinal cord of 10-day-old larvae and becomes limited to the tip of the tail in juvenile fish (15 days) (Supplementary Fig. 6). These findings suggest that only presynaptic cholinergic genes in the spinal cord undergo the rostral to caudal downregulation during development, which continues until juvenile stages.

Rostro-caudal gradient of ChAT and VAChT in larvae. To verify if the downregulation of presynaptic cholinergic mRNA transcript expression is consistent with a decrease in protein levels, we carried out immunohistochemistry (IHC) for ChAT in the *Tg*(*mnx1:GFP*) transgenic line. First, we found in 24 hpf embryos that while the rostral spinal cord contained higher number of motoneurons (17.14 ± 4.14 vs. 10.27 ± 3.8 l; $p = 0.0009$), there was no difference in the number of ChAT$^+$ neurons between the rostral and caudal spinal cord (Fig. 4A–C; 13.17 ± 3.13 vs. 11.19 ± 5.01; $p = 0.444$). In addition, we found that ChAT is expressed in most motoneuron soma and axons in the spinal cord at this stage of development (Fig. 4A, D; 87 ± 17%). In 6-day-old larvae, while the number of motoneurons in the rostral vs. caudal spinal cord was similar (23 ± 8.92 vs. 26 ± 5.74; $p = 0.417$), there was almost twice as many ChAT$^+$ neurons in the caudal spinal cord (Fig. 4E–G; 15 ± 2.8 vs. 29 ± 8.26; $p = 0.0028$). In fact, the caudal motoneurons mostly co-expressed ChAT (93 ± 9.1%), as found in 24 hpf embryos. However,the rostral spinal cord showed a decrease in the percentage of motoneurons that co-express ChAT (Fig. 4H;63 ± 18%; $p = 0.005$). These results show that ChAT protein expression is correlated with its mRNA transcript expression, and suggest that ChAT is downregulated in the rostral spinal cord during larval development.

To see whether the difference in the number of ChAT$^+$ neurons in the spinal cord affects the number of putative ACh release sites, we next carried out IHC for VAChT, which functions to package ACh into vesicles at its release sites. We quantified the number of VAChT puncta at the neuromuscular junctions in the rostral vs. caudal myosepta, which have been shown to contain high levels of nAChRs[37]. Again, we found that there was a significantly lower number of VAChT puncta in the rostral compared to caudal myosepta (Fig. 5; 6.68 ± 2.4 vs. 16.788 ± 4.56; $p = 2.67391E{-}08$), suggesting a rostro-caudal gradient of VAChT in the spinal motoneuron projections to the myosepta in 6-day-old larvae. This gradient is consistent with *vachta* ISH results (Supplementary Fig. 5A) further providing evidence that downregulation of presynaptic cholinergic component mRNA expression does indeed result in decreased protein levels.

Reduced AChE activity in the rostral spinal cord. Another cholinergic gene that was decreased in the rostral spinal cord in larvae is *ache*. We carried out Karnovsky staining to assay for esterase activity[38]. First, we performed this in 24 hpf embryos where we found stronger staining in the rostral compared with the caudal spinal cord (Fig. 6A), which is consistent with *ache* expression pattern (Fig. 1D). This staining was completely lost when embryos are treated with eserine (Fig. 6B), an esterase inhibitor, showing the specificity of the staining. In 6-day-old larvae, we found stronger staining in the caudal compared with the rostral spinal cord (Fig. 6C–F), which is lost when treated with eserine (Fig. 6D′, F′). This result is consistent with the rostro-caudal gradient in *ache* expression (Supplementary Fig. 5C), and indicates that the level of AChE enzymatic activity is determined by *ache* transcript expression.

Downregulation of cholinergic signaling is not due to neurotransmitter switch in motoneurons. Downregulation of presynaptic cholinergic gene expression during development may be explained by a change in the neurotransmitter type utilized by motoneurons in the spinal cord during later stages of development. Indeed, studies have shown co-release of ACh and glutamate in motoneurons in the perinatal and adult mouse[39,40] and in the adult zebrafish[36]. Only the *vesicular glutamate transporter 2* (*vglut2*), and not *vglut1* is expressed in the zebrafish spinal cord in embryo and larvae[41]. We assayed whether motoneurons co-express *vglut2* by analyzing the *Tg*(*mnx1:GFP;vglut2:DsRed*) double transgenic line. Our results show that in 24 hpf embryos *vglut2:*DsRed neurons are located dorsal to the *mnx1:*GFP neurons (Supplementary Fig. 7A), consistent with a previous study suggesting that only interneurons utilize glutamate as their neurotransmitter in the zebrafish embryo[41]. In 6-day-old larvae, interneurons continue expressing *vglut2*, while less than 5% of *mnx1:*GFP$^+$ neurons co-express *vglut2:*DsRed (Supplementary Fig. 7B, C; 2.9 ± 2.5%). Together, these

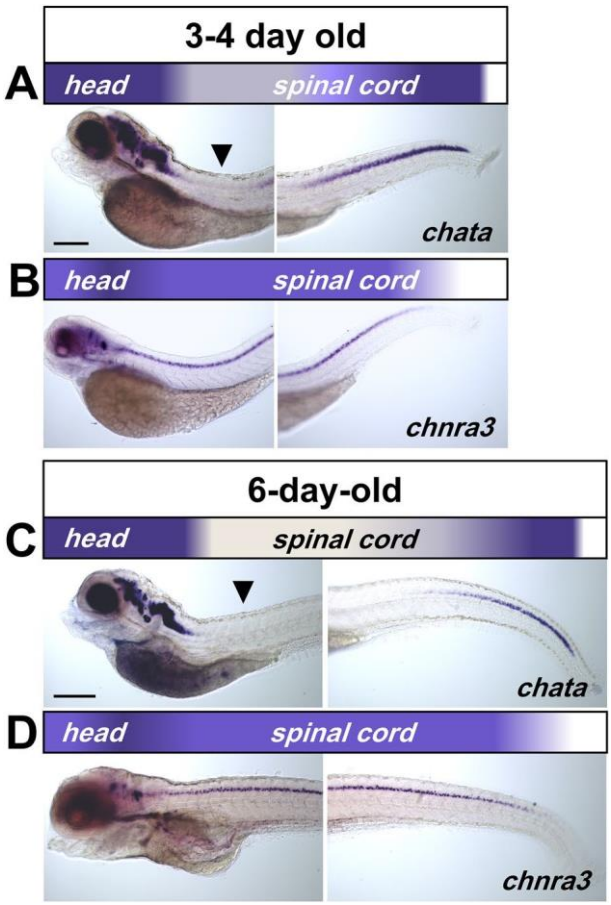

Figure 3. Downregulation of presynaptic cholinergic gene transcript in larval spinal cord. (**A**, **C**) Lateral view of 3–4 and 6-day-old larvae processed by in situ hybridization showing a rostro-caudal gradient for *chata*. Arrowheads point toward reduced transcript levels in rostral spinal cord. (**B**, **D**) *chrna3* remain expressed in a uniform pattern along the entire spinal cord. The rostro-caudal expression pattern of the transcript is represented by the colored gradient bar on top of each image. Note that there is no change in transcript levels in the brain. Magnification is the same for all images in (**A**–**D**). Scale bar: 200 μm.

findings suggest that the decrease in cholinergic phenotype in motoneurons is not due to the acquisition of the gluta-matergic phenotype.

Discussion

We carried out a detailed spatiotemporal analysis of one of the most ancient signaling systems in living forms, the cholinergic system, which can be perturbed by external sources including nicotine and neonicotinoid pesticides. This spatiotemporal map revealed that while 1-day-old embryos express the full machinery for ACh release in motoneurons and interneurons express different subunits for the nicotinic ACh receptors, there is an unexpected decrease in presynaptic cholinergic components in the rostral spinal cord during development (Fig. 7). The downregulation of presynaptic cholinergic transcripts was validated by the reduction in ChAT-expressing neurons, as well as the number of VAChT puncta along the myosepta in the rostral versus caudal spinal cord. Finally, acetylcholinesterase activity staining confirmed that the rostral to caudal gradient of *ache* transcript translates to reduced AChE function in the rostral spinal cord.

In the spinal cord, there is a rostral to caudal delay in the differentiation of neurons during development. In other words, rostral neurons are more mature than caudal neurons[30]. The higher number of ChAT$^+$ neurons, VAChT$^+$ protein puncta and AChE activity in the caudal compared with the rostral spinal cord suggest that there is a dynamic downregulation of cholinergic neurons during development. It is possible that the downregulation of cholinergic neurons may be due to programmed cell death (PCD) as around 40% of cells from the lateral motor column undergo PCD in the chick embryo[42]. However, studies in rat, mouse or chick show conflicting results on whether there is indeed a rostro-caudal gradient of PCD[42,43]. Furthermore, PCD was not observed in motoneurons[44] and appears to mainly occur in sensory neurons in the zebrafish spinal cord during early development[45]. Regardless, even if the reduction in ChAT$^+$ neurons in the rostral spinal cord may be partly due to PCD, this cannot fully explain the lower levels of mRNA transcript staining, which becomes even more difficult to detect in juvenile larvae (15-days-old), except at the tip of the tail. As the staining is maintained at high levels in the brain throughout development, the difference in staining intensity is unlikely due to technical issues.

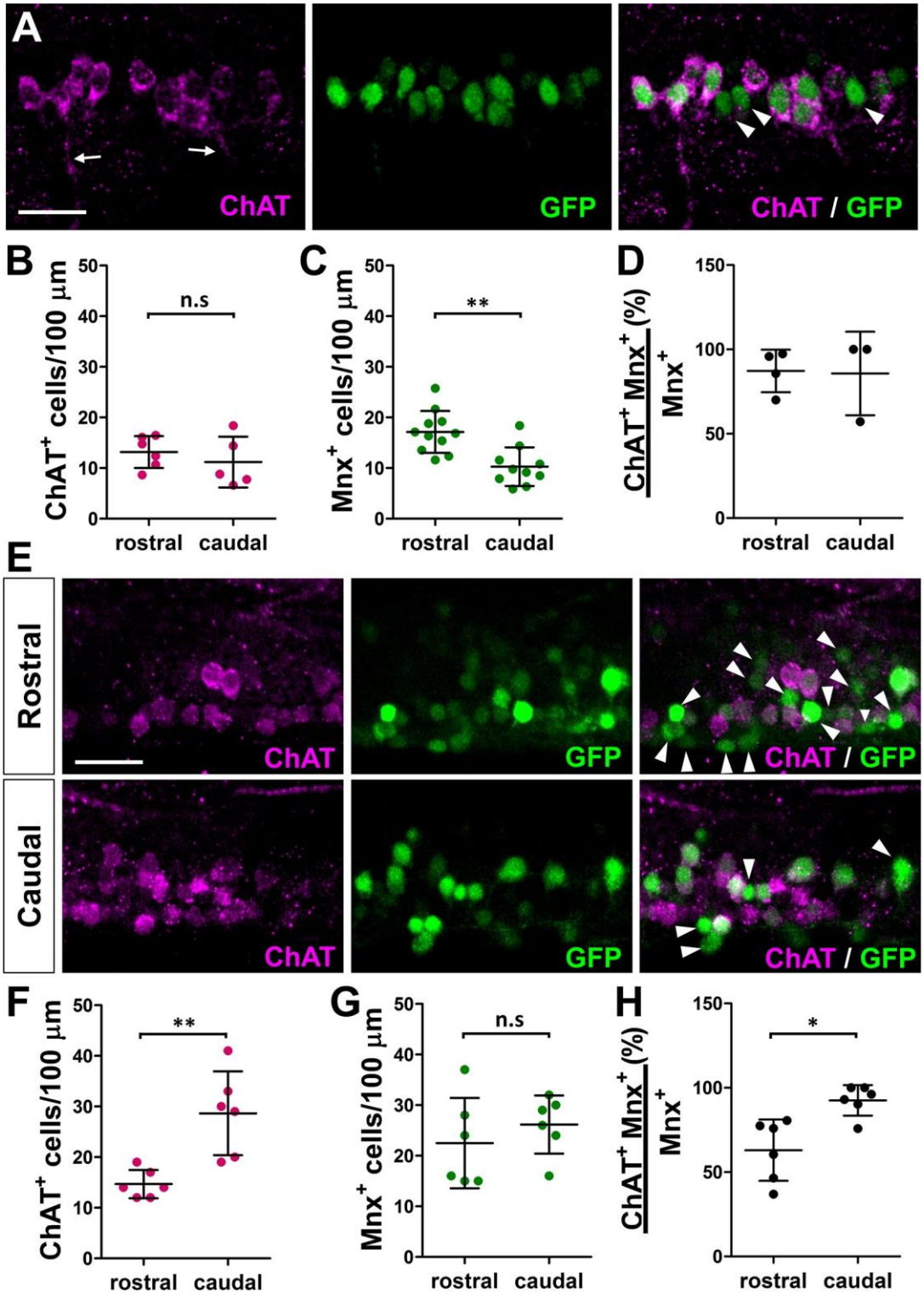

Figure 4. Expression of ChAT in *Tg*(*mnx1*:GFP) spinal motoneurons. (**A**) Confocal images of a lateral view of 24 hpf embryos processed with antibody labeling showing ChAT in MN soma and axons (arrows). Arrowheads point to ChAT$^-$ *mnx1*:GFP$^+$ cells. (**B–D**) Quantification of ChAT and *mnx1*:GFP labeled cells in 24 hpf *Tg*(*mnx1:GFP*) embryos. (**B**) ChAT$^+$ and (**C**) *mnx1:*GFP labeledcell numbers in 100 µm segment in rostral and caudal spinal cord of 24 hpf embryos. (N=10 embryos; 527 *mnx1:*GFP$^+$ neurons,

307 ChAT$^+$ neurons). (**D**) Percentage of ChAT expressing *mnx1:*GFP neurons in rostral and caudal spinal cord. (N = 7 embryos; 186 *mnx1:*GFP$^+$ neurons, 172 ChAT$^+$ neurons). (**E**) Confocal images of a lateral view of a 6-day-old larva processed with antibody labeling showing that ChAT$^-$ *mnx1:*GFP$^+$ cells (arrowheads) are found more in the rostral than caudal spinal cord. (**F–H**) Quantification of ChAT and *mnx1:*GFP labeled cells in 6-day-old *Tg*(*mnx1:GFP*) larvae. (**F**) ChAT$^+$ and (**G**) *mnx1:*GFP labeled cell numbers in 100 µm segment in the rostral and caudal spinal cord of 6-day-old *Tg*(*mnx1:GFP*) larvae. (**H**) Percentage of ChAT expressing *mnx1:*GFP neurons in rostral and caudal spinal cord. (N = 6 larvae; 499 *mnx1:*GFP$^+$ neurons, 381 ChAT$^+$ neurons). All images are oriented with rostral towards the left and dorsal to the top. Scale bar: 20 µm. 2-tailed non-paired Student's *t* test; n.s.: not significant; *$p<0.05$;**$p<0.005$.

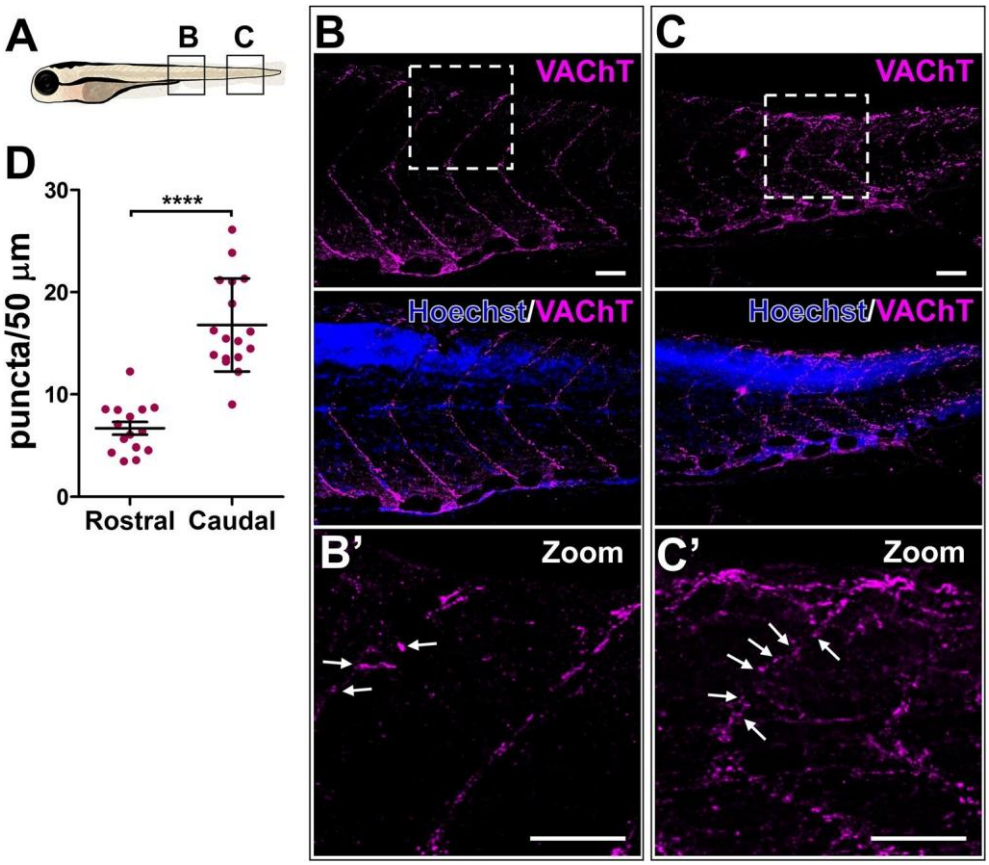

Figure 5. Decreased VAChT expression along the rostral myosepta of 6-day-old larva. (**A**) Schematic representation of the imaged areas in (**B**, **C**). (**B**, **C**) Confocal image of a lateral view of larva showing a rostro-caudal gradient of VAChT puncta in MN axons projecting along the dorsal myosepta. Nuclei are labeled by Hoechst (blue). (**B′**, **C′**) Zoomed in images of the boxed areas in (**B**, **C**). White arrows point toward VAChT positive signals along the myosepta. Scale bars: 50 µm. (**D**) Quantification of VAChT puncta in the dorsal myosepta. N = 4 larvae (15 rostral axons, 17 caudal axons). 2-tailed non-paired Student's *t* test; ****$p < 0.0001$.

Studies in perinatal and adult mouse have shown that spinal motoneurons exhibit developmental plasticity by co-releasing acetylcholine and glutamate in the CNS[39,40]. Recent study in adult zebrafish found evidence that motoneurons co-release glutamate at the neuromuscular junction depending on their physiological and pathophysiological conditions to regulate motor behaviors[36]. We hypothesized that the reduction in cholinergic neurons in the rostral spinal cord may be due to a transition to a glutamatergic neurotransmitter phenotype. However, as less than 5% of *mnx1:*GFP^{+} neurons appear to be glutamatergic, this cannot fully account for the ~ 30% reduction in ChAT-expressing motoneurons in the rostral spinal cord.

One characteristic of ACh is that it functions as both a neurotransmitter, mediating fast synaptic transmission and a neuromodulator, to alter neuronal excitability and/or coordinate firing of groups of neurons[46]. It functions as a neurotransmitter at the neuromuscular junction (NMJ) between the motoneuron and muscles. In the brain, evidence of ACh function as a neurotransmitter is scarce, instead, it is released at non-synaptic sites through exocytosis and/or volume transmission and is believed to function as a neuromodulator[46,47]. In vertebrates including rodents and chick, cholinergic signaling mediates the emergence of spontaneous neuronal activity (SNA) in the embryonic spinal circuit[11–13]. However, this effect is transitory as ChAT mutant mice recover their SNA, albeit at reduced levels compared with wild-type animals[12]. We propose that in embryonic stages, ACh released by MNs functions as a neuromodulator for the synchronized activation of interneurons. Indeed, ACh released from motoneurons is necessary for the activation of GABAergic and glutamatergic interneurons in the embryonic mice spinal cord[48]. Later, as spinal neurons mature in a rostral to caudal sequence, ACh may be mainly released by motoneurons at the neuromuscular junction and functions as a neurotransmitter in regulating fast synaptic currents, necessary for the precise control of locomotion.

The relationship between gene expression patterns with mRNA levels, decay, stability or protein levels appear complex as it varies depending on many factors including the developmental stage and cellular location, as well as function of the protein[49,50]. An interesting hypothesis to explore in future studies would be to test whether the high and low levels of presynaptic mRNA transcript result in either neuromodulation or neurotransmitter functions during cholinergic signaling, respectively.

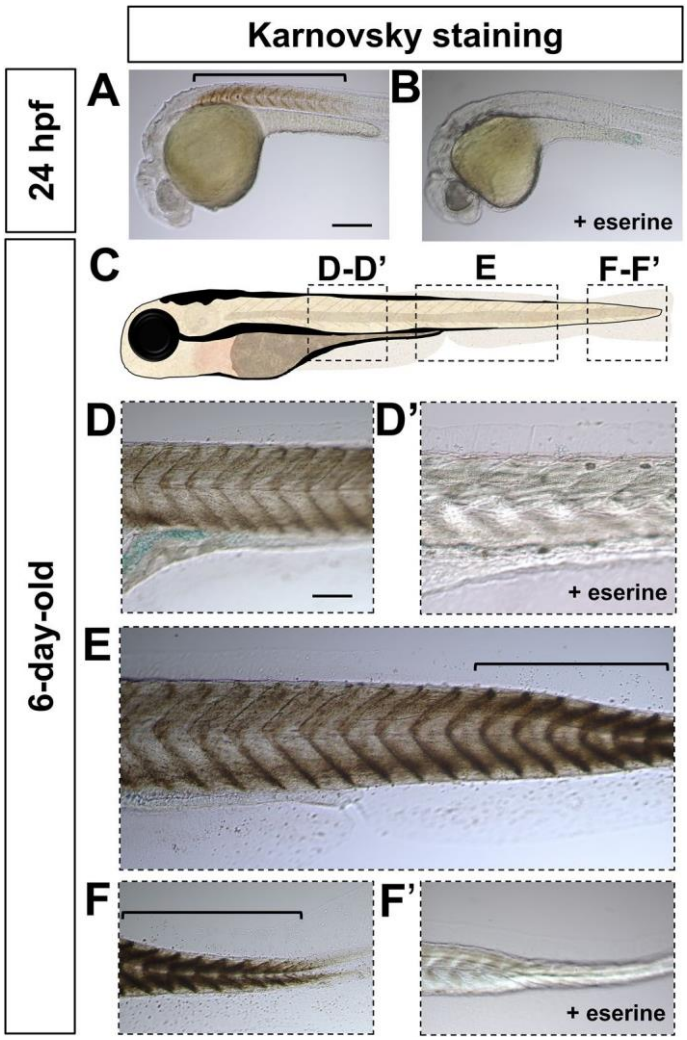

Figure 6. Spatiotemporal Acetylcholinesterase enzymatic activity pattern in the spinal cord during early development. (**A**, **B**) Lateral view of 24 hpf embryos processed with Karnovsky staining showing Acetylcholinesterase enzymatic activity (bracket) in the absence (**A**), but not in presence (**B**) of eserine, an AChE inhibitor. (**C**) Schematic representation of the imaged areas in (**D**–**F**′). Lateral view of 6-day-old larvae showing a rostro-caudal gradient of AChE activity revealed by Karnovsky staining (**D**–**F**′). (**D**, **D′**) Anterior trunk in the absence (**D**) or presence (**D**′) of eserine. (**E**) Mid trunk in the absence of eserine. (**F**, **F′**) Tip of the tail in the absence (**F**) or presence (**F**′) of eserine. Brackets indicate high levels of Karnovsky staining in (**E**, **F**). Magnification is the same for all images in (**A**, **B**) and (**D**–**F**′). Scale bar: 200 µm.

The emergence of spinal SNA in 16 h to 1-day-old zebrafish embryo[51,52], when cholinergic genes start being expressed, suggests that cholinergic signaling plays a role in the generation of SNA and spinal circuit formation, as have been described in other vertebrate animals[11–13]. However, previous studies have concluded that this may not be the case as they failed to observe an effect on embryonic spinal neuron activity upon application of cholinergic antagonists in zebrafish[53,54]. Our work unequivocally shows that the cholinergic machinery is present in 1-day-old embryos, which is then downregulated during development. These results strongly suggest that cholinergic signaling may indeed play a key conserved role during embryonic CNS development.

Together, these findings showing the complexity, dynamics and conservation of zebrafish spinal cholinergic neurons during development, warrant further investigation on the role of cholinergic signaling in SNA and circuit formation in the zebrafish embryo.

Materials and methods

Zebrafish embryos. All animals were maintained at 28 °C in a 14/10 h light/dark cycle at the IBPS core facility according to established procedures. Wild-type AB strain, *Tg*(*mnx1:GFP*)[31], and *Tg*(*vglut2:DsRed*)[55] lines were used in this study. Maintenance of zebrafish stocks and experiments on larvae were carried out in accord-ance with the "Comité d'éthique Charles Darwin" (APAFIS#15,909–2,018,070,912,072,530 v5). The fish facility has been approved by the French "Service for animal protection and health" (A-75-05-25). Zebrafish embryos

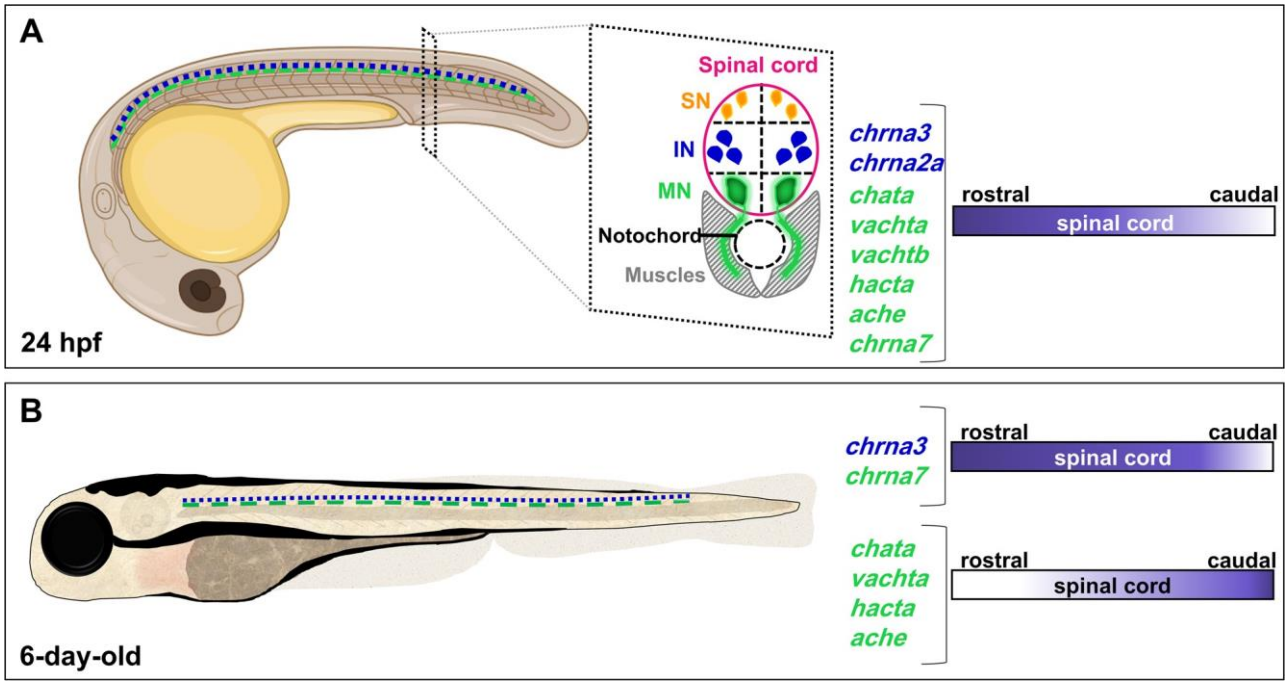

Figure 7. Spatiotemporal cholinergic gene map in embryonic and larval zebrafish. (**A**, **B**) Illustration of 24 hpf embryo (**A**) and 6-day-old larva (**B**) summarizing the cholinergic genes expressed in spinal motoneurons (green) and interneurons (blue). The rostro-caudal expression pattern of the transcripts is represented by the colored gradients on the right. Abbreviations: sensory neurons (SN), interneurons (IN), motoneurons (MN).

were collected and allowed to develop at 28.5 °C. To prevent pigment formation, 0.2 mM phenylthiourea (PTU) was added to the fish water starting 24 h post fertilization (hpf).

RNA colorimetric and fluorescent In-situ hybridization (ISH). Colorimetric ISH on whole-mount zebrafish embryos and larvae was performed as described in[56]. Plasmids used for antisense RNA probes preparation were described in[47]. Restriction enzymes and RNA polymerases used to synthesize the probes were: *vachta* (BamH1/SP6), *vachtb* (EcoRI/T7), *chata* (Not1/Sp6), *chatb* (Not1/Sp6), *hacta* (Not1/SP6), *chrna2a* (Not1/Sp6), *chrna3* (BamH1/T7), *chrna7* (Not1/Sp6), and *ache* (HindIII/T7). Briefly, probes were labeled with UTP-digoxigenin and incubated with embryos overnight in 50% formamide-containing hybridization solution. Probes were then detected using alkaline phosphatase conjugated anti-Digoxigenin antibodies (Roche) and visualized by 5-bromo-4-chloro-3-indolyl-phosphate (BCIP) and 4-nitro blue tetrazolium (NBT) staining. When the desired labeling intensity is reached, embryos/larvae were washed extensively and stored in PBS at 4 °C until imaging.

Fluorescent in situ hybridization (FISH) was performed on 24 hpf embryos as described in[47]. Briefly, UTP-digoxigenin labeled probes were incubated with embryos overnight in 50% formamide-containing hybridization solution. Probes were then detected using horseradish peroxidase conjugated anti-Digoxigenin antibody (Roche) in Maleic acid blocking buffer (150 mM Maleic acid, pH 7.5 & 100 mM NaCl). To amplify the signal, homemade tyramide-FITC was used as described in[57]. Embryos were incubated with tyramide-FITC (1:250) in TSA reactionbuffer (100 mM borate pH 8.5, 0.1% tween-20, 2% dextran sulfate, 0.003% H_2O_2, and 200 µg/ml 4-iodophenol) for 30–45 min in the dark. The reaction was then stopped by abundant washes of 0.1% Tween-20 in PBS (PBT). Embryos were incubated overnight at 4 °C in PBS, 0.1% Triton, 10% sheep serum with rabbit anti-GFP antibody (Thermofisher) or mouse anti-HuC/HuD antibody (Life Technologies) to detect GFP or neurons, respectively. Embryos were washed in PBT and incubated at 4 °C overnight with goat anti-rabbit Alexa594 antibody or goat anti-mouse Alexa555 antibody (Thermofisher), respectively. Finally, embryos were abundantly washed and stored in PBS at 4 °C in the dark until imaging.

Immunohistochemistry. Immunohistochemistry (IHC) was performed either on whole-mount or sec- tioned larvae as described in[58], with some modifications. Larvae were fixed for 1.5 h at 4 °C in 4% paraformalde-hyde, then washed (3 × 5 min) in PBS with 0.2% Triton X-100 (PBST). Samples were then blocked on shaker for 3 h in PBS with 1% BSA, 1% DMSO, 5% Normal Sheep Serum, and 0.2% Triton X-100. Larvae were then incubated with rabbit polyclonal anti-VAChT antibody (1:500, Synaptic systems) in PBST with 1% BSA, overnight at 4 °C on a shaker. Samples were washed in PBST, and incubated with anti-rabbit Alexa594 for 5 h, then Hoechst (Thermofisher) for 30 min at room temperature on a shaker. After several PBST washes, larvae were stored in PBS at 4 °C until imaging. ChAT IHC was performed on whole-mount embryos and larvae. Briefly, embryos/larvae were fixed for 5 h at 4 °C in 4% paraformaldehyde, washed with PBS, and then permeabilized with 0.8% PBST for 1 h on shaker. Samples were then incubated with goat anti-ChAT (1:100, Millipore) for 72 h at 4 °C on

shaker. After 3 washes of PBS, samples were incubated with anti-goat Alexa594 overnight at 4 °C on shaker. After several PBST washes, larvae were stored in PBS at 4 °C until imaging.

Detection of AChE enzymatic activity. AChE activity was detected using a method adapted from Karnovsky and Roots[38]. Briefly, larvae were fixed for 7 h in BT-Fix[59] at room temperature, then washed in PBS with 0.1% Triton X-100. Larvae were then incubated 4–5 h in 60 mM sodium acetate buffer (pH 6.4), 5 mM sodium citrate, 4.7 mM $CuSO_4$, 0.5 mM $K_3(Fe(CN)_6)$, and 1.7 mM acetylthiocholine iodide. When the desired labeling intensity was reached, larvae were washed extensively and stored in PBS at 4 °C until imaging. To check for the specificity of the staining, acetylcholinesterase inhibitor eserine was used at a final concentration of 10^{-4} M.

Sectioning and microscopy. To prepare sections, embryos processed with ISH or IHC were embedded in 4% low-melt agarose prepared in PBS and sectioned at 35 µm (transverse) or 50 µm (sagittal) using a vibratome (LEICA VT1000S). ISH sections were then mounted in Mowiol (Sigma-Aldrich) on glass slides, covered with coverslips and stored at 4 °C in the dark until imaging.

Embryos/larvae processed with ISH or Karnovsky staining were transferred to a glass microscope slide with single cavity well containing 50% glycerol. Bright-field images were acquired on Nikon Eclipse E800 microscope equipped with a Nikon DXM1200 digital camera using Lucia G software. The same system was used to imageslides with sections.

Larvae processed with FISH and IHC were mounted laterally in a drop of 2% low-melt agarose in medium petri dishes, then covered with PBS. Fluorescent Z-stack images were captured at 0.5–3 µm increments with a Leica SP5 confocal microscope using a 20X water immersion objective. Acquisition parameters were identical when imaging rostral and caudal areas of the same fish.

Fluorescent in situ hybridization and immunohistochemistry analysis. Quantifications of *hacta*$^+$/*mnx1*:GFP, *chrna3*$^+$/*mnx1*:GFP, *ache*$^+$/*mnx1*:GFP, *chrna7*$^+$/*mnx1*:GFP, *chrna3*$^+$/HuC, ChAT$^+$/*mnx1*:GFP neurons and VAChT puncta were performed manually using ImageJ. VAChT analysis was performed on axon branches of the rostral and caudal motoneurons along the dorsal myosepta. For each axon, the length of the myosepta was measured and VAChT$^+$ puncta were counted. Labeled puncta were defined as areas containing at least four attached pixels. At least three rostral and three caudal myosepta segments were analyzed per fish.

Statistical analysis. Results are represented as mean ± standard deviation (SD). Differences among groups were analyzed with GraphPad Prism 6.0 software (GraphPad Software Inc., San Diego USA) using a Student's *t* test.

Received: 26 May 2020; Accepted: 18 August 2020
Published online: 18 September 2020

References

1. Yamada, T. *et al.* Expression of acetylcholine (ACh) and ACh-synthesizing activity in Archaea. *Life Sci.* **77**, 1935–1944 (2005).
2. Ahmed, N. Y., Knowles, R. & Dehorter, N. New insights into cholinergic neuron diversity. *Front. Mol. Neurosci.* https://doi.org/10.3389/fnmol.2019.00204 (2019).
3. D'Souza, G. X. & Waldvogel, H. J. Targeting the cholinergic system to develop a novel therapy for Huntington's disease. *J. Huntingtons Dis.* **5**, 333–342 (2016).
4. Gratwicke, J., Jahanshahi, M. & Foltynie, T. Parkinson's disease dementia: a neural networks perspective. *Brain* **138**, 1454–1476 (2015).
5. Hampel, H. *et al.* The cholinergic system in the pathophysiology and treatment of Alzheimer's disease. *Brain* **141**, 1917–1933 (2018).
6. Dwyer, J. B., McQuown, S. C. & Leslie, F. M. The dynamic effects of nicotine on the developing brain. *Pharmacol. Ther.* **122**, 125–139 (2009).
7. Svoboda, K. R., Vijayaraghavan, S. & Tanguay, R. L. Nicotinic receptors mediate changes in spinal motoneuron development and axonal pathfinding in embryonic zebrafish exposed to nicotine. *J. Neurosci.* **22**, 10731–10741 (2002).
8. Holbrook, B. D. The effects of nicotine on human fetal development. *Birth Defects Res. C Embryo Today Rev.* **108**, 181–192 (2016).
9. Sun, Y. A. & Poo, M. M. Evoked release of acetylcholine from the growing embryonic neuron. *Proc. Natl. Acad. Sci.* **84**, 2540–2544 (1987).
10. Welle, T. M., Alanis, K., Colombo, M. L., Sweedler, J. V. & Shen, M. A high spatiotemporal study of somatic exocytosis with scan- ning electrochemical microscopy and nanoITIES electrodes. *Chem. Sci.* **9**, 4937–4941 (2018).
11. Blankenship, A. G. & Feller, M. B. Mechanisms underlying spontaneous patterned activity in developing neural circuits. *Nat. Rev. Neurosci.* **11**, 18–29 (2010).
12. Myers, C. P. *et al.* Cholinergic input is required during embryonic development to mediate proper assembly of spinal locomotorcircuits. *Neuron* **46**, 37–49 (2005).
13. Hanson, M. G. & Landmesser, L. T. Characterization of the circuits that generate spontaneous episodes of activity in the early embryonic mouse spinal cord. *J. Neurosci.* **23**, 587–600 (2003).
14. Enjin, A. *et al.* Identification of novel spinal cholinergic genetic subtypes disclose Chodl and Pitx2 as markers for fast motor neurons and partition cells. *J. Comp. Neurol.* **518**, 2284–2304 (2010).
15. Cho, H.-H. *et al.* Isl1 Directly controls a cholinergic neuronal identity in the developing forebrain and spinal cord by forming cell type-specific complexes. *PLoS Genet.* **10**, e1004280 (2014).
16. Hellström-Lindahl, E., Gorbounova, O., Seiger, Å, Mousavi, M. & Nordberg, A. Regional distribution of nicotinic receptors during prenatal development of human brain and spinal cord. *Dev. Brain Res.* **108**, 147–160 (1998).

17. Keiger, C. J. H., Prevette, D., Conroy, W. G. & Oppenheim, R. W. Developmental expression of nicotinic receptors in the chick and human spinal cord. *J. Comp. Neurol.* **455**, 86–99 (2003).

18. Broide, R. S., Winzer-Serhan, U. H., Chen, Y. & Leslie, F. M. Distribution of α7 nicotinic acetylcholine receptor subunit mRNA in the developing mouse. *Front. Neuroanat.* https://doi.org/10.3389/fnana.2019.00076 (2019).
19. Friedrich, R. W., Jacobson, G. A. & Zhu, P. Circuit neuroscience in zebrafish. *Curr. Biol.* **20**, R371–R381 (2010).
20. Portugues, R., Severi, K. E., Wyart, C. & Ahrens, M. B. Optogenetics in a transparent animal: circuit function in the larval zebrafish. *Curr. Opin. Neurobiol.* **23**, 119–126 (2013).

21. Leung, L. C., Wang, G. X. & Mourrain, P. Imaging zebrafish neural circuitry from whole brain to synapse. *Front. Neural Circuits* https://doi.org/10.3389/fncir.2013.00076 (2013).

22. Vanwalleghem, G. C., Ahrens, M. B. & Scott, E. K. Integrative whole-brain neuroscience in larval zebrafish. *Curr. Opin. Neurobiol.*
50, 136–145 (2018).

23. Goulding, M. Circuits controlling vertebrate locomotion: moving in a new direction. *Nat. Rev. Neurosci.* **10**, 507–518 (2009).
24. Fetcho, J. R. & McLean, D. L. Some principles of organization of spinal neurons underlying locomotion in zebrafish and their implications. *Ann. N. Y. Acad. Sci.* **1198**, 94–104 (2010).
25. Seredick, S. D., Van Ryswyk, L., Hutchinson, S. A. & Eisen, J. S. Zebrafish Mnx proteins specify one motoneuron subtype and suppress acquisition of interneuron characteristics. *Neural Dev.* **7**, 35 (2012).
26. Arenzana, F. J. *et al.* Development of the cholinergic system in the brain and retina of the zebrafish. *Brain Res. Bull.* **66**, 421–425 (2005).
27. Thisse, C. & Thisse, B. High throughput expression analysis of ZF-models consortium clones. ZFIN Direct Data Submission (2005).
28. Ackerman, K. M., Nakkula, R., Zirger, J. M., Beattie, C. E. & Boyd, R. T. Cloning and spatiotemporal expression of zebrafish neu- ronal nicotinic acetylcholine receptor alpha 6 and alpha 4 subunit RNAs. *Dev. Dyn.* **238**, 980–992 (2009).
29. Zirger, J. M., Beattie, C. E., McKay, D. B. & Thomas Boyd, R. Cloning and expression of zebrafish neuronal nicotinic acetylcholine receptors. *Gene Expr. Patterns* **3**, 747–754 (2003).
30. Kimmel, C. B., Ballard, W. W., Kimmel, S. R., Ullmann, B. & Schilling, T. F. Stages of embryonic development of the zebrafish. *Dev. Dyn.* **203**, 253–310 (1995).
31. Flanagan-Steet, H., Fox, M. A., Meyer, D. & Sanes, J. R. Neuromuscular synapses can form in vivo by incorporation of initiallya-neural postsynaptic specializations. *Development* **132**, 4471–4481 (2005).
32. Hui, S. P., Dutta, A. & Ghosh, S. Cellular response after crush injury in adult zebrafish spinal cord. *Dev. Dyn.* **239**, 2962–2979 (2010).
33. Kim, C.-H. *et al.* Zebrafish elav/HuC homologue as a very early neuronal marker. *Neurosci. Lett.* **216**, 109–112 (1996).
34. Sherriff, F. E. & Henderson, Z. A cholinergic propriospinal innervation of the rat spinal cord. *Brain Res.* **634**, 150–154 (1994).
35. Sherriff, F. E., Henderson, Z. & Morrison, J. F. B. Further evidence for the absence of a descending cholinergic projection from the brainstem to the spinal cord in the rat. *Neurosci. Lett.* **128**, 52–56 (1991).
36. Bertuzzi, M., Chang, W. & Ampatzis, K. Adult spinal motoneurons change their neurotransmitter phenotype to control locomo-tion. *Proc. Natl. Acad. Sci.* **115**, E9926–E9933 (2018).
37. Bradley, S., Tossell, K., Lockley, R. & McDearmid, J. R. Nitric oxide synthase regulates morphogenesis of zebrafish spinal cord motoneurons. *J. Neurosci.* **30**, 16818–16831 (2010).
38. Karnovsky, M. J. & Roots, L. A 'direct-coloring' thiocholine method for cholinesterases. *J. Histochem. Cytochem.* **12**, 219–221 (1964).
39. Nishimaru, H., Restrepo, C. E., Ryge, J., Yanagawa, Y. & Kiehn, O. Mammalian motor neurons corelease glutamate and acetylcholineat central synapses. *Proc. Natl. Acad. Sci.* **102**, 5245–5249 (2005).
40. Lamotte d'Incamps, B., Bhumbra, G. S., Foster, J. D., Beato, M. & Ascher, P. Segregation of glutamatergic and cholinergic transmis- sion at the mixed motoneuron Renshaw cell synapse. *Sci. Rep.* **7**, 4037 (2017).
41. Higashijima, S.-I., Mandel, G. & Fetcho, J. R. Distribution of prospective glutamatergic, glycinergic, and GABAergic neurons in embryonic and larval zebrafish. *J. Comp. Neurol.* **480**, 1–18 (2004).
42. Hamburger, V. Cell death in the development of the lateral motor column of the chick embryo. *J. Comp. Neurol.* **160**, 535–546 (1975).
43. Yamamoto, Y. & Henderson, C. E. Patterns of programmed cell death in populations of developing spinal motoneurons in chicken, mouse, and rat. *Dev. Biol.* **214**, 60–71 (1999).
44. Myers, P. Z., Eisen, J. S. & Westerfield, M. Development and axonal outgrowth of identified motoneurons in the zebrafish. *J. Neu-rosci.* **6**, 2278–2289 (1986).
45. Cole, L. K. & Ross, L. S. Apoptosis in the developing zebrafish embryo. *Dev. Biol.* **240**, 123–142 (2001).
46. Picciotto, M. R., Higley, M. J. & Mineur, Y. S. Acetylcholine as a neuromodulator: cholinergic signaling shapes nervous system function and behavior. *Neuron* **76**, 116–129 (2012).
47. Hong, E. *et al.* Cholinergic left-right asymmetry in the habenulo-interpeduncular pathway. *Proc. Natl. Acad. Sci.* **110**, 21171–21176 (2013).
48. Czarnecki, A. *et al.* Acetylcholine controls GABA-, glutamate-, and glycine-dependent giant depolarizing potentials that govern spontaneous motoneuron activity at the onset of synaptogenesis in the mouse embryonic spinal cord. *J. Neurosci.* **34**, 6389–6404 (2014).
49. Nouaille, S. *et al.* The stability of an mRNA is influenced by its concentration: a potential physical mechanism to regulate gene expression. *Nucleic Acids Res.* **45**, 11711–11724 (2017).
50. Burow, D. A. *et al.* Dynamic regulation of mRNA decay during neural development. *Neural Dev.* **10**, 11 (2015).
51. Plazas, P. V., Nicol, X. & Spitzer, N. C. Activity-dependent competition regulates motor neuron axon pathfinding via PlexinA3. *Proc. Natl. Acad. Sci.* **110**, 1524–1529 (2013).

52. Warp, E. *et al.* Emergence of patterned activity in the developing zebrafish spinal cord. *Curr. Biol.* **22**, 93–102 (2012).
53. Saint-Amant, L. & Drapeau, P. Motoneuron activity patterns related to the earliest behavior of the zebrafish embryo. *J. Neurosci.* **20**, 3964–3972 (2000).

54. Saint-Amant, L. & Drapeau, P. Synchronization of an embryonic network of identified spinal interneurons solely by electrical coupling. *Neuron* **31**, 1035–1046 (2001).
55. Kani, S. *et al.* Proneural gene-linked neurogenesis in zebrafish cerebellum. *Dev. Biol.* **343**, 1–17 (2010).
56. Thisse, B. & Thisse, C. In situ hybridization on whole-mount zebrafish embryos and young larvae. *Methods Mol. Biol.* **1211**, 53–67 (2014).
57. Davidson, L. A. & Keller, R. E. Neural tube closure in Xenopus laevis involves medial migration, directed protrusive activity, cell intercalation and convergent extension. *Development* **126**, 4547–4556 (1999).

58. Fierro, J., Haynes, D. R. & Washbourne, P. 4.1Ba is necessary for glutamatergic synapse formation in the sensorimotor circuit of developing zebrafish. *PLoS ONE* **13**, e0205255 (2018).
59. Westerfield, M. *The zebrafish book: a guide for the laboratory use of zebrafish (Brachydanio rerio)* (University of Oregon, 1995).

Acknowledgements

We would like to thank Edson Rodrigues for help with experiments and Jean-Pierre Coutanceau for aid in zebrafish husbandry. We would like to thank Alex Bois, Stéphane Tronche, and Abdelkarim Mannioui from the aquatic animal facility in the Institut de Biologie Paris-Seine (IBPS; Sorbonne University, Paris, France) for fish care and France Lam, Jean-François Gilles and Susanne Bolte from the IBPS imaging facility for their assistance in confocal microscopy. This study was supported by the ATIP-Avenir young investigator grant (to E.H), Fondation pour la Recherche Médicale grant (to J.M.M, P.L and E.H) and the PhD fellowship from the Alexis and Anne Marie Habib Foundation and the Institut de Reeducation Audio Phonetique (to M.A.Y).

Author contributions

M.R., P.L., J.M.M. and E.H. designed research; M.R., Y.L., M.A.Y., E.B. and E.H. performed experiments; M.R.,

M.A.Y. and E.H. analyzed data; M.R. and E.H. wrote the manuscript with input from all authors.

Competing interests

The authors declare no competing interests.

Additional information

Supplementary information is available for this paper at https://doi.org/10.1038/s41598-020-72524-3.

Correspondence and requests for materials should be addressed to E.H.

Reprints and permissions information is available at www.nature.com/reprints.

Publisher's note Springer Nature remains neutral with regard to jurisdictional claims in published maps and institutional affiliations.

Supplementary Figures

Dynamic regulation of the cholinergic system in the spinal central nervous system

Mohamad Rima[1,2], Yara Lattouf[1,3], Maroun Abi Younes[1,3], Erika Bullier[1], Pascal Legendre[1], Jean-Marie Mangin[1], Elim Hong[1*]

[1] Sorbonne Université, INSERM, CNRS, Neurosciences Paris Seine - Institut de Biologie Paris Seine (NPS - IBPS), 75005 Paris, France

[2] current address : Institut de Génétique et de Biologie Moléculaire et Cellulaire (IGBMC), INSERM,CNRS, Université de Strasbourg, 67400 Illkirch, France

[3] equal contribution

[*] Corresponding author

Correspondence to elim.hong@inserm.fr

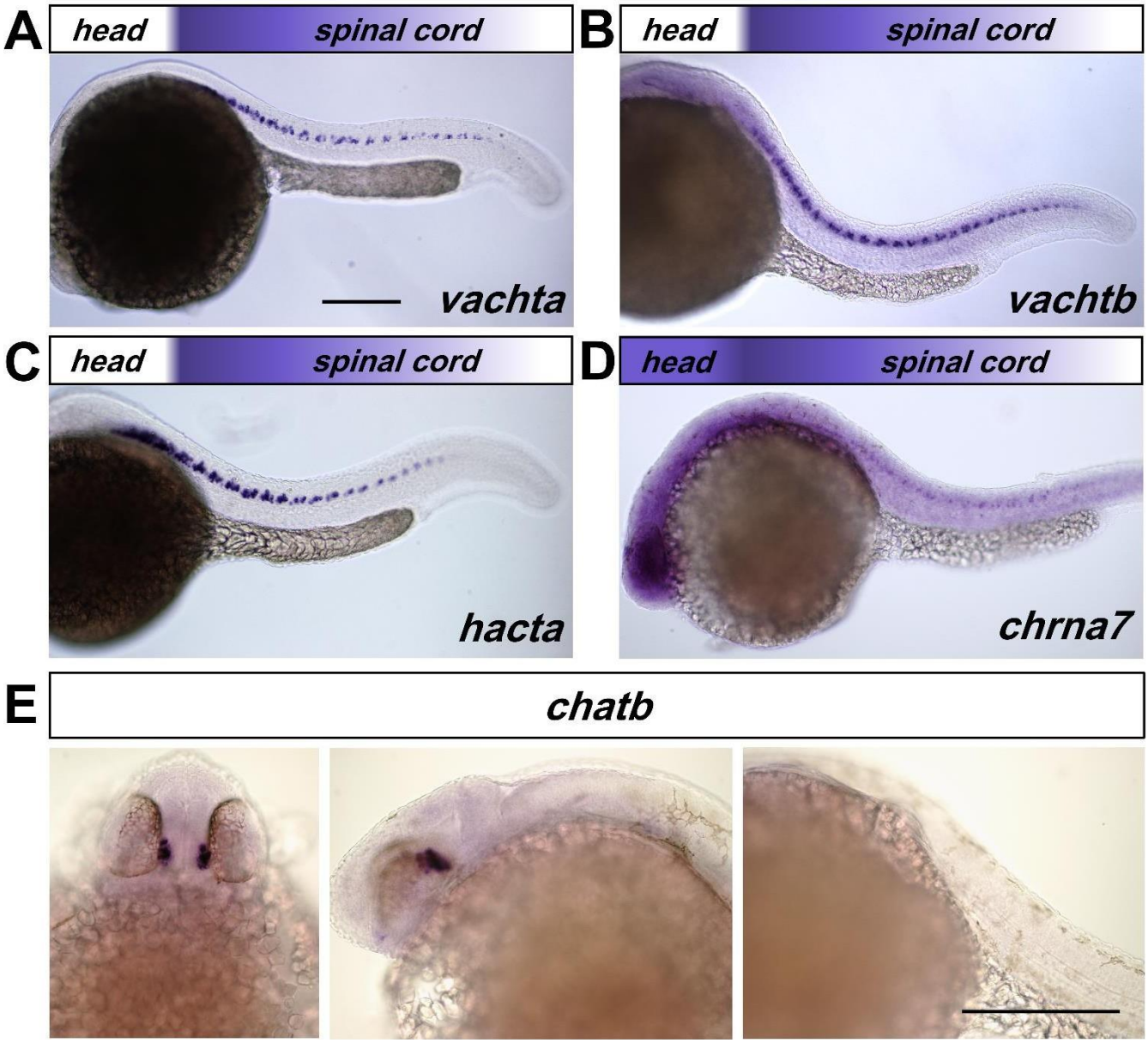

Supplementary Figure 1. Expression pattern of cholinergic markers in the 22-24 hpf embryonic spinal cord.**(A-D)** Lateral view of 22-24 hpf zebrafish embryos processed by *in situ* hybridization showing presynaptic cholinergic transcripts *vachta* (A), *vachtb* (B), and *hacta* (C) in spinal neurons. nAChRs subunit transcript for*chrna7* (D) is expressed in spinal neurons and ubiquitously in the brain. The rostro-caudal expression pattern of the transcript is represented by the colored gradient bar on top of each image. Magnification is the same forall images in (A-D). Scale bar: 200 μm. **(E)** Dorsal (left panel) and lateral (middle, and right panels) view of 22-24 hpf zebrafish embryos processed by *in situ* hybridization showing presynaptic cholinergic transcript *chatb* in the putative oculomotor neurons, but not in the spinal cord. Magnification is the same for all imagesin (E). Scale bar: 200 μm.

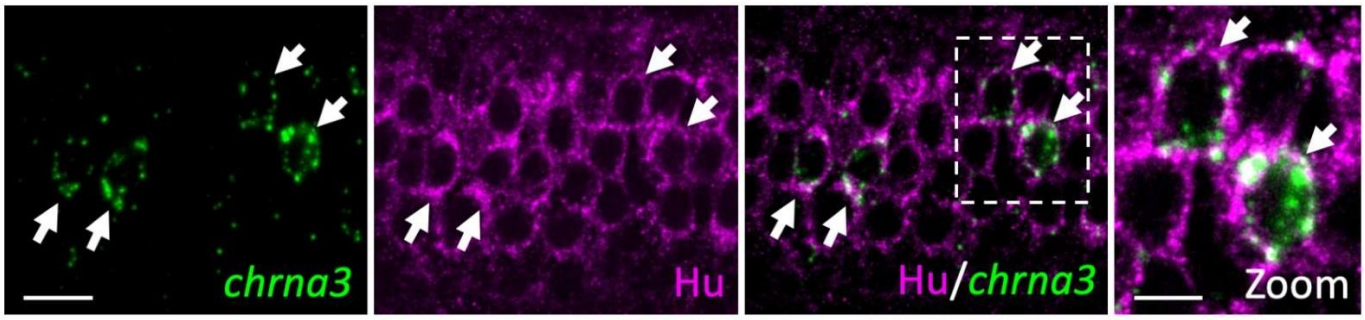

Supplementary Figure 2. Nicotinic acetylcholine receptor subunit *chrna3* is expressed in interneurons. Lateral view of a 24 hpf zebrafish embryo processed by fluorescent *in situ* hybridization for *chrna3* (green) followed by anti-Hu labeling (magenta) shows co-localization of the two signals (white arrows) in 100% of the *chrna3*$^{+}$ cells. Far right panel (Zoom) shows a close-up image of the white boxed region in the third panel.N = 9 embryos (197 *chrna3*$^{+}$ cells). Scale bar: 10 μm. Scale bar (Zoom): 5 μm.

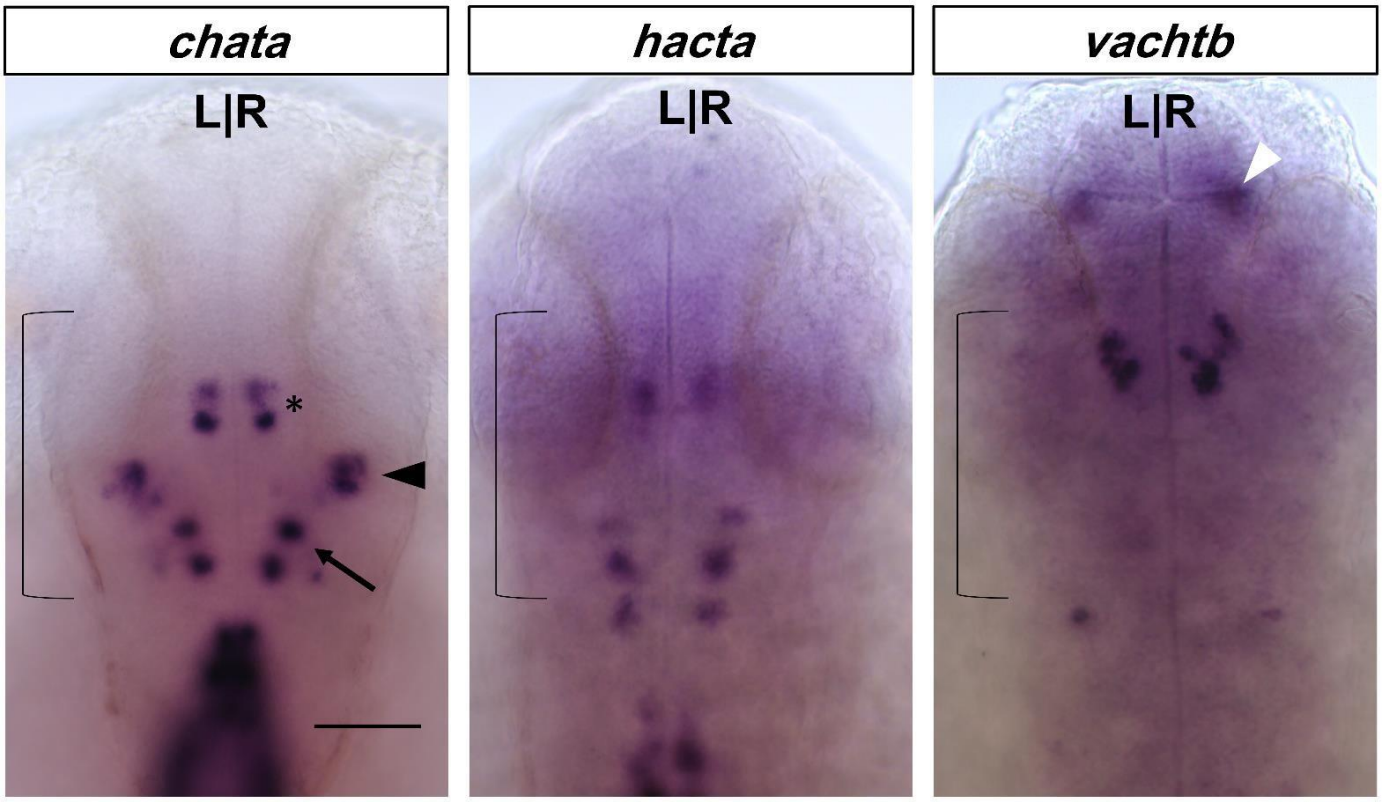

Supplementary Figure 3. Cholinergic gene expression in the brain. Dorsal view of 2-day-old embryos processed by *in situ* hybridization showing *chata*, *hacta* and *vachtb* transcripts bilaterally in the midbrain (brackets). *chata* is expressed in the oculomotor (asterisk), secondary gustatory (arrowhead) and trigeminal motor (arrow) nuclei. *vachtb* is detected symmetrically in the habenula (white arrowhead) at this stage. **L**: left;**R:** right. Scale bar: 200 μm.

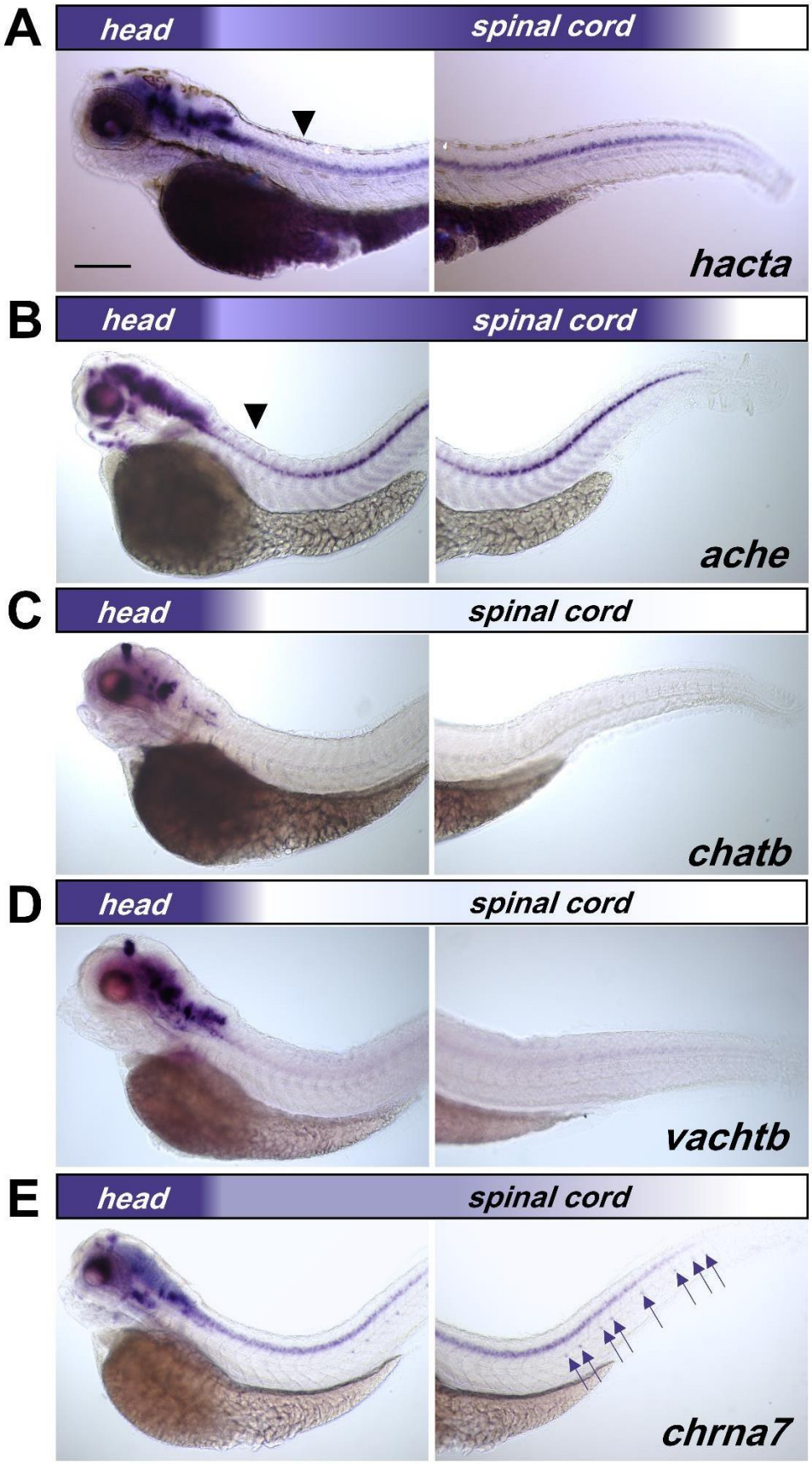
A
head
spinal cord
hacta
B
head
spinal cord
ache
C
head
spinal cord
chatb
D
head
spinal cord
vachtb
E
head
spinal cord
chrna7

Supplementary Figure 4. Downregulation of presynaptic cholinergic gene expression in the spinal cord of 3-day-old embryos. **(A-E)** Lateral view of embryos processed by *in situ* hybridization showing rostro-caudalgradient for *hacta* (A), and *ache* (B). These transcripts remain highly expressed in the brain. *chatb* (C) and *vachtb* (D) are only expressed in the brain. Transcript for the nAChRs subunit *chrna7* (E) remain expressed all along the spinal cord and is also found in the brain and neuromasts (arrows). The rostro-caudal expressionpattern of the transcript is represented by the colored gradient bar on top of each image. Magnification is the same for all images in (A-E). Scale bar: 200 μm.

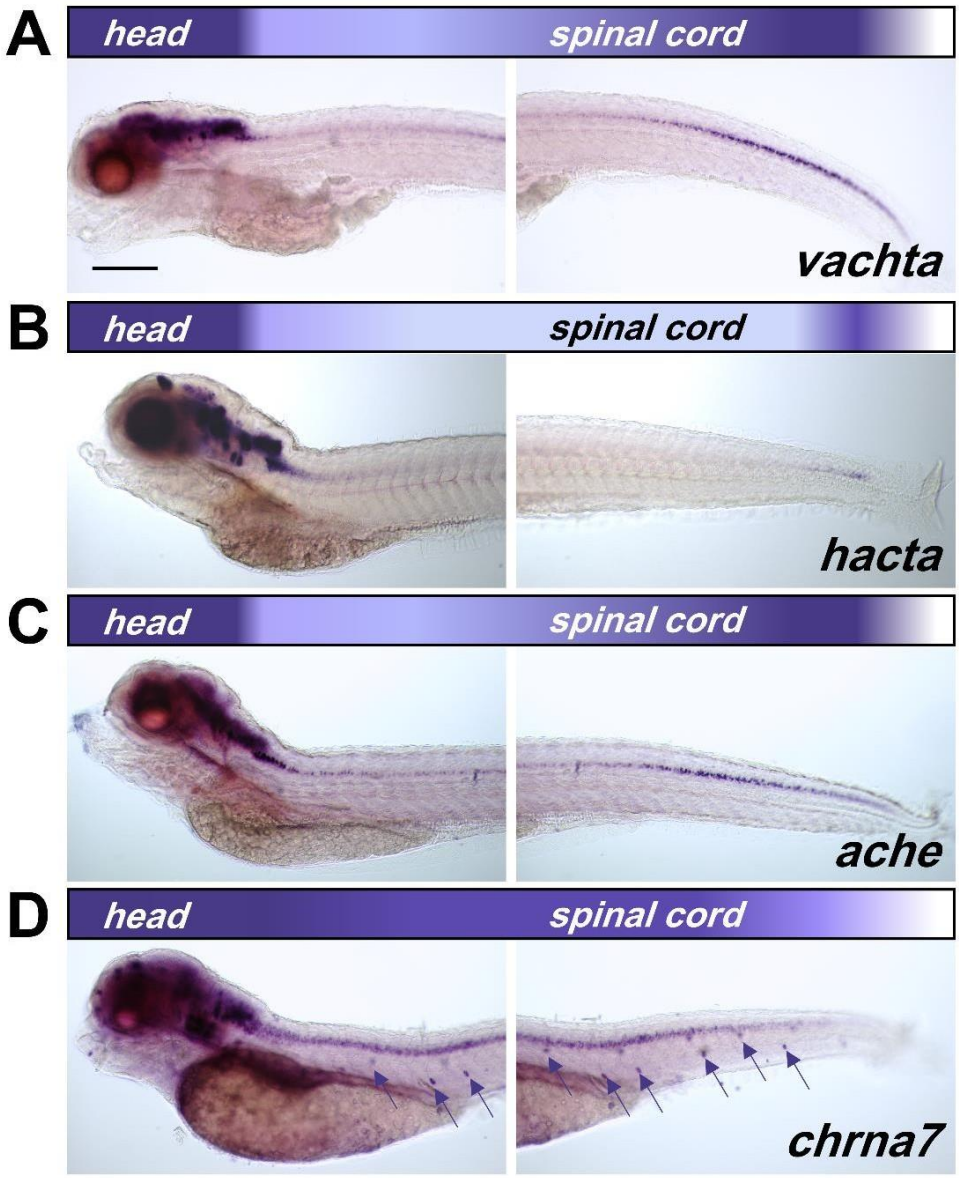

Supplementary Figure 5. Progressive downregulation of presynaptic cholinergic gene expression in 6-day- old larvae. **(A-D)** Lateral view of zebrafish larvae processed by *in situ* hybridization showing the rostro-caudalexpression gradient of cholinergic transcripts *vachta* (A), *hacta* (B), and *ache* (C). Note the strong expressionof the transcripts in the brain. nAChRs subunit transcript for *chrna7* (D) is also found in the brain, in neuromasts (arrows) and remain uniformly expressed all along the spinal cord. The rostro-caudal expression pattern of the transcript is represented by the colored gradient bar on top of each image. Magnification is the same for all images in (A-D). Scale bar: 200 μm.

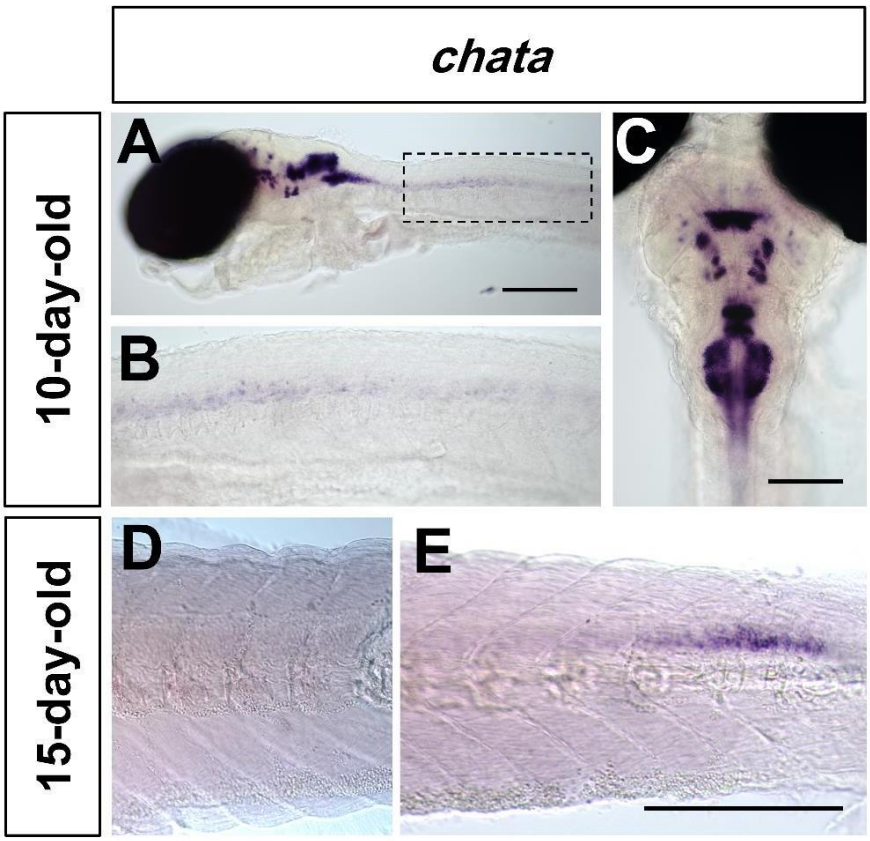

Supplementary Figure 6. Low levels of *chata* expression in the spinal cord persists in 15-day-old larvae. **(A,B)** Lateral and **(C)** dorsal view of a 10-day-old larva processed by *in situ* hybridization showing the decreasein *chata* expression at the rostral spinal cord (A, B), while the transcript remains highly expressed in the brain(C). Panel (B) shows a close-up image of the boxed region in panel (A). Scale bar: 200 μm. **(D)** Lateral viewof the rostral spinal cord and **(E)** the tip of the tail of 15-day-old larva processed by *in situ* hybridization showing very faint *chata* expression at the rostral spinal cord, while it remains present at the tip of the tail. Magnification is the same for images in (D, E). Scale bar: 200 μm.

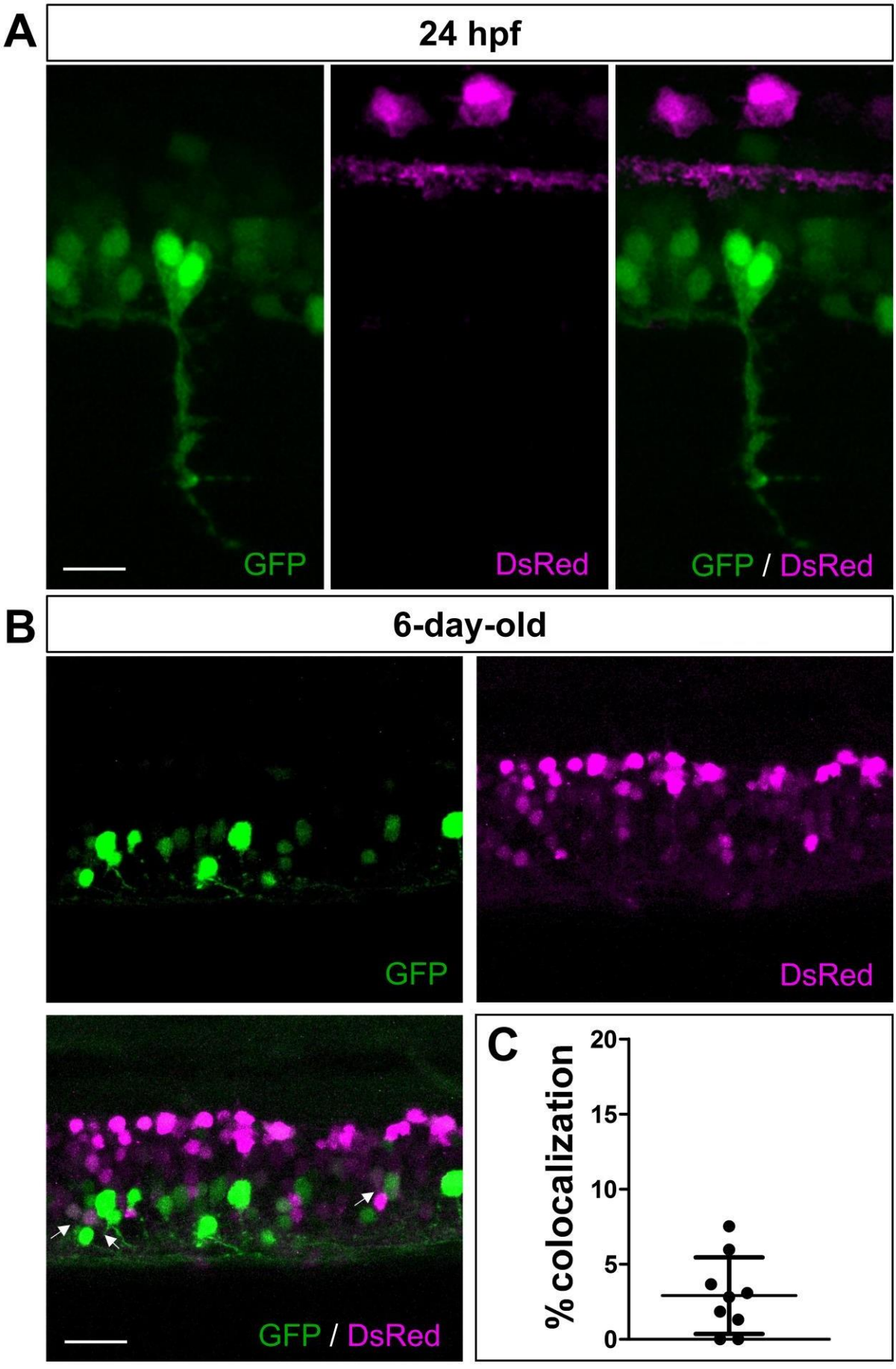
A
24 hpf
GFP
DsRed
GFP / DsRed
B
6-day-old
GFP
DsRed
GFP / DsRed
C
% colocalization
20
15
10
5
0

Supplementary Figure 7. Most *mnx1:*GFP neurons are not glutamatergic in the 6-day-old larvae. **(A-B)** Confocal images of the spinal cord in *Tg(mnx1:GFP;vglut2:DsRed)* line showing no or very few cells co- expressing *mnx1:*GFP (green) and *vglut2:*DsRed (magenta) in 24 hpf embryo (A) or 6-day-old larva (B), respectively. Scale bar: 15 µm in (A) and 20 µm in (B). **(C)** Percentage of *mnx1:*GFP*;vglut2:*DsRed cells in 6-day-old larvae. N=5 larvae (487 *mnx1:*GFP^{+}neurons, 590 *vglut2:*DsRed^{+} neurons).

Chapter 3:

Acetylcholine promotes rhythmic motor activity in the zebrafish embryo

Acetylcholine promotes rhythmic motor activity in the zebrafish embryo

Maroun Abi Younes[1], Mohamad Rima[1], Ninon Peysson[1], Jean-Pierre Coutanceau[1], Erika Bullier[1], Jean-Marie Mangin[1] and Elim Hong[1,2]

[1]INSERM, CNRS, Neurosciences Paris Seine - Institut de Biologie Paris Seine (NPS - IBPS), Sorbonne Université, 75005, Paris, France

[2] corresponding author: elim.hong@inserm.fr

Abstract

Cholinergic signaling plays a critical role in numerous biological processes throughout development. In rodent and chick, cholinergic signaling is crucial for the initiation and maintenance of spontaneous neural activity, the coordinated activation of large groups of neurons during embryogenesis. Maternal smoking causes nicotine to enter the fetal circulation and interact with nicotinic acetylcholine receptors (nAChR), leading to disturbances in cholinergic signaling that can negatively impact the development and function of the nervous system. While studies have shown the adverse effects of nicotine in the peripheral nervous system and muscles, how it affects the spinal central nervous system development is less understood.

By carrying out calcium imaging on large groups of neurons in the spinal cord of 1 day old zebrafish embryos, we discovered that neurons display different patterns of neural activity, consisting of high or low frequency activity. Using a transgenic line that labels motoneurons revealed that groups of neurons displaying high or low frequency activity contain both moto- and interneurons. In addition, we found that neurons that display low frequency activity contain earlier born primary motoneurons, whereas those with high frequency activity contain later born secondary motoneurons. These results suggest that neurons that are born together form microcircuits that first display high frequency activity, which transitions to low frequency activity. To investigate the role of cholinergic signaling during spontaneous neural activity, we performed calcium imaging in the mutant for *cholineacetyltransferse a* (*chata*), which encodes an enzyme

for acetylcholine synthesis. We found that the emergence of correlated activity is altered in mutants. The highly rhythmic events observed in WT siblings are not present in the *chata* mutants as they display higher interval variability between the calcium transients. Application of nicotine increased the frequency, suggesting that the high frequency activity is mediated by nicotinic acetylcholine receptors. The results attribute a yet undescribed role for cholinergic signaling through the nicotinic acetylcholine receptors in modulating highly rhythmic activity during early spontaneous neural activity. Taken together, we show that both genetic and environmental factors that modify cholinergic signaling alter early spontaneous neural activity, suggesting that the cholinergic system plays a critical role in the formation and recruitment of neural circuits in the developing zebrafish spinal cord.

Introduction

Common to all vertebrates is the ability to move and navigate through the environment to seek shelter, forage for food, and find mates. Understanding the complex interplay between neural circuits and motor behavior has long been a focus of interest in the field of neuroscience. Spontaneous movements of the trunk of the body have been observed in developing embryos and fetuses across different species (Preyer, 1885; Hamburger, 1963) and studies in embryonic chick spinal cords showed that this activity is non-reflexogenic as it occurs independently of external stimuli (Hamburger, Wenger and Oppenheim, 1966). Over the years, pharmacological, genetic, and optogenetic approaches combined with electrophysiological recordings and calcium imaging revealed the occurrence of spontaneous neural activity (SNA) across a multitude of species in different developing circuits, including the retina, cochlea and the spinal cord (Feller, 1999; Blankenship and Feller, 2010; Kirkby *et al.*, 2013). SNA plays a role in the maturation of neural circuits (Kirkby *et al.*, 2013) as perturbing SNA during critical developmental periods in the spinal cord and other developing systems resulted in aberrant effects on axonal projection (Hanson and Landmesser, 2006; Kastanenka and Landmesser, 2010; Tezuka *et al.*, 2022), neurotransmitter specification (Gu and Spitzer, 1995; Watt *et al.*, 2000; Borodinsky *et al.*, 2004), cellular differentiation (Stevens *et al.*, 2002) and cell death (Warm *et al.*, 2022).

In the developing spinal cords of chick and mouse embryos, SNA is initiated when motoneurons start extending their axons toward the muscles (O'Donovan and Landmesser, 1987; Hanson and Landmesser, 2003). SNA consists of patterned recurring activity that progresses from synchronized activity in the whole spinal cord to alternating between the left and right sides (O'Donovan and Landmesser, 1987; Momose-Sato and Sato, 2013). SNA is initially dependent on cholinergic signaling as blocking nicotinic acetylcholine receptors using pharmacological agents including nicotine results in silencing SNA (Milner and Landmesser, 1999; Momose-Sato and Sato, 2020). However, knockdown of the *cholineacetyltransferase (chat*) gene, which encodes an enzyme necessary for the synthesis of acetylcholine, delayed and altered the patterned activity of SNA in mice (Myers, 2005), suggesting the presence of redundant mechanisms in maintaining SNA.

In the zebrafish spinal cord, SNA is first observed at 17 hours post fertilization (hpf), and is primarily dependent on gap junctions and calcium ion conductance (Saint-Amant and Drapeau, 2001). Calcium imaging shows that the activity begins around 17 hpf in groups of neighboring cells, which become ipsilaterally correlated and contralaterally anti-correlated within a few hours (Warp *et al.*, 2012; Wan *et al.*, 2019). The frequency of left right alternating SNA decreases during the first day of development to eventually become silent (Saint-Amant, 2010). Due to the rapid development of the zebrafish embryo, several rounds of neurogenesis occur within the first day. However, whether and how different groups of sequentially born neurons incorporate into the spinal circuit have not been investigated. Moreover, in contrast to mammals, pharmacological application of antagonists for nicotinic acetylcholine receptors (nAChRs) showed no effect on SNA in the zebrafish embryo (Saint-Amant and Drapeau, 2001; Warp *et al.*, 2012). Given the conservation of the locomotor spinal circuit in vertebrates (Goulding, 2009), as well as the presence of pre- and postsynaptic cholinergic components in the zebrafish spinal cord as early as 20 hpf (Rima *et al.*, 2020), we aimed to reassess the role of cholinergic signaling during SNA in the zebrafish embryo.

We performed calcium imaging recordings of neurons in the spinal cord of zebrafish embryos co-expressing GCaMP in most post-mitotic spinal neurons and red fluorescent protein (RFP) in motoneurons *Tg(elavl3:GCaMP6f ; mnx1:Gal4;UAS:RFP)*. Calcium recordings of rostral spinal segments reveal that

spontaneous neural activity consists of rhythmic calcium peaks occurring around every 4 seconds (high frequency), which then transitions to long lasting bursts of activity separated by long quiescent periods lasting around 30 seconds (low frequency). The transition from early to late type activity is accompanied by the emergence of another microcircuit consisting of newly born motoneurons and interneurons displaying high frequency activity. Chronic perturbation of cholinergic signaling in the *cholineacetyltransferase* (*chat*) mutants resulted in increased variability between calcium events during high frequency activity, suggesting cholinergic signaling is necessary in maintaining stable rhythmic early spontaneous activity. Nicotine perfusion increased activity frequency, suggesting that cholinergic signaling via the nicotinic acetylcholine receptors is crucial in promoting high frequency activity during early SNA. Taken together, our results demonstrate that cholinergic signaling plays a yet undescribed role in maintaining rhythmic activity during early spontaneous neural activity in the zebrafish embryo. This study shows that acetylcholine plays an essential role in shaping neural circuit dynamics during spontaneous neural activity, highlighting a conserved role of cholinergic signaling in the embryonic vertebrate motor circuit and firmly establishes the zebrafish embryo as an in vivo model for elucidating the role of cholinergic signaling in spinal neural circuit formation.

Materials and Methods

Zebrafish

Adult fish were reared at 28°C in a 14/10h light/dark cycle in a fish facility approved by the French Service for animal protection and health (A-75-05-25), and the experiments were performed in compliance with relevant regulations and guidelines. Fish were paired overnight using separators and dividers in mating tanks, and the eggs were collected the following morning after removing the separators. Wild-type AB strain, the *cholineacetyltransferase* (*chat*) mutant fish (Granato *et al.*, 1996), *Tg(mnx1:GFP)* (Flanagan-Steet *et al.*, 2005), *Tg(NeuroD:GCaMP6f^{icm05})* (Rupprecht et al., 2016), *Tg(elavl3:H2B-GCaMP6f)* (Chen et al., 2013), *Tg(elavl3:GCaMP6s^{CY14})* *Tg(elavl3:GCaMP6s^{CY44})* (Vladimirov et al., 2014), *Tg(elavl3:jRGECO1b) (Mu et al., 2019), Tg(elavl3:GCaMP6f)^{a12200}* (Wolf *et al.*, 2017), *Tg(mnx1:Gal4)* (Flanagan-Steet *et al.*, 2005), *Tg(UAS :RFP)* (Asakawa and Kawakami, 2009) were used in this study.

Fluorescent in situ hybridization with antibody labeling

Fluorescent in situ hybridization (FISH) was performed on 24 hpf embryos as described in Rima et al., 2020. Not1 and Sp6 were used to linearize and synthesize the UTP-digoxigenin labelled *chrna7* probe, respectively. Briefly, dehydrated embryos in methanol were rehydrated by successive washes of decreasing ratio of methanol:PBS solutions. They were then permeabilized and incubated in 50% formamide containing hybridization mixture for three hours before an overnight incubation with UTP-digoxigenin labelled probes. Probes were then detected using horseradish peroxidase conjugated anti-Digoxigenin antibody (Roche) in Maleic acid blocking buffer (150 mM Maleic acid, pH 7.5 & 100 mM NaCl). Signal amplification was performed using homemade tyramide-FITC as described in Davidson & Keller, 1999. Embryos were incubated with tyramide-FITC (1:250) in TSA reaction buffer (100 mM borate pH 8.5, 0.1% tween-20, 2% dextran sulfate, 0.003% H2O2, and 200 µg/ml 4-iodophenol) for 45 min in dark. The reaction was stopped by washing in 0.1% Tween-20 in PBS (PBT). Embryos were incubated overnight at 4 °C in PBS, 0.1% Triton, 10% sheep serum with rabbit anti-GFP antibody (Thermofisher) to detect GFP. Embryos were washed in PBT and incubated at 4 °C overnight with goat anti-rabbit Alexa594 antibody (Thermofisher). Finally, embryos were washed and mounted laterally in a drop of low melt agarose (2%) and imaged using the Leica SP5 confocal microscope using a 20X water immersion objective.

Genotyping

DNA was extracted from tail biopsies (adults) or whole embryos using DNA extraction buffer (10mM Tris pH 8.2, 10 mM EDTA, 200mM NaCl, 0.5% SDS, 200µg/ml proteinase K). PCR amplification of the *chat* gene was carried out using primers from (Wang, Wen and Brehm, 2008) and the mutation was confirmed by sequencing.

Pharmacology

Nicotine (Acros Organics) was prepared at a concentration of 10uM in E3 the day of the experiment. For the first 15 minutes of acquisition, E3 was pumped into the petri dish using a perfusion peristaltic pump (Ismatec) at a rate of 1.47 mL/min. 15 minutes into the acquisition, nicotine was perfused into the petri dish for the next 15 minutes.

The tubes of the peristaltic pump were thoroughly cleaned with E3 between each acquisition.

Calcium imaging

Embryos were individually transferred to a 70mm petri dish and mounted using a drop of low melt agarose (2% in E3) with pancuronium bromide (300µM). Calcium imaging recordings were carried out on a spinning disk microscope (Zeiss Axio Examiner.Z1) using a 40X water immersion objective (NA = 0.95) acquired at a rate of 3.3 Hz [*Tg(elavl3:GCaMP*)] or 10Hz [*Tg(elavl3:GCaMP;mnx1:gal4;UAS:RFP*)] using the 480 nm laser. The 532 nm laser was used for the z-stack acquisition of mnx1:RFP^{+} cells. The duration of acquisition ranged from 12 – 30 min depending on the experiment.

Calcium imaging analysis

FIJI

Regions of interests (ROIs) were manually drawn on the soma of neurons exhibiting GCaMP fluorescent transients and the average fluorescence intensity was extracted for all recorded frames using FIJI (Schindelin *et al.*, 2012). Further analysis was done on MATLAB (The MathWorks, Inc. 2022).

MATLAB

The values for the average fluorescence intensity for each ROI per frame were imported into MATLAB using custom written scripts. Z-score was used to analyze calcium activity according to the formula:

$$\frac{\Delta F}{F} = \frac{F_i - F_m}{F_{std}}$$

F_i is the mean intensity in a single ROI at a single time point while F_m is the moving mean in a single ROI for 500 frames and F_{std} is the standard deviation for the entire recording. Clustering of neurons was performed using *k-means* function and manually verified based on pairwise linear correlation coefficients. Each calcium event was identified using *findpeaks* (Signal Processing Toolbox, MATLAB) function in MATLAB and verified manually. All plots and graphs were made on MATLAB.

Alternation index was calculated as:

$$\frac{event_{sp} + event_{ps}}{event_T - 1}$$

where $event_{sp}$ is the total number of time when calcium transient in the ipsilateral soma is followed by an event in the puncta, $event_{ps}$ is the total number of time when calcium transient in the puncta is followed by an event in the ipsilateral soma and $event_T$ is the sum of events in the ipsilateral soma and puncta.

Symmetry index was calculated as:

$$\frac{|event_s - event_p|}{event_s + event_p}$$

where $event_s$is the total number of events in the ipsilateral soma, $event_p$ being the total number of events in the puncta displaying contralateral activity.

Muscle contraction imaging and analysis

Microscope and mounting setup were identical to calcium imaging (10Hz) with the exception of using bright field to image muscle contractions in non-paralyzed embryos mounted in low melt agarose (2% in E3). Prior to imaging muscle contractions, z-stack acquisition of mnx1:RFP$^+$ cells was performed using the 532 nm laser. The recordings were analysing using FIJI where a ROI was drawn in an area that displayed a distinct morphology (i.e. muscle segment, edge of embryo, etc.) and manually verified for a change in pixel intensity upon movement.

Heartbeat and length acquisition and analysis

Embryos were phenotyped into moving (WT sibling) and non-moving (mutant) and laterally mounted and embedded in 1.5% low melt agarose. 1 min recordings were taken using a color camera (Leica IC80 HD) mounted on a stereomicroscope (Leica M80). Heartbeat was manually counted for the duration of the recording. The outline of the embryo from the nose tip to the tail tip were traced using FIJI to calculate the length of the embryos.

Statistics

Statistical comparisons between two independent groups were conducted using a Wilcoxon rank sum test. Comparison between more than 2 dependent groups were

conducted by a Kruskal-Wallis test followed by a Bonferroni test. Statistical tests were performed on MATLAB. Specific information on statistical test, sample size, value representation (mean ± std) and p values are indicated in the figure legends.

Results

Spinal neurons display distinct patterns of spontaneous activity

To analyze spontaneous neural activity (SNA), we first carried out calcium imaging on embryos expressing GCaMP under different pan-neuronal promoters. While all 6 transgenic lines displayed calcium transients at 5 days, only one line [*Tg(elavl3:GCaMP6f ^{12200a})*] (Wolf *et al.*, 2017) showed activity at 1 day (Supplemental Table 1). This result was surprising as at least two other transgenic lines were shown to display calcium activity in 1 day old embryos in a previous study (Wan et al., 2019). These results suggest that the signal-to-noise ratio of GCaMP activity differ between individuals but becomes more robust during development.

We carried out calcium imaging of 2-3 segments of the rostral spinal cord (above the beginning of the thin yolk sac) in 1 day old laterally mounted *Tg(elavl3:GCaMP6f ^{12200a})* embryos expressing the GCaMP transgene in most spinal neurons, including the motoneurons (Figure 1A). We found that around 35 (34.5 ± 8.9%) percent of imaged neurons showed at least one calcium transient during the 10 min recording (Figure 1B). We also found that the ventral spinal cord, consisting of motoneurons and interneurons, contained more active neurons compared with the dorsal domain, which largely contains sensory neurons easily identifiable due to their rounder soma (Williams and Ribera, 2020) expressing higher baseline GCaMP fluorescence (Figure 1A), consistent with what has been reported in other studies (Saint-Amant and Drapeau, 2001). In contrast to previous studies showing that all active spinal neurons display synchronized activity (Saint-Amant and Drapeau, 2001; Warp *et al.*, 2012), we observed groups of neurons exhibiting distinct patterns of activity. We carried out *k-means* clustering analysis and determined that $k = 3$ was sufficient to group neurons into highly correlated clusters with each cluster containing at least 10 % of active neurons (Figure 1C-E). The calcium transients consisted of at least two distinct profiles: 1. Calcium event consisting of fluorescence increase followed by a decay to the baseline (peak) and 2. Fluorescence increase immediately followed by a series of

events resulting in a sequence of peaks (burst) before decreasing to baseline levels

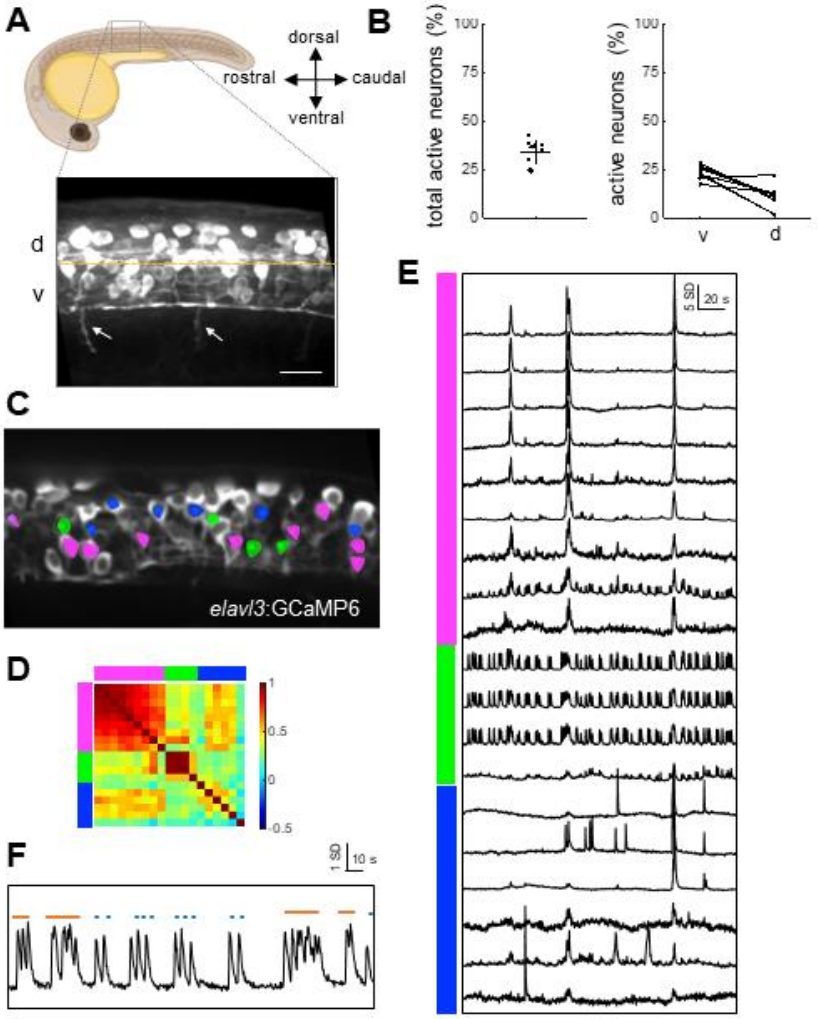

Figure 1. ***1 day old embryos display distinct patterns of spontaneous activity***

(A) Schematic of a lateral view of a 1 day old embryo indicating the calcium imaging area (dotted box). Close up z composite image of the recorded area along the spinal cord in a *Tg(elavl3:GCaMP6*) embryo. Orange horizontal line demarcates dorsal (d) vs. ventral (v) regions quantified in (B). Note the motoneuron axons exiting the spinal cord (arrows). Double arrowheads indicate rostral, caudal, dorsal, ventral axis of the embryo. Scale bar = 20 μm.

(B) Graphs showing the percentage of total *elavl3:GCaMP*$^{+}$ cells displaying calcium events (active neurons) 34.2 ± 6.37% (left) and those located in the dorsal (23.6 ± 3.4%) vs. ventral (10.6 ± 6.1%) spinal cord domains (right). mean ± SD. N = 9 embryos, n_T = 419 total neurons, n_A = 144 active neurons.

(C-E) *k*-means clustering (*k* = 3) reveals neuron groups tat display distinct patterns of calcium activity in a representative 1 day old *Tg(elavl3:GCaMP6*) embryo. 8 min recording. 3Hz.

(C) Spinning disk image of the imaged region showing the location of the different neuron groups overlaid by colored circles. (D) Correlation coefficient matrix of active neurons indicating the degree of correlation between neurons within each group and with other groups. (E) Z-score plot of the 3 groups of neurons revealed by *k*-means clustering. Neurons in different clusters are indicated by the color coded bar on left.

(F) Plot of one representative neuron from the green cluster displaying calcium peaks (blue circle) or bursts (orange line).

with low correlated activity within the cluster as well as with the first two groups (Figure 1D). In general, we found that while neurons in the third group were located mostly in the dorsal area, neurons in the first and second groups were intermingled in the ventral spinal cord (Figure 1C). As motoneurons are largely restricted to the most ventral spinal cord, the result suggests that neurons in the first and second clusters are composed of both interneuron and motoneurons.

Microcircuits with high and low frequency activity are co-active during spontaneous activity

To confirm whether the first two clusters consist of motoneuron and interneurons, we imaged spontaneous activity in embryos that co-express red fluorescent protein (RFP) mainly in motoneurons (Flanagan-Steet *et al.*, 2005; Asakawa and Kawakami, 2009) [*Tg(elavl3:GCaMPf;mnx1:gal4;UAS:RFP*)]. The three primary motoneurons that are the first born neurons in each hemisegment of the spinal cord are the CaP, MiP and RoP MNs that target the ventral, dorsal and medial muscle fibres, respectively (Figure 2A) (Myers, 1985; Moreno and Ribera, 2009). Zebrafish embryos undergo rapid development, with approximately 2 somites added to their trunk every hour during somitogenesis (D'Costa and Shepherd, 2009). To tightly control the developmental stage of the embryos, we used the number of RFP^+ cells per hemisegment to compare calcium transients between embryos. Consistent with our previous observation (Figure 1), we found that spinal neurons could be grouped into 3 different clusters based on their activity pattern in embryos with 4-5 motoneurons per hemisegment (Figure 2B-E). The first two clusters showed high levels of correlated activity within each cluster as well as between the clusters (Figure 2E). First group of neurons displayed low frequency (LF) activity consisting mainly of bursts whereas the second group of neurons showed high frequency (HF) activity consisting of peaks and bursts (Figure 2C-C"). The two neuronal clusters contained both RFP^+ and RFP^-negative neurons (Figure 2B-C"), suggesting the presence of distinct motor microcircuits containing motoneurons and interneurons that display LF or HF activity. The third cluster of neurons showed low correlation with the first two clusters and did not contain any RFP^+ cells (Figure 2B,E), suggesting that these are interneurons that are not yet recruited into the LF or HF circuits.

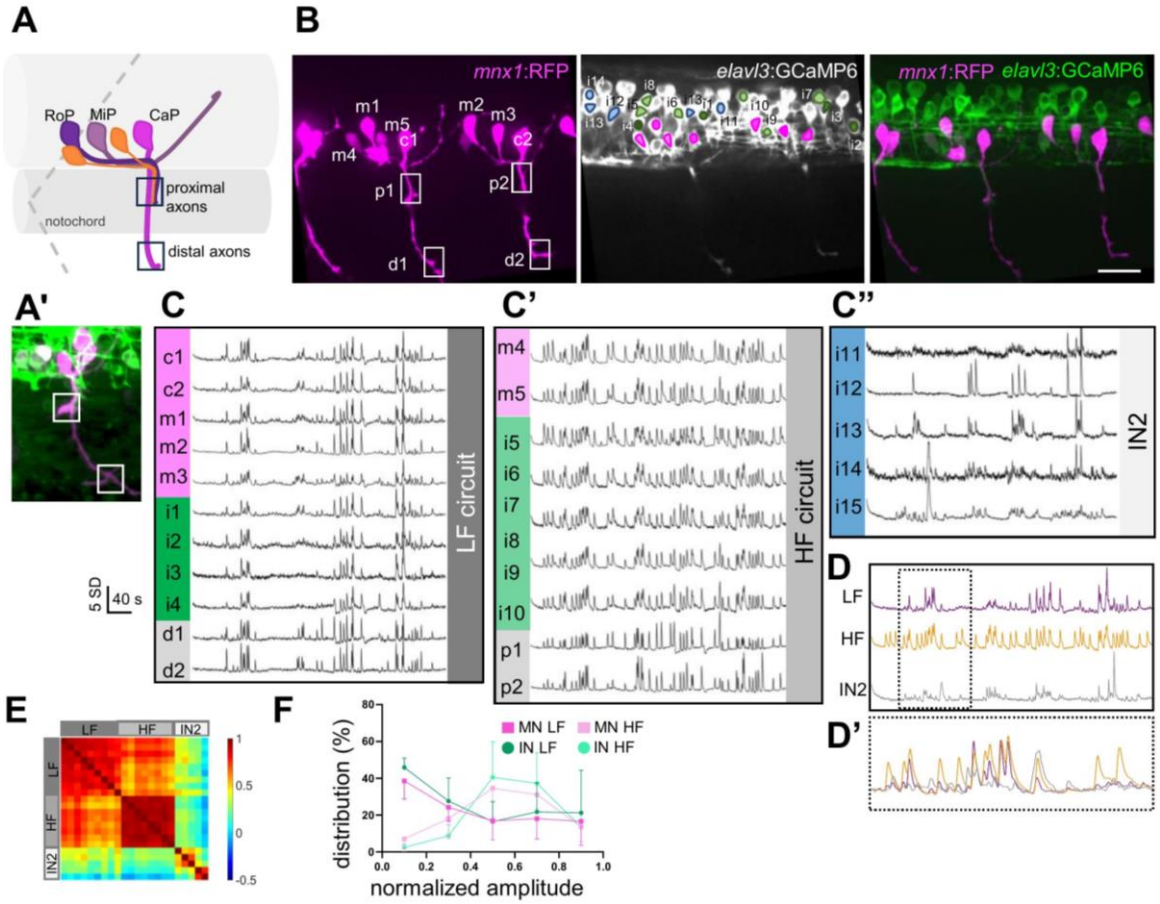

Figure 2. ***Functionally distinct microcircuits are present during spontaneous activity***

(A,A') Schematic of primary (CaP, MiP, RoP) and secondary (orange) motoneurons and their axon projections displaying stereotypical organization within the hemisegment (A). Note that the proximal axons represent those from both the primary and secondary motoneuron, whereas, the distal axons represent mainly the CaP axon in <36 hour old embryos based off of confocal image in (A') with proximal and distal axons in white squares.

(B) Composite image of 7.5 um in the z axis of the recorded area in the spinal cord of a *Tg(elavl3:GCaMP6 ; mnx1:RFP)* embryo showing *mnx1:RFP*$^{+}$ (left panel, magenta), *elavl3:GCaMP6*$^{+}$ (middle panel, white) and *elavl3:GCaMP6 ; mnx1:RFP*$^{+}$ (right panel) neurons. Neuron type are color-coded (motoneurons: magenta, interneurons: green, blue) and identifiers noted (m: motoneuron, c: CaP, i: interneuron, p: proximal axons, d: distal axons). Scale bar = 20 μm.

(C-C") Activity plot of a 5-minute calcium imaging recording. Neurons types are color-coded (motoneurons: magenta, interneurons: green, blue, axons: grey) and identifiers noted to the left of the panel (m: motoneuron, c: CaP, i: interneuron, p: proximal axons, d: distal axons). Neurons belonging to distinct circuits are color-coded in different shades of grey to the right of the panel (HF: high frequency circuit, LF: low frequency circuit).

(D,D') Average plots of neurons in LF (purple), HF (orange) circuits and IN2 type (grey) (D), and close up overlay of the average plots in dotted rectangle (D').

(E) Pairwise correlation coefficient matrix between neurons. Neurons in functional circuits are indicated by grey bars left and above the matrix.

(F) Histogram showing the distribution of normalized amplitudes from MNs and INs in the HF and LF circuits. n=10 embryos, n = 1101 events.

One possibility for the presence of microcircuits is that they consist of neurons that are born and recruited at different times. We consistently found that the first-born primary CaP motoneurons, easily identified based on the location of the soma directly over the axon bundle exiting the spinal cord, displayed LF activity. By contrast, motoneurons with smaller soma and fainter RFP expression showed HF activity (Figure 2A-C'). We next analyzed calcium transients in the proximal and distal areas of the motoneuron axon bundles. The distal part of the motoneuron axon fascicles contains mainly CaP axons whereas the proximal motoneuron axon fascicles contains both MiP and RoP axons as well as later born secondary motoneuron axons that exit the spinal cord to target the ventral muscles (Figure 2A,A'). If the LF circuit consists of earlier born neurons while the HF circuit contains later born neurons, we expected to observe LF activity in the distal axons and HF activity in the proximal axons. Indeed, we found that the distal area showed LF activity while the proximal area displayed HF activity (Figure 2B-C'). Taken together, these results suggest that the LF and HF circuits consist of earlier born (older) and later born (younger) MNs, respectively.

Overlaying the average traces between the LF and HF circuits revealed that when neurons displaying LF activity have calcium events, those in the HF circuit are also active. However, calcium events that occur in neurons with HF activity are not always observed in neurons with LF activity (Figure 2D, D'). We next analyzed the amplitude of calcium events and found that the HF circuit consisted of events that were more uniform between each other, whereas neuron activity in the LF circuit showed events with variable amplitudes (Figure 2F).

Early spontaneous activity consists of synchronized high-frequency activity

If in embryos with 4-5 motoneurons per hemisegment contains a LF circuit composed of early-born older neurons and a HF circuit composed of late-born younger neurons, we expected that younger embryos with 3 or less motoneurons would only have one circuit exhibiting HF activity. We analyzed the frequency and pattern of calcium activity in embryos with 1 motoneuron per segment consisting only of the primary CaP neuron. We found that the motoneurons displayed only one type of HF calcium activity: highly rhythmic HF peaks (Figure 3A-D). We found two types activity in interneurons (IN); one that synchronized (IN1) and another that had low correlation (IN2) with motoneuron activity (Figure 3A-D). These results show that neurons that are recently born exhibit HF rhythmic activity. In addition, we analyzed the activity type in the CaP

primary motoneurons in younger (1-3 motoneurons) or older (4-7 motoneurons) embryos. We found that CaP neurons exhibit HF activity in the younger embryos, whereas in older embryos, they largely showed LF activity (Figure 3E), supporting our hypothesis that the HF and LF circuits are composed of younger and older neurons, respectively. One surprising noteworthy observation was the presence of puncta and/or axons that displayed alternating activity with the neurons in the HF circuit (F-F"). We suspected that the alternating activity in these puncta and/or axons was due to the activation of the contralateral motor circuit.

Spontaneous calcium activity corresponds to trunk contractions

The earliest spontaneous movement occurring around 17 hpf in the zebrafish embryo is left-right coiling, whereby muscle contractions alternate with a regular delay between the left and right sides at around 0.5 Hz frequency (Saint-Amant and Drapeau, 1998). This movement transitions to a double coiling behavior at approximately 21 hpf and occurs at 0.75 Hz frequency, which is characterized by the occurrence of multiple consecutive coils on one side of the body, followed by a series of coiling movements to the other side. (Saint-Amant and Drapeau, 1998). To test whether the alternating activity in the puncta may be due to the contralateral activation of the motor circuit due to left-right coiling of the embryo, we first analyzed muscle contractions in non-paralysed agarose-restrained embryos expressing RFP in MNs. In embryos with 1-2 motoneurons per segment, we identified two types of alternating contractions around every 2 sec, likely corresponding to the ipsilateral vs. contralateral muscle contractions that occur during left-right coiling (Figure 5A-B). Next, to confirm that the calcium events in motoneurons correlate with muscle contractions, we carried out simultaneous calcium imaging of motoneuron calcium events with muscle contractions (Figure 5C-D). We found that calcium events in motoneurons co-occurred with around half of the muscle contractions. This result suggests that the motoneuron activity

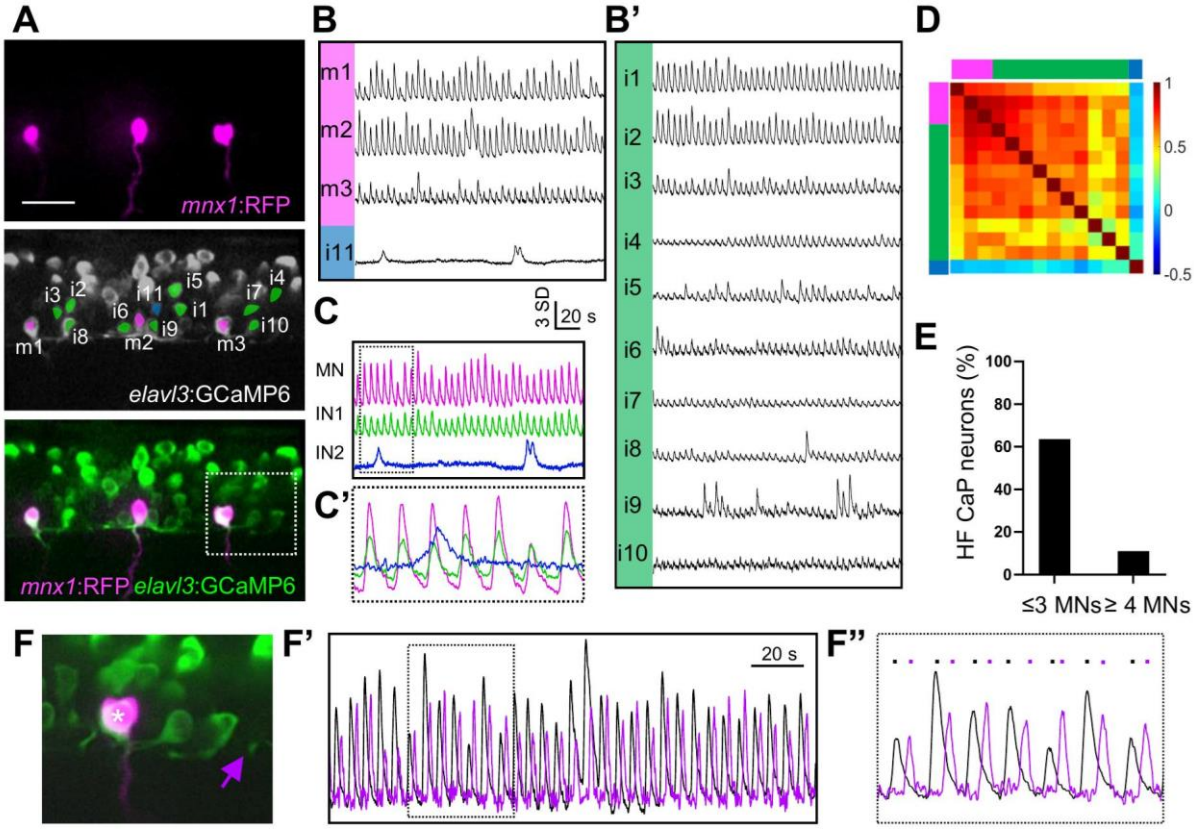

Figure 3. ***Early-stage embryos exhibit fast rhythmic activity***

(A) Composite image of 7.5 um in the z axis of the recorded area in the spinal cord of a representative *Tg(elavl3:GCaMP6 ; mnx1:RFP)* embryo showing *mnx1:RFP*$^{+}$ (magenta, top panel), *elavl3:GCaMP6*$^{+}$ (white, middle panel) and *elavl3:GCaMP6 ; mnx1:RFP* $^{+}$ (bottom panel) neurons. Active neuron soma of motoneurons (MNs, magenta), interneuron type 1 (IN1, green), interneuron type 2 (IN2, blue) and their identifiers are indicated (middle panel). Scale bar = 20 μm.

(B,B') Z-score plot of a 3.5 minute calcium activity recording. Neurons are ordered by type: MNs (magenta), interneurons that display correlated activity with motoneurons (IN1, green) and interneuron with no correlation to motoneuron activity (IN2); blue). Neuron type (colored bars on left) and identifiers are indicated.

(C,C') Average (D) and close up overlay (D', dotted rectangle) activity plots of MNs (magenta), IN1 (green) and IN2 (blue).

(D) Correlation coefficient matrix of active neurons. MNs (magenta), IN1 (green), and IN2 (blue) are are indicated by colored bars on top and left of the matrix.

(E) Bar graph displaying the percentage of primary CaP neurons displaying HF activity in early vs late embryos. (N=17 embryos, n= 28 CaP neurons).

(F-F") (F) Close up image of MN soma (asterisk) and puncta (purple arrow) outlined in (A) that display alternating calcium activity. MN soma (black plot) and puncta (purple plot) (F'). (F") Close up of activity plot in the dotted rectangle in (F'). Colored circles above the activity plot indicate soma (black) or puncta (purple) activity.

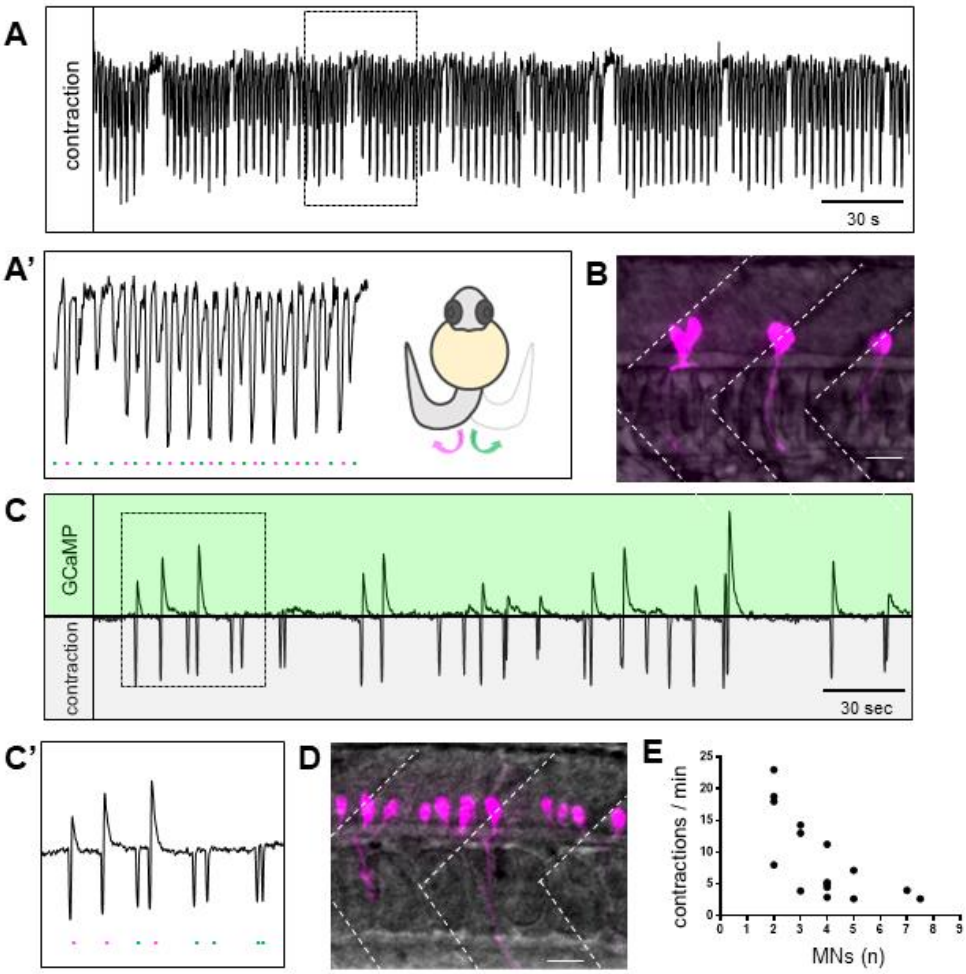

Figure 4. ***Muscle contractions correlate with motoneuron calcium activity and frequency***

(A) Muscle contractions during a 5-minute recording of an early-stage embryo.
(A') Zoomed in muscle activity plot from time shown in (A, rectangle). Putative ipsilateral (magenta) and contralateral (green) contractions are indicated by colored circles. Cartoon of zebrafish embryo from a frontal view showing left-right coiling corresponding to ipsilateral (magenta) or contralateral (green) contractions.

(B) Lateral view showing motoneurons (magenta) and muscle (grey) in an early stage *Tg(mnx1:RFP)* embryo containing 2 MNs per hemisegment. White dotted lines delineate the somite boundaries.

(C) Ipsilateral motoneuron activity (top, green) and muscle contraction (bottom, grey) during a 5-minute recording of a late-stage embryo. Scale bar = 20 μm.

(C') Zoomed in muscle activity plot from time shown in (D, rectangle). Ipsilateral (magenta) and contralateral (green) contractions are indicated by colored circles.

(D) Lateral view showing motoneurons (magenta) and muscle (grey) in late-stage embryo containing 5 MNs per hemisegment. White dotted lines delineate the somite boundaries. Scale bar = 20 μm.

(E) Scatter plot showing negative correlation between developmental stage (identified by number of *mnx1*$^{+}$ cells per hemisegment) and frequency of muscle contraction. n=15 embryos.

induces ipsilateral muscle contractions whereas the muscle contractions that occur without calcium events are due to the activation of contralateral motoneurons. Altogether, the results demonstrate that the calcium activity in the motor circuit translates to muscle contractions and suggest that the alternating calcium activity observed in the puncta is due to the activation of the contralateral motor circuit. Finally, we analyzed the frequency of muscle contractions with the number of motoneurons and found a negative correlation (Figure 5E), consistent with that observed during calcium activity.

In summary, we propose a model for the evolution of spontaneous activity in the motor circuit. During the first wave of neurogenesis (1-3 motoneurons per hemisegment), primary motoneurons and INs display near-synchronous oscillating activity consisting of calcium peaks that occur at regular intervals and amplitudes. As the embryo develops following the second wave of neurogenesis (≥4 MNs per hemisegment), the older microcircuit transitions to exhibit LF activity while the newly born microcircuit displays HF activity (Figure 5).

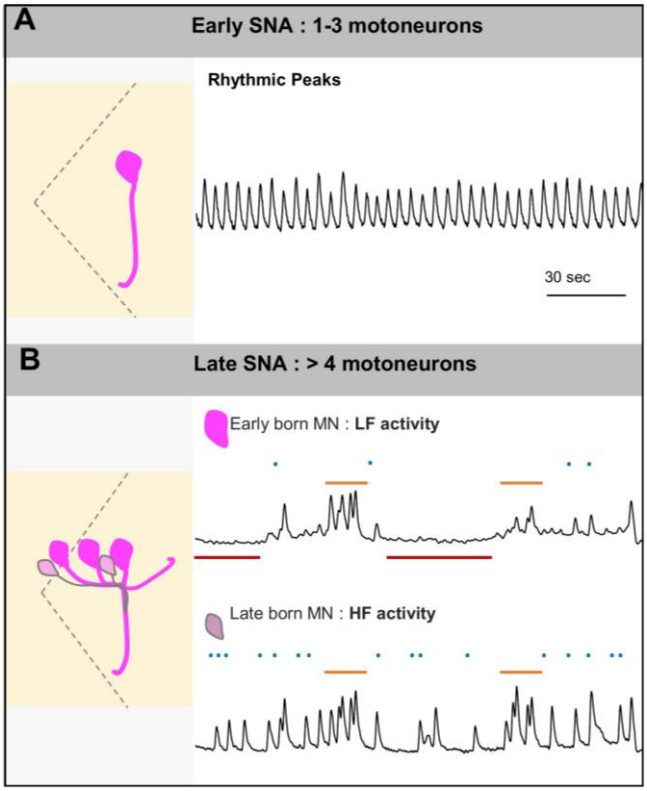

Figure 5. ***Schematic model for the evolution of spontaneous neural activity (SNA) in zebrafish spinal neurons.***

(A) Early SNA occurs in embryos containing 1-3 motoneurons per hemisegment, consisting of cells displaying high frequency rhythmic peaks that correlate with left-right muscle contractions. (B) Late SNA occurs in embryos containing over 4 motoneurons per hemisegment, which consists of early born (mature) neurons that display low-frequency (LF) activity characterized by calcium bursts (orange line) separated by long quiescent periods (red line) and late-born (young) neurons displaying high-frequency (HF) activity containing bursts (orange line) nested within peaks (blue dots).

Cholinergic signaling is required for symmetric rhythmic activity at the onset of spontaneous neural activity

To investigate whether cholinergic signaling plays a role during spontaneous neural activity, we performed calcium imaging in mutants for *cholineacetyltransferase a* (*chat*) (Wang, Wen and Brehm, 2008) expressing GCaMP in most neurons and RFP in most motoneurons [*Tg(elavl3:GCaMP6f;mnx1:gal4;UAS:RFP*); *chat*$^{-/-}$]. First, we confirmed that there was no overt difference in the development of the embryos by measuring the length and heartbeat frequency between the mutant and WT siblings. Next, we quantified the percentage of active cells and found no significant difference between mutant and WT siblings (29.2±16.7% vs. 34.5 ± 7.9 %) (Supplemental Figure 1A-C). We analyzed the calcium activity pattern and also found similar percentage of active motoneurons, IN1 and IN2 in the *chat* mutants to that in the WT embryos (Supplemental Figure 1E). We found that with the exception of one embryo, the early (1-3 motoneurons) *chat* mutant embryos mostly showed one type of HF activity, as in WT siblings. In later developmental stages (over 4 motoneurons), embryos contained distinct microcircuits showing HF and LF activity, similar to that in WT embryos (Supplemental Figure 1F).

However, a careful inspection of the calcium events revealed that the rhythmic oscillatory activity appeared less regular in *chat* mutants compared to WT embryos (Figure 6A-A'). Indeed, analysis of the interval time between consecutive calcium events revealed that the duration between the events was more widespread in the *chat* mutants compared to the WT embryos (Figure 6A-B). We wondered whether the longer interval time between events was due to absence of general activity or rather because the contralateral side was active. We calculated the alternation index by analyzing the number of alternations between the ipsilateral soma activity and contralateral puncta activity (Figure 6C-D). If there is perfect alternation between the ipsi- and contralateral sides, the alternation index would be 1. In WT embryos, we were able to fit a linear regression model between the alternation index and number of motoneurons. Alternatively, we found that the *chat* mutants had a lower alternation index compared with WT of a similar developmental stage that could not be fit via linear regression, suggesting that *chat* mutants exhibit less consistent left right alternating activity. Although the left right alternation may be defective in the *chat* mutants, the total number of events in the left vs. right sides could still remain the

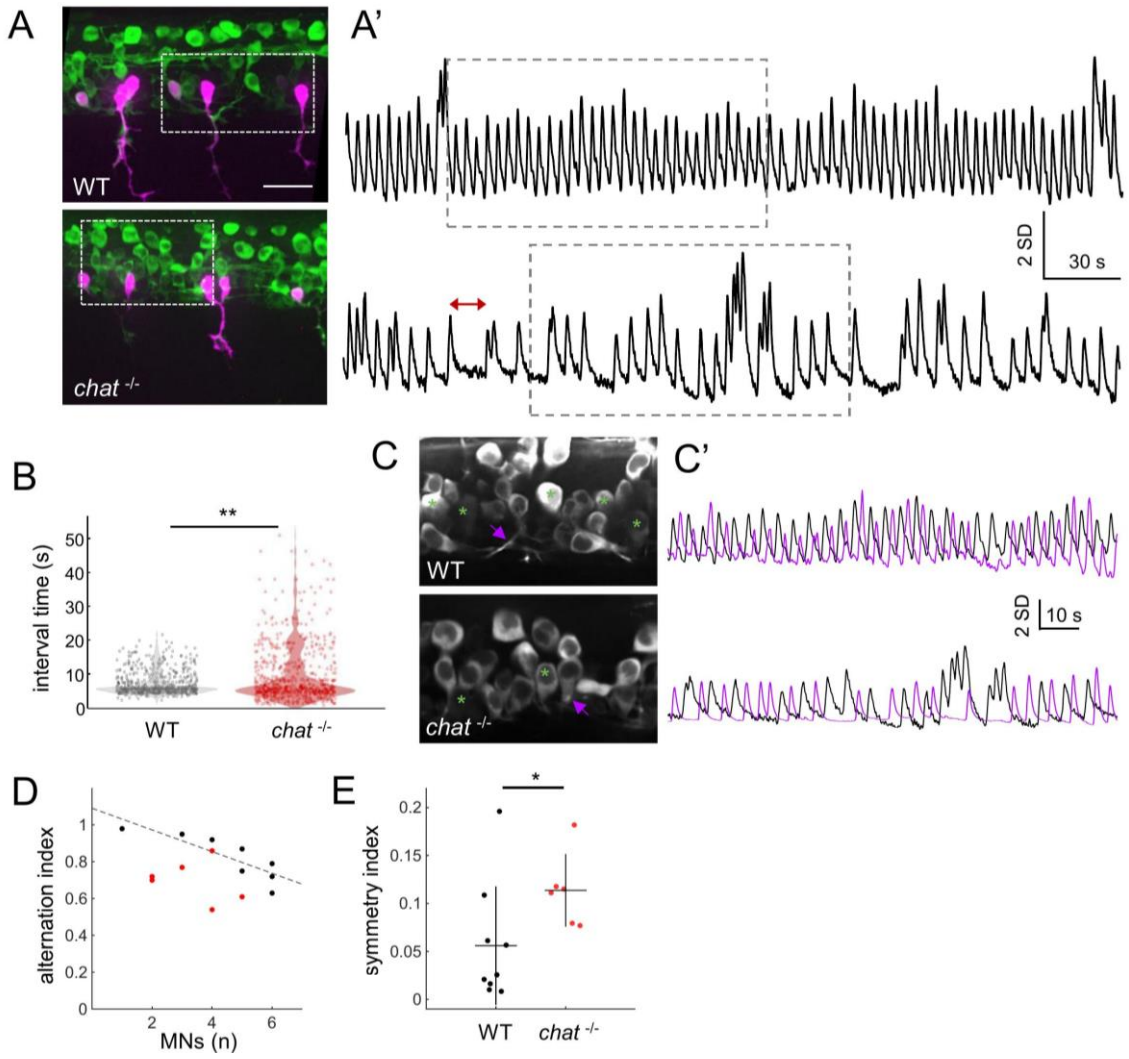

Figure 6. ***Cholinergic signaling is required for maintaining early rhythmic spontaneous activity.***

(A,A') Images of recorded spinal area showing MNs (magenta) (A) with plots of representative neurons in WT (top) or *chat*$^{-/-}$ (bottom) embryos (A').

(B) Scatter plots showing the interval time between two consecutive peaks (red double arrow in A') WT (black) or *chat*$^{-/-}$ (red) embryos. WT : n = 4 embryos, n = 720 events; *chat*$^{-/-}$: 6 embryos, n = 720 events. Wilcoxon rank-sum test ** p = 1.3e-5.

(C,C') Image showing neuron soma (asterisks) and puncta (purple arrow) outlined in white dotted rectangles in (A, A') that display alternating activity (C'). Close up of calcium activity in soma (black) and puncta (purple) in WT (top) and *chat*$^{-/-}$ (bottom) embryos outlined by grey dashed rectangle in A'.

(D) Linear regression of alternation index between developing WT (black) and *chat*$^{-/-}$ (red).

(E) Symmetry index show *chat*$^{-/-}$ embryos display less left right symmetry in calcium events compared with WT siblings. Each circle represents the symmetry index for an embryo, triangles show mean value. WT vs. *chat*$^{-/-}$: 0.056 ± 0.062 vs. 0.114 ± 0.038 (mean ± std). WT: n = 8 embryos, n = 555 events, *chat*$^{-/-}$: n = 6 embryos, n = 566 events. Wilcoxon rank-sum test. * p = 0.0256

same. We analyzed the symmetry index where if there are the same number of events between the left and right sides, the value would be 0. We found that the *chat* mutants have a higher value for their symmetry index compared with their WT siblings, suggesting that the left and right sides are less symmetrically active in the mutants compared to their WT siblings. These results indicate that cholinergic signaling is necessary for modulating rhythmic high frequency activity as well as left right symmetric activity in the zebrafish embryo.

Nicotinic receptors modulate high frequency activity

If cholinergic signaling does play a role in modulating rhythmic high frequency, we hypothesized that application of an agonist would increase spontaneous activity. As nicotinic acetylcholine receptor (nAChR) subunits α2 and α3 are expressed in the INs and α7 in motoneurons at 20 hpf (Rima *et al.*, 2020), we sought to determine whether activation of these receptors via nicotine could increase the frequency of spontaneous activity. We carried out calcium imaging while perfusing the embryo with nicotine or control medium. In embryos with more than 4 motoneurons containing the HF and LF microcircuits, spinal neurons did not show any changes in their activity patterns during the first 5 min following nicotine perfusion. However, between 5-10 min in nicotine, the frequency of calcium events increased by around 1.3-fold in both HF and LF microcircuits. After 10- 15min in nicotine, some embryos showed a further increase in their frequency whereas others became inhibited (Figure 7A-B'). These results show that nicotine activates nAChRs in embryos that display HF and LF circuit activity to increase their frequency.

Discussion

Emergence of distinct functional microcircuits in the developing embryo

By carrying out calcium imaging in a large group of spinal neurons with labelled motoneurons, we found the presence of functional micro motor circuits with distinct patterns of activity that have low-frequency (LF) or high-frequency (HF) activity. While all events that occur in the HF circuit are not observed in the LF circuit, all activity in the LF is correlated with that in the HF circuit. In other words, the LF activity is nested within the HF activity. There are several rounds of neurogenesis in motoneurons resulting in primary vs. secondary motoneurons (Lewis and Eisen, 2003) and the spontaneous activity frequency has been shown to decrease during development

(Momose-Sato and Sato, 2013). Based on the morphology and topography of motoneuron soma and axons, we found that the older motoneurons display LF activity whereas the younger motoneurons show HF activity (Figure 2). Calcium imaging in younger embryos revealed the presence of only one type of HF oscillatory activity, containing strikingly rhythmic activity (Figure 3). Taken together, our model for the emergence of spontaneous neural activity depicts that upon primary neurogenesis, a group of primary INs and motoneurons establish a microcircuit consisting of rhythmic HF activity driven by gap junctions coupled to a ‘pacemaker cell’. Later, the decrease

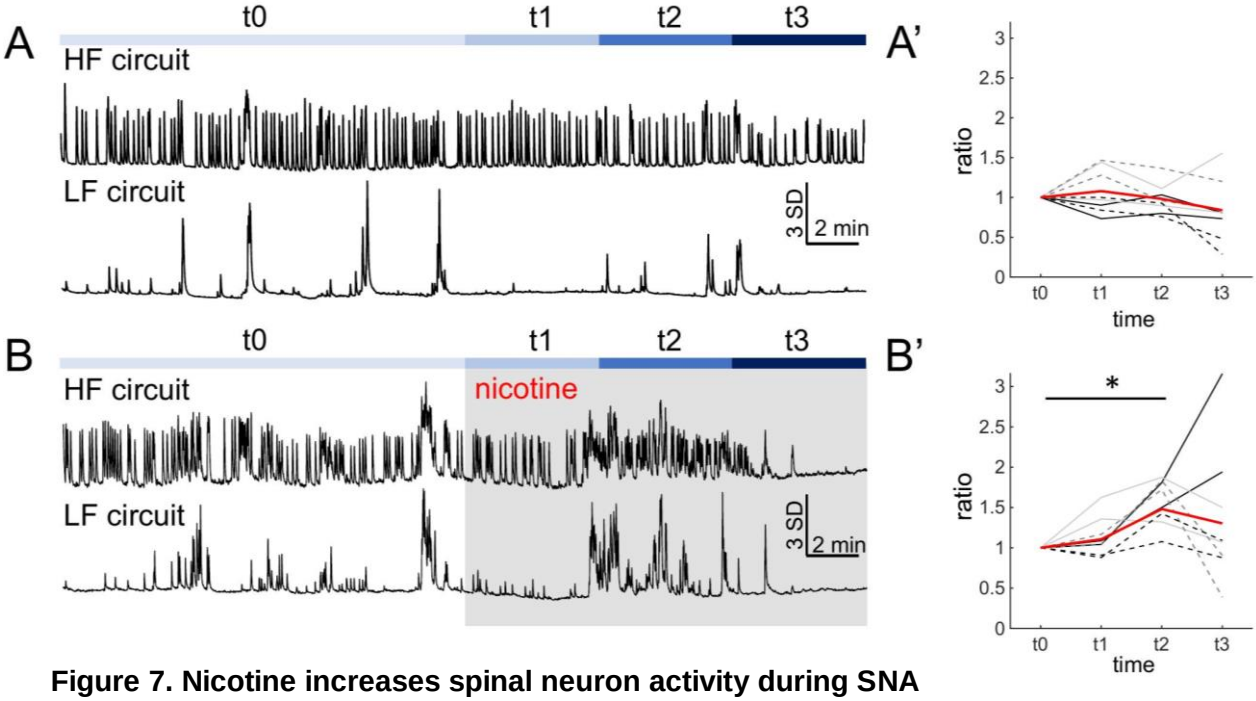

Figure 7. Nicotine increases spinal neuron activity during SNA

(A, B) Activity plots of representative neurons in the high frequency (HF) and low frequency (LF) circuits during baseline (t0), 0-5 min (t1), 5-10 min (t2), and 10-15 min (t3) after the start of perfusing control E3 medium (A) or nicotine (B). (A’, B’) Graph showing the number of calcium events normalized by the number of events during t0 for the four sections (t0, t1, t2, t3, t4). Each color and line type represent events in HF and LF circuits in the same embryo. Mean values are plotted in red. (B’) t2/t0 = 1.48 ± 0.32 (mean ± std). n = 4 (control), n = 5 (nicotine), HF and LF circuits analyzed for each embryo. Kruskal-Wallis followed by Bonferroni test * p = 0.0055.

in gap junctions between earlier born neurons and accordingly, the influence of the ‘pacemaker cell’ between these neurons leads to decreased activity in them, resulting in the LF circuit. Meanwhile, upon secondary neurogenesis, a group of secondary INs and motoneurons form another distinct microcircuit with HF activity. The HF microcircuit activity does not appear to be as regular as in the younger embryos that contain only one rhythmic HF activity. This may be due to the

competing influence of gap junctions and chemical synapses that are rapidly modified during development (Knogler *et al.*, 2014).

Fast and slow swimming behavior have been shown to be mediated by a dorsal-ventral topological map of neurons that correspond to birth date order (McLean et al., 2007). One intriguing future study would be to test whether the different microcircuits are maintained throughout development to contribute to the distinct fast and slow swimming movements.

Validating ipsilateral calcium activity with left-right muscle contractions

We performed high resolution calcium imaging on laterally mounted embryos, which allowed us to simultaneously record the activity in ipsilateral spinal neurons and ipsilateral motoneuron axons. Surprisingly, we also observed the presence of puncta and axons that display anti-correlated activity to the ipsilateral neurons, suggesting that these signals correspond to the activation of contralateral neurons. Analysis of muscle contractions in unparalysed embryos showing two distinct types of alternating muscle contractions strongly supports this notion. The signals pertaining to the contralateral activity enabled the reconstruction of the left-right coiling behavior during SNA in the zebrafish embryo. Combining muscle contractions and calcium imaging data demonstrate that movement can be inferred from calcium imaging.

Role of cholinergic signaling in maintaining rhythmic activity and left right alternation in early spontaneous neural activity

In contrast to rodent and chick, studies using cholinergic antagonists in the zebrafish embryo failed to disturb SNA (Saint-Amant and Drapeau, 2001), suggesting that the neurotransmission mechanisms underlying SNA is different in the zebrafish to other vertebrates. However, due to the many similarities between the vertebrate spinal circuits (Goulding, 2009) including the expression of early cholinergic markers in the zebrafish embryo (Rima et al., 2020), we wanted to re-examine the role of cholinergic signaling in SNA in the zebrafish. For this purpose, using a non-invasive calcium imaging approach, we analyzed neural activity in mutant embryos for the *cholineacetyltransferase a (chat)* gene*,* which encodes an enzyme for acetylcholine synthesis. Due to the lack of the *chata* gene, the embryos are unable to exhibit any motor movements. Through detailed analysis of neural activity, we found that in contrast to the highly uniform activity in the WT embryos, the mutants exhibited a larger

degree of variability in the duration of intervals between events as well as in the sequence of activity between the left and right sides. Interestingly, mouse *chat* mutants also exhibit different frequency in activity as well as defects in left right coordination (Myers et al., 2005), suggesting that contrary to previously thought, the role of cholinergic signaling is highly conserved in the embryonic spinal cord during SNA.

During SNA, most neurons in the spinal cord are still extending their axons and dynamically forming and pruning synapses onto their targets (see Supplemental Figure 2A). The presence of ipsilaterally synchronized activity that is alternating between the left and right sides indicate that both excitatory and inhibitory neurons are functional. However, due to the rostral to caudal development of the spinal cord, different number and types of neurons are present for each repeating circuit modules in the segments. In other words, one segment may contain more excitatory synapses onto one neuron type, while in the other segment, there may be more inhibitory synapses.

How do these differing segments communicate to maintain uniform activity in frequency, interval periods and left-right coordination? Inhibiting cholinergic signaling results in aberrant non-rhythmic activity and asymmetry between the left and right circuit activity. These results suggest that cholinergic signaling is necessary to maintain uniform symmetric activity in frequency and left-right alternation during early SNA. We have previously shown that different nAChR subunits are expressed in INs at this stage of development (Rima et al., 2020). We propose a model where acetylcholine released from motoneurons during SNA activates nAChRs in ascending, descending and commissural INs to strengthen their connection with other neurons, allowing yet weakly connected neurons to exert their full weight in influencing each others' activity. In the absence of acetylcholine, neurons that have more inhibitory inputs would fire less, resulting in longer intervals between events while neurons with more excitatory inputs would exhibit higher frequency in their activity. Overall, we propose that cholinergic signaling plays a role in enhancing the uniformity of events, both at the level of intersignal duration and left right alternation during early SNA.

Where is the source and site of acetylcholine release? To our knowledge, there is no descending cholinergic neurons from the brain at this stage of development (Rima et

al., 2020), which suggests that the only neurons that release acetylcholine are the motoneurons. We propose that the rhythmic activity during early SNA results in the release of acetylcholine from motoneurons that is augmented via the activation of α7 nAChRs first in the primary CaP and later in all motoneurons (Rima et al., 2020; Supplemental Figure 2B). Acetylcholine release could be from two non-mutually exclusive sites: from either the soma of the motoneurons or at the axo-dendritic site between the motoneuron and INs, modulating IN activity via their presynaptic nicotinic acetylcholine receptors (Rima et al., 2020). In the CNS, ACh is released at non-synaptic sites through volumetric release (Picciotto, Higley and Mineur, 2012). Moreover, somatic release of ACh was reported in cultured *Xenopus* motoneurons (Young, 1986; Sun and Poo, 1987; Welle *et al.*, 2018). Future studies using an acetylcholine sensor will help determine the release site for acetylcholine from motoneurons during SNA (Jing *et al.*, 2020).

Modulation of high frequency activity by cholinergic signaling

In our model, the high frequency rhythmic activity occurring during early SNA transitions to LF activity while the newly born neurons display HF activity. However, the HF activity in developed embryos is not as uniform in frequency and left-right alternation as during early SNA. We proposed above that the difference may be due to the change in the chemical composition of the environment due to increased and/or modification of old and/or new genes. Interestingly, the HF microcircuit activity during late SNA in WT embryos resembles the activity profile of the *chat* mutants during early SNA, suggesting that this is due to a decrease in the influence of cholinergic signaling. If so, increasing cholinergic signaling should convert the late HF activity to the early rhythmic HF activity. To test this hypothesis, we perfused nicotine, an agonist/antagonist for the nAChRs. We found a general increase in the frequency of activity, providing support to our hypothesis. Due to the variability in their response, more studies are necessary to fully conclude that enhancing cholinergic signaling can revert the activity to the highly rhythmic HF activity occurring during early SNA.

In conclusion, we found that birth-date formed microcircuits emerge during spontaneous activity: firstly, a group of early-born motoneuron and INs display synchronized rhythmic oscillatory activity that later, transitions into lower frequency activity (LF circuit). Later-born motoneurons and INs form another microcircuit

exhibiting high frequency activity (HF circuit), which co-exist with the early-born LF circuit. We also found that cholinergic signaling plays a crucial role in maintaining fast rhythmic oscillatory activity. Overall, our work illustrates the emergence of birth-date determined functional microcircuits, highlighting the role of cholinergic signaling in the maintenance of rhythmic oscillatory activity in newly born neurons and provides support for a conserved role of cholinergic signaling in vertebrates.

References

Asakawa, K. and Kawakami, K. (2009) 'The Tol2-mediated Gal4-UAS method for gene and enhancer trapping in zebrafish', *Methods (San Diego, Calif.)*, 49(3), pp. 275–281. Available at: https://doi.org/10.1016/j.ymeth.2009.01.004.

Blankenship, A.G. and Feller, M.B. (2010) 'Mechanisms underlying spontaneous patterned activity in developing neural circuits', *Nature Reviews. Neuroscience*, 11(1), pp. 18–29. Available at: https://doi.org/10.1038/nrn2759.

Borodinsky, L.N. *et al.* (2004) 'Activity-dependent homeostatic specification of transmitter expression in embryonic neurons', *Nature*, 429(6991), pp. 523–530. Available at: https://doi.org/10.1038/nature02518.

Davidson, L.A. and Keller, R.E. (1999) 'Neural tube closure in Xenopus laevis involves medial migration, directed protrusive activity, cell intercalation and convergent extension', *Development*, 126(20), pp. 4547–4556. Available at: https://doi.org/10.1242/dev.126.20.4547.

D'Costa, A. and Shepherd, I.T. (2009) 'Zebrafish Development and Genetics: Introducing Undergraduates to Developmental Biology and Genetics in a Large Introductory Laboratory Class', *Zebrafish*, 6(2), pp. 169–177. Available at: https://doi.org/10.1089/zeb.2008.0562.

Feller, M.B. (1999) 'Spontaneous Correlated Activity in Developing Neural Circuits', *Neuron*, 22(4), pp. 653–656. Available at: https://doi.org/10.1016/S0896-6273(00)80724-2.

Flanagan-Steet, H. *et al.* (2005) 'Neuromuscular synapses can form in vivo by incorporation of initially aneural postsynaptic specializations', *Development*, 132(20), pp. 4471–4481. Available at: https://doi.org/10.1242/dev.02044.

Goulding, M. (2009) 'Circuits controlling vertebrate locomotion: moving in a new direction', *Nature Reviews Neuroscience*, 10(7), pp. 507–518. Available at: https://doi.org/10.1038/nrn2608.

Granato, M. *et al.* (1996) 'Genes controlling and mediating locomotion behavior of the zebrafish embryo and larva', *Development (Cambridge, England)*, 123, pp. 399–413. Available at: https://doi.org/10.1242/dev.123.1.399.

Gu, X. and Spitzer, N.C. (1995) 'Distinct aspects of neuronal differentiation encoded by frequency of spontaneous Ca2+ transients', *Nature*, 375(6534), pp. 784–787. Available at: https://doi.org/10.1038/375784a0.

Hamburger, V. (1963) 'Some Aspects of the Embryology of Behavior', *The Quarterly Review of Biology*, 38(4), pp. 342–365.

Hamburger, V., Wenger, E. and Oppenheim, R. (1966) 'Motility in the chick embryo in the absence of sensory input', *Journal of Experimental Zoology*, 162(2), pp. 133–159. Available at: https://doi.org/10.1002/jez.1401620202.

Hanson, M.G. and Landmesser, L.T. (2006) 'Increasing the frequency of spontaneous rhythmic activity disrupts pool-specific axon fasciculation and pathfinding of embryonic spinal motoneurons', *The Journal of Neuroscience: The Official Journal of the Society for Neuroscience*, 26(49), pp. 12769–12780. Available at: https://doi.org/10.1523/JNEUROSCI.4170-06.2006.

Jing, M. *et al.* (2020) 'An optimized acetylcholine sensor for monitoring in vivo cholinergic activity', *Nature Methods*, 17(11), pp. 1139–1146. Available at: https://doi.org/10.1038/s41592-020-0953-2.

Kastanenka, K.V. and Landmesser, L.T. (2010) 'In vivo activation of channelrhodopsin-2 reveals that normal patterns of spontaneous activity are required for motoneuron guidance and maintenance of guidance molecules', *The Journal of Neuroscience: The Official Journal of the Society for Neuroscience*, 30(31), pp. 10575–10585. Available at: https://doi.org/10.1523/JNEUROSCI.2773-10.2010.

Kirkby, L. *et al.* (2013) 'A role for correlated spontaneous activity in the assembly of neural circuits', *Neuron*, 80(5), pp. 1129–1144. Available at: https://doi.org/10.1016/j.neuron.2013.10.030.

Knogler, L.D. *et al.* (2014) 'A Hybrid Electrical/Chemical Circuit in the Spinal Cord Generates a Transient Embryonic Motor Behavior', *Journal of Neuroscience*, 34(29), pp. 9644–9655. Available at: https://doi.org/10.1523/JNEUROSCI.1225-14.2014.

Lewis, K.E. and Eisen, J.S. (2003) 'From cells to circuits: development of the zebrafish spinal cord', *Progress in Neurobiology*, 69(6), pp. 419–449. Available at: https://doi.org/10.1016/S0301-0082(03)00052-2.

Milner, L.D. and Landmesser, L.T. (1999) 'Cholinergic and GABAergic Inputs Drive Patterned Spontaneous Motoneuron Activity before Target Contact', *Journal of Neuroscience*, 19(8), pp. 3007–3022. Available at: https://doi.org/10.1523/JNEUROSCI.19-08-03007.1999.

Momose-Sato, Y. and Sato, K. (2013) 'Large-scale synchronized activity in the embryonic brainstem and spinal cord', *Frontiers in Cellular Neuroscience*, 7. Available at: https://www.frontiersin.org/articles/10.3389/fncel.2013.00036 (Accessed: 28 August 2023).

Momose-Sato, Y. and Sato, K. (2020) 'Prenatal exposure to nicotine disrupts synaptic network formation by inhibiting spontaneous correlated wave activity', *IBRO reports*, 9, pp. 14–23. Available at: https://doi.org/10.1016/j.ibror.2020.06.003.

Moreno, R.L. and Ribera, A.B. (2009) 'Zebrafish Motor Neuron Subtypes Differ Electrically Prior to Axonal Outgrowth', *Journal of Neurophysiology*, 102(4), pp. 2477–2484. Available at: https://doi.org/10.1152/jn.00446.2009.

Myers, C. (2005) 'Cholinergic Input Is Required during Embryonic Development to Mediate Proper Assembly of Spinal Locomotor Circuits'. Available at: https://core.ac.uk/reader/82664400 (Accessed: 13 March 2023).

Myers, P.Z. (1985) 'Spinal motoneurons of the larval zebrafish', *The Journal of Comparative Neurology*, 236(4), pp. 555–561. Available at: https://doi.org/10.1002/cne.902360411.

O'Donovan, M.J. and Landmesser, L. (1987) 'The development of hindlimb motor activity studied in the isolated spinal cord of the chick embryo', *Journal of Neuroscience*, 7(10), pp. 3256–3264. Available at: https://doi.org/10.1523/JNEUROSCI.07-10-03256.1987.

Picciotto, M.R., Higley, M.J. and Mineur, Y.S. (2012) 'Acetylcholine as a neuromodulator: cholinergic signaling shapes nervous system function and behavior', *Neuron*, 76(1), pp. 116–129. Available at: https://doi.org/10.1016/j.neuron.2012.08.036.

Preyer, W.T. (1885) 'Special Physiology of the Embryo'.

Rima, M. *et al.* (2020) 'Dynamic regulation of the cholinergic system in the spinal central nervous system', *Scientific Reports*, 10(1), p. 15338. Available at: https://doi.org/10.1038/s41598-020-72524-3.

Saint-Amant, L. and Drapeau, P. (1998) 'Time course of the development of motor behaviors in the zebrafish embryo', *Journal of Neurobiology*, 37(4), pp. 622–632. Available at: https://doi.org/10.1002/(SICI)1097-4695(199812)37:4<622::AID-NEU10>3.0.CO;2-S.

Saint-Amant, L. and Drapeau, P. (2001) 'Synchronization of an Embryonic Network of Identified Spinal Interneurons Solely by Electrical Coupling', *Neuron*, 31(6), pp. 1035–1046. Available at: https://doi.org/10.1016/S0896-6273(01)00416-0.

Schindelin, J. *et al.* (2012) 'Fiji - an Open Source platform for biological image analysis', *Nature methods*, 9(7), p. 10.1038/nmeth.2019. Available at: https://doi.org/10.1038/nmeth.2019.

Sun, Y.A. and Poo, M.M. (1987) 'Evoked release of acetylcholine from the growing embryonic neuron.', *Proceedings of the National Academy of Sciences of the United States of America*, 84(8), pp. 2540–2544.

Tezuka, Y. *et al.* (2022) 'Developmental stage-specific spontaneous activity contributes to callosal axon projections', *eLife*, 11, p. e72435. Available at: https://doi.org/10.7554/eLife.72435.

Wan, Y. *et al.* (2019) 'Single-Cell Reconstruction of Emerging Population Activity in an Entire Developing Circuit', *Cell*, 179(2), pp. 355-372.e23. Available at: https://doi.org/10.1016/j.cell.2019.08.039.

Wang, M., Wen, H. and Brehm, P. (2008) 'Function of neuromuscular synapses in the zebrafish choline-acetyltransferase mutant bajan', *Journal of Neurophysiology*, 100(4), pp. 1995–2004. Available at: https://doi.org/10.1152/jn.90517.2008.

Warm, D. *et al.* (2022) 'Spontaneous Activity Predicts Survival of Developing Cortical Neurons', *Frontiers in Cell and Developmental Biology*, 10. Available at: https://www.frontiersin.org/articles/10.3389/fcell.2022.937761 (Accessed: 9 September 2023).

Warp, E. *et al.* (2012) 'Emergence of patterned activity in the developing zebrafish spinal cord', *Current biology: CB*, 22(2), pp. 93–102. Available at: https://doi.org/10.1016/j.cub.2011.12.002.

Watt, S.D. *et al.* (2000) 'Specific Frequencies of Spontaneous Ca2+ Transients Upregulate GAD 67 Transcripts in Embryonic Spinal Neurons', *Molecular and Cellular Neuroscience*, 16(4), pp. 376–387. Available at: https://doi.org/10.1006/mcne.2000.0871.

Welle, T.M. *et al.* (2018) 'A high spatiotemporal study of somatic exocytosis with scanning electrochemical microscopy and nanoITIES electrodes', *Chemical Science*, 9(22), pp. 4937–4941. Available at: https://doi.org/10.1039/C8SC01131A.

Williams, K. and Ribera, A.B. (2020) 'Long-lived zebrafish Rohon-Beard cells', *Developmental Biology*, 464(1), pp. 45–52. Available at: https://doi.org/10.1016/j.ydbio.2020.05.003.

Wolf, S. *et al.* (2017) 'Sensorimotor computation underlying phototaxis in zebrafish', *Nature Communications*, 8(1), p. 651. Available at: https://doi.org/10.1038/s41467-017-00310-3.

Young, S.H. (1986) ‘Spontaneous release of transmitter from the growth cones of Xenopus neurons in vitro: The influence of Ca2+ and Mg2+ ions’, *Developmental Biology*, 113(2), pp. 373–380. Available at: https://doi.org/10.1016/0012-1606(86)90172-7.

Supplementary Figures

Transgenic line	Calcium events (1 dpf)	Calcium events (5 dpf)	N	Reference
Tg(elavl3:H2B-GCaMP6f)	no	yes	3	Chen et al., 2013
Tg(NeuroD:GCaMP6f^{icm05})	no	yes	3	Rupprecht et al., 2016
Tg(elavl3:GCaMP6s^{CY14})	no	yes	3	Vladimirov et al., 2014
Tg(elavl3:GCaMP6s^{CY44})	no	yes	3	Vladimirov et al., 2014
Tg(elavl3:jRGECO1b)	no	yes	3	Mu et al., 2019
Tg(elavl3:GCaMP6f^{f12200a})	yes	yes	>3	Wolf et al., 2017

Supplemental Table 1. ***Transgenic lines expressing calcium sensors that were tested for calcium transients in 1 day post fertilization (dpf) embryos***

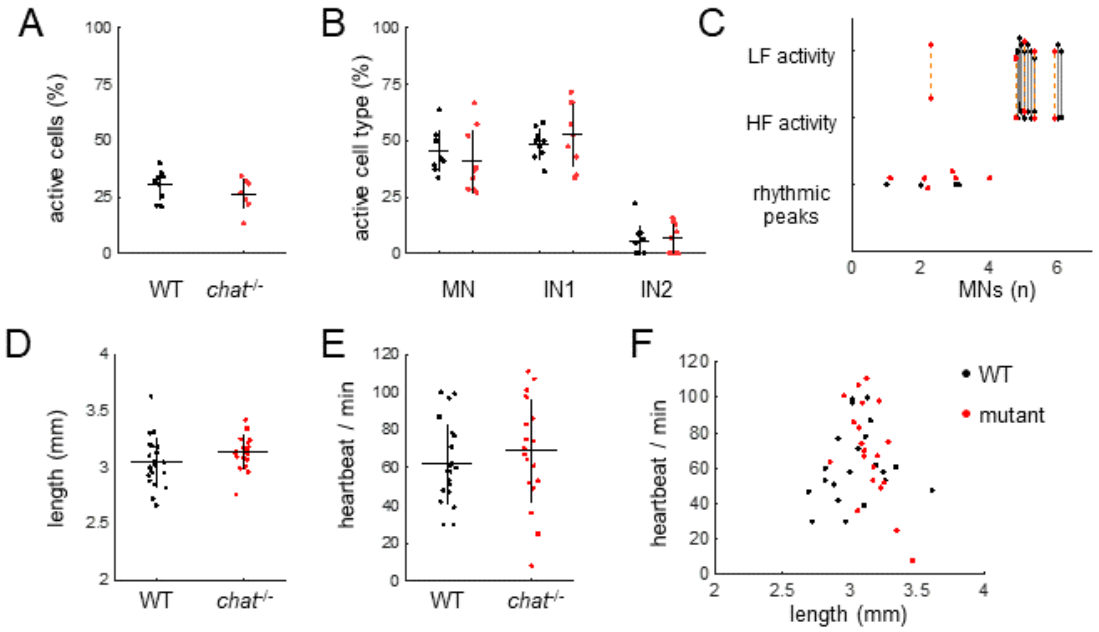

Supplemental Figure 1. *chat* mutants do not display overt differences with their WT siblings.

(A) Scatter plot showing the percentage of active cells in WT and *chat* $^{-/-}$ 1 dpf embryos (WT = 12, *chat*$^{-/-}$ = 10, Mann-Whitney test p=0.1915).

(B) Scatter plot showing the percentage of neuron types (MN, IN1, & IN2) in active cells between WT and *chat*$^{-/-}$ embryos (WT (n =12) vs. *chat*$^{-/-}$ (n= 10), MN: 43±9.5 vs. 44.4±12.21 %, IN1: 46.7±11.1 vs. 46.17±12 %, IN2: 12.9±7.3 vs. 15.6±8 %).

(C) Scatter plot of the the distribution of activity types in embryos staged by the number of mnx1^{+} cells per hemisegment. Activity types on the left y-axis correspond to rhythmic peaks, high frequency (HF) or low frequency (LF) activity. Later stage embryos displaying microcircuits are indicated by a line between HF and LF activity. WT = 12, *chat*$^{-/-}$ = 11.

(D) Number of heartbeats in 1 min WT (n = 27) vs. mutant (n = 32) embryos: 54.4 ± 23.9 vs. 55.9 ± 29.1. Length of embryos in WT (, n = 21) and mutant (n = 20) embryos: 3 ± 0.21 vs. 3.1 ± 0.16 mm. Embryos were also divided into those with regular or irregular heartbeats.

Regular heartbeats: WT (n = 21) vs mutant (n = 20), 62 ± 21.1 vs. 69.2 ± 27.4 heartbeats per min; 3 ± 0.22 vs. 3.1 ± 0.15 mm length.

Irregular heartbeats: WT (n = 6) vs mutant (n = 12), 28 ± 10.3 vs. 33.8 ± 10.3 heartbeats per min. 3.1 ± 0.16 vs. 3.2 ± 0.18 mm length. Mean ± SD.

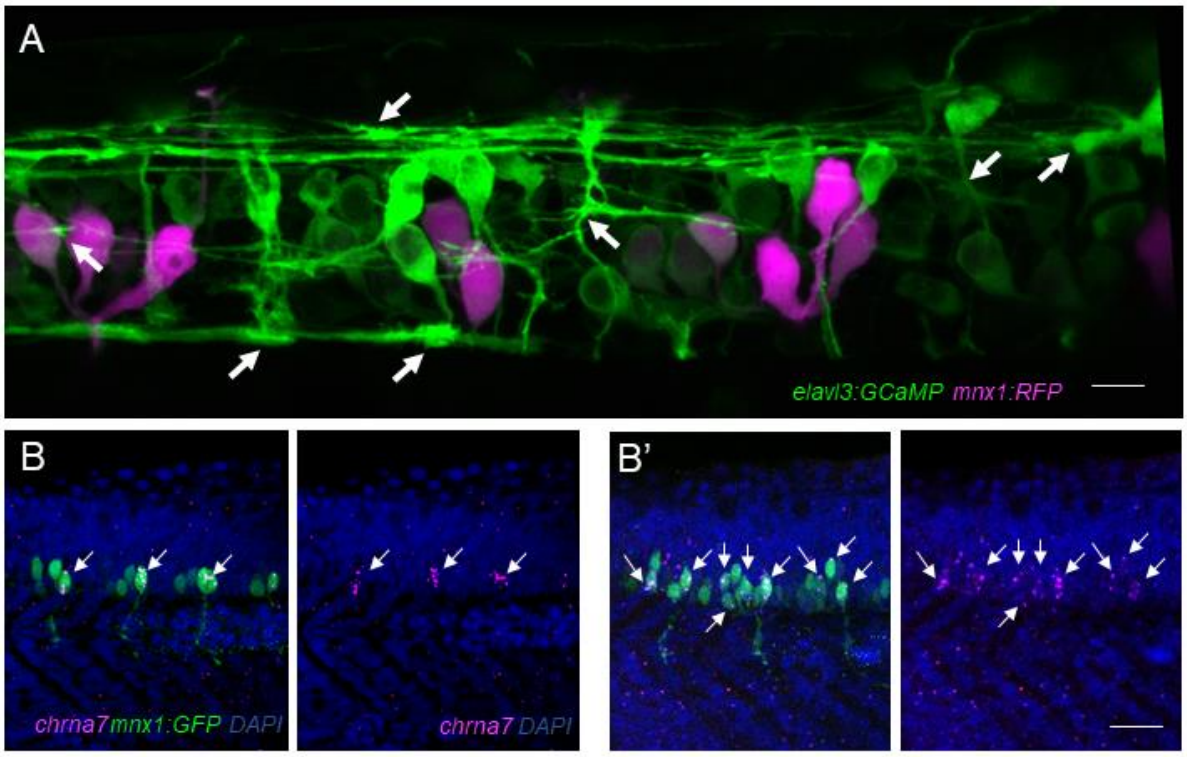

Supplemental Figure 2. ***Dynamic changes occur during early embryonic stages.***
(A) Axon elongation and dynamic protrusions occur in many spinal neurons during the evolution of spontaneous neural activity. Z-stack composite confocal image of *Tg(elavl3:GCaMP6f;mnx1:gal4;UAS:RFP*) embryo showing motoneurons (magenta) and spinal neurons (green). White arrows point to putative growth cones. Scale bar = 10 μm.
(B,B') Fluorescent in situ hybridization of *chrna7* (magenta) in *Tg(mnx1:GFP)* (green) embryos. Note that *chrna7* is first expressed only in CaP motoneurons (B) but later becomes expressed in most motoneurons (B'). Arrows indicate *chrna7* labeling. Scale bar = 50 μm.

Chapter 4: Thesis Discussion

The aim of this thesis was to study spontaneous neural activity (SNA) during the first day of embryonic development and study the influence of cholinergic signaling during SNA. SNA is a phenomenon that occurs across multiple regions of the nervous system and in a multitude of organisms (Hamburger, Wenger and Oppenheim, 1966; Hubel and Wiesel, 1970; Galli and Maffei, 1988; Nishimaru *et al.*, 1996; Saint-Amant and Drapeau, 2000). It is important because it influences certain biological processes related to the assembly of functional neural networks (Feller, 1999; Kirkby *et al.*, 2013). One of the prominent neurotransmitters to influence the initiation and maintenance of SNA is acetylcholine (ACh). In the chick spinal cord, the emergence of SNA is dependent on cholinergic signaling as blocking cholinergic signaling led to the total abolishment of activity (O'Donovan and Landmesser, 1987; Milner and Landmesser, 1999). In mice, SNA is initially mediated by electrical and cholinergic transmission, whereby blocking cholinergic transmission led to the abolishment of activity at early stages and disruption of frequency at later stages (Hanson and Landmesser, 2003; Myers, 2005). However, studies in zebrafish suggest that cholinergic signaling does not play a role SNA (Saint-Amant and Drapeau, 2001). This discrepancy was surprising since there is a conservation in transcription factor gradients that specify cellular domains in the spinal cord among vertebrates (Jessell, 2000; Grillner and Jessell, 2009). There is also homology among different spinal interneuron types between vertebrates. For instance, the CiA, CiD, and VeLD interneurons are some of the first INs to differentiate and be active in the zebrafish spinal cord, and are homologous to the V1, V2a, and V2b INs in the mouse spinal cord, respectively (Alvarez *et al.*, 2005; Goulding, 2009). In short, there is conservation of pathways and genes that guide the assembly of the spinal circuit in vertebrate animals. For this reason, we wanted to revisit the contribution of cholinergic signaling during embryonic SNA in the zebrafish spinal cord.

Cholinergic signaling components are expressed in the embryonic spinal cord at the time of the emergence of correlated spontaneous activity

We first characterized the cholinergic system in wild-type (WT) zebrafish embryos. We saw that pre- and post- synaptic components are expressed as early as 20 hours post fertilization (hpf) (Rima *et al.*, 2020), around the emergence of correlated activity (Warp *et al.*, 2012). Motoneurons express all components necessary for the synthesis,

packaging, release, and hydrolysis of acetylcholine as well as the machinery to uptake choline (VAChT, ChAT, ACHE, HACT). MNs also express one of the receptor subunits, the nAChRα7, while interneurons express receptor subunits a2, and a3 (Rima *et al.*, 2020). Presynaptic components remain expressed in the spinal cord until 3 days post fertilization (dpf), where they become confined to the tip of the tail, while the expression of genes that encode the receptor subunits remain unchanged and are expressed throughout the entire spinal cord (Rima *et al.*, 2020).

Knowing that cholinergic system is involved in several biological processes involved in neural network formation, and establishing that it is expressed during early embryonic development at around 20hpf indicates that it could play a role in spinal spontaneous neural activity. To study the role that cholinergic signaling plays in spinal SNA, we decided to use a *cholineacetyltransferase (chat$^{-/-}$)* mutant where cholinergic signaling is abolished. But before that, we needed to further study the progression of SNA in the spinal cord down to a single cell level to better understand the contribution of ACh to SNA.

Birthdate determined microcircuits emerge among active neurons in the zebrafish spinal cord

We recorded calcium transients during SNA in WT zebrafish spinal cords during day 1 of embryonic development. The line we utilized is the *Tg(elavl3:GCaMP6; mnx1:Gal4;UAS:RFP)* which expresses GCaMP in most post-mitotic neurons and RFP in MNs. Even when the time of egg fertilization was controlled and monitored, we saw embryos with different developmental stages even though they were born within the same clutch. To better control for the developmental stage of the embryos we imaged, we opted to use the number of MNs per hemisegment as a marker of developmental stage since MN soma occupy stereotypical positions in the developing zebrafish spinal cord. The zebrafish spinal cord goes through several rounds of neurogenesis during embryonic development. The first round of neurogenesis results in the differentiation of primary MNs and a few INs that mediate early locomotor behavior and spontaneous activity, while the second round of embryonic spinal neurogenesis results in the differentiation of secondary MNs and other classes of INs (Lewis and Eisen, 2003). After the first round of neurogenesis between 20-24hpf (1-3 MNs per hemisegment), cells only display high frequency oscillatory activity. This

oscillatory activity arises due to the linking of the active cells to each other via gap junctions, among these cells being a subset of INs with pacemaker properties (IC neurons), which may drive the patterned activity (Tong and McDearmid, 2012).

Following the second round of neurogenesis at around 25 hpf (4+ MN per hemisegment), we observed that even within the population of MNs (RFP labeled cells), there are two types of activity (consisting of low frequency (LF) or high frequency (HF) activity), which are correlated yet occurring at different frequencies. When neurons in the LF microcircuit are active, neurons in the HF microcircuit are also active. However, not all events in the HF circuit co-occur with those in the LF microcircuit. The activity pattern of the HF microcircuit differs from the rhythmic oscillatory activity observed in younger embryos. The difference is that upon the emergence of microcircuits, neurons begin to exhibit trains of activity that occur with shorter intervals, resulting in a 'burst'-like activity. The primary MNs (RFP^+) in the embryos with microcircuits predominantly display LF activity. These neurons are easy to identify based on their soma positions and axonal trajectories. On the other hand, secondary MNs born during the subsequent round of neurogenesis display HF activity. These neurons are identified based on their smaller soma nested within the intensely labelled and bigger soma of the stereotypically positioned primary MNs. The identification of two distinct activity patterns within the MNs, with LF activity attributed to primary MNs and HF activity to secondary MNs, suggests that the microcircuits are forming based on the birthdates of the neurons. The molecular mechanisms that underly the transition from rhythmic HF to LF activity should be addressed in future studies.

What changes in the spinal circuit induce the emergence of microcircuits? The dynamical behavior of developing systems means that they are constantly forming and removing connections. In the mouse embryo, SNA is initially mediated through cholinergic signaling and later through glutamatergic transmission, while in chick embryos the GABAergic and glycinergic systems take over the activity after cholinergic signaling (Kirkby *et al.*, 2013). The establishment of new connections and the differentiation of additional IN classes signifies an increased input to the postsynaptic cell which might change its firing pattern. The earlier born neurons including the CaP MNs establish connections with or express receptors that respond to inhibitory neurons which decrease the frequency of firing, as well as to excitatory neurons that excite them for a longer time period allowing them to display bursts. This

happens while the neurons in HF circuit still rely mainly on gap junctions to propagate and synchronize the activity as previously described in younger embryos (Saint-Amant and Drapeau, 2001). It is still unclear whether the HF neurons establish chemical synapses with the same neurons that induce bursting activity in the LF neurons, or if the bursts of activity the HF neurons display are due to the gap junctions they have with the LF neurons. It is unlikely due to gap junctions, as this would imply that the gap junctions between the HF and LF neurons are different from those between the HF neurons themselves, otherwise the entire system would display one activity pattern and frequency.

To test the neurotransmitter responsible for activating the LF circuit, we would need to conduct calcium imaging recordings while applying receptor antagonists for glycinergic and glutamatergic neurotransmission after the emergence of microcircuits. An alternative method would be cell-type specific laser ablation, however, the caveat is that the effects cannot be reversed. Another way would be to express opsins that either depolarize (channelrhodopsin) or hyperpolarize (halorhodopsin) specific neurons (glycinergic or glutamatergic) upon illumination. If the activity changes, that would confirm our hypothesis on which neurotransmitter-releasing neurons are activate the LF circuit.

After observing the microcircuits, another question is raised: Are the neurons in either microcircuit during embryonic development part of the same circuit that controls specific aspects of locomotion or speed of swimming in larval fish? Zebrafish hatchlings and young larvae exhibit a singular swimming mode, characterized by high-speed bouts of swimming. This high speed is mediated by the early-born primary MNs and INs mentioned earlier (Saint-Amant and Drapeau, 2000; McLean *et al.*, 2007). Based on the bursting activity (longer lasting depolarization of the neuron) observed in the LF microcircuit neurons, it is likely that they drive the fast swimming bout. Additionally, as swimming speed increases, excitatory INs in higher domains of the spinal cord get recruited (McLean and Fetcho, 2009). For example, the CiD INs (*alx*$^{+}$*)* are among the first excitatory INs to be born and to become active. They are located in the dorsal half of the spinal cord and are implicated in fast swimming bouts in zebrafish larvae (Kimura, Okamura and Higashijima, 2006). Knowing that the CiD INs are active during early SNA (Saint-Amant and Drapeau, 2001), are glutamatergic

(Kimura, Okamura and Higashijima, 2006), and are correlated with the MN activity (Knogler *et al.*, 2014), it would be interesting to investigate their activity pattern progression at different embryonic stages.

Prior to the functional study, I first wanted to investigate whether the CiD INs were indeed recruited in the LF microcircuit. I crossed the *Tg[alx:Gal4;UAS:RFP]* that labels the V2a glutamatergic INs (mostly CiD INs) that are homologous to the *chx10* neurons in mice (Kimura, Okamura and Higashijima, 2006) with the pan-neuronal calcium sensor line to analyze their activity. Unfortunately, I did not see expression of the transcription factor mediated reporter protein at the developmental stage of interest. I used other IN lines to see which IN types are recruited during SNA. The INs lines I used were the following: *Tg[evx2:Gal4;UAS:RFP]* that labels the inhibitory INs in the V0 domain (Menelaou, Kishore and McLean, 2019), *Tg[eng1:Gal4;UAS:RFP]* which labels a single subset of glycinergic ipsilaterally ascending INs (CiA) (Higashijima *et al.*, 2004), *Tg[vgluT:DsRed]* that labels excitatory glutamatergic INs (Kinkhabwala and Fetcho, 2011), and finally the *Tg[gad1b:Gal4;UAS:RFP]* which labels the GABAergic INs (Filosa *et al.*, 2016). Again, the majority of transgenic lines started to express the reporter protein at 3 dpf. The only transgenic line to show expression of the reporter protein at around 1 dpf was the *Tg[gad1b:Gal4;UAS:RFP]* line. After performing calcium imaging on these embryos, I did not observe any calcium transients in cells that are double positive for GCaMP and RFP. This result suggests that *gad1b*-expressing GABAergic neurons are not recruited at this stage of development. However, further experiments need to be conducted to confirm this finding.

What could be the role of the HF microcircuit? We recorded activity within the distal axons of CaP MNs, which innervate the ventral myotome, and captured the activity in proximal axon bundles—the location where the three primary MN axons and secondary MN axons bundle together as they exit the spinal cord. Our observations revealed LF activity in the distal axons that connect with the ventral muscle. In contrast, we noted HF activity within the proximal axon bundle, where the secondary MNs are still extending their axons to reach their respective muscle targets. Thus, I propose that the HF activity could be a main factor for the proper extension of axons to their targets, either the muscles (MN axons) or other neurons within the spinal cord (IN axons). To test this hypothesis, I would express opsins under the *mnx*1 promoter that

would lead to the hyperpolarization of MNs upon illumination. Possible candidates would be either an anion channelrhodopsin or an inward chloride pump (Antinucci *et al.*, 2020). I would then analyze the length of the MN axon and the location of the MN axon target site. In chick embryos, this hypothesis was tested by pharmacological inhibition of SNA during the period when axons were extending towards muscle targets. This blockade of activity resulted in faulty axonal projections. However, when the appropriate frequency of activity was optogenetically reinstated within the motoneurons under the same conditions of activity suppression, a positive outcome was observed: the axons projected accurately towards the intended muscle targets (Kastanenka and Landmesser, 2010). Conversely, enhancing the frequency of activity also led to improper axonal projection in a manner different from what was seen under activity blockade (Hanson and Landmesser, 2006).

Why have researchers studying zebrafish spinal SNA not reported the existence of microcircuits? Originally, the first lab to describe SNA in the zebrafish spinal cord utilized paired electrophysiological recordings to study the correlation between cells (Saint-Amant and Drapeau, 2001). Although a very powerful tool in recording neural activity, this method is not very effective to studying large groups of neurons, as only the activities of a few cells can be recorded at once. Other labs that have performed calcium imaging used α-Bungarotoxin while we used Pancuronium Bromide to paralyze the fish and record calcium transients. One team cut the tail tip of the embryos, subsequently incubating them in fish medium mixed with α-BTX (Warp *et al.*, 2012). Meanwhile, the other team injected α-BTX mRNA into fertilized eggs at the one-cell stage, resulting in the widespread expression of the protein, most likely within the CNS (Wan *et al.*, 2019). The difference between the two paralyzing agents is that Pancuronium Bromide predominantly binds to nAChRα1 subunits that are exclusively found at the NMJ (Gotti *et al.*, 2021), while α-Bungarotoxin also binds to nAChRα7 subunits which are found in the NMJ and in the MNs of the embryonic spinal cord (Rima et al). The experiments assessing receptor affinity for antagonists were initially performed on mammals (Gotti *et al.*, 2021). However, it is worth noting that the receptor subunits that were cloned in mammals have also been cloned in zebrafish. These cloned subunits display a significant degree of similarity in terms of both structure and physiological distribution (Zirger *et al.*, 2003; Papke *et al.*, 2012).

A model for the progression of SNA in the embryonic zebrafish spinal cord

We propose a model for how microcircuits emerge during embryonic zebrafish spinal cord development (Figure 1): As the embryos undergo the first round of neurogenesis in the spinal cord, this leads to the differentiation of primary MNs and a few classes of INs that will modulate early motor activity. These are the first cells to be active in the spinal cord, and at the emergence of correlated activity, they all display oscillatory HF peaks of activity with an average duration of 2 seconds between peaks. The early activity among them is highly correlated, patterned, synchronized among cells on one side of the spinal cord, shows relatively uniform amplitudes, and is mainly dependent on gap junctions. Subsequent rounds of neurogenesis generate the secondary MNs and additional classes of INs. The emergence of microcircuits occurs at this stage. We propose the cells that resulted from the first round of neurogenesis have established new connections with earlier and/or later born neurons, and are now operated by a chemical/electrical hybrid circuit, and gradually adopt a LF activity pattern.

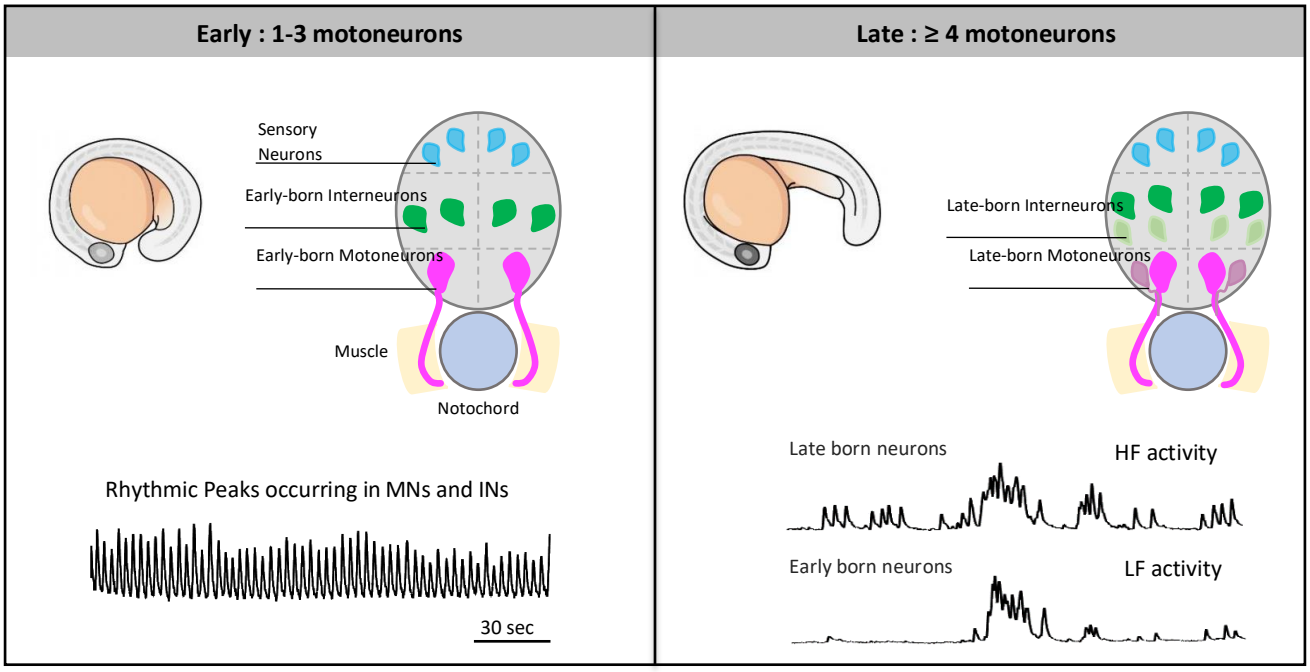

Figure 1. Schematic model for the progression of spontaneous activity in the embryonic zebrafish spinal cord. At the 1-3 MN per hemisegment stage, only the primary MNs and a few classes of INs are born and display HF activity. After the second round of neurogenesis, secondary MNs and additional classes of INs are born, adopting a HF activity pattern, while the earlier born neurons transition to a LF activity pattern after forming chemical synapses with other neurons.

The LF activity consists of both bursts and peaks of activity, which are more widely spaced in time and exhibit less uniform amplitudes. Meanwhile, the neurons from the

second round of neurogenesis display a HF activity which is similar but not identical to the early activity previously described for the early born neurons.

Cholinergic signaling is involved in maintaining the rhythmicity of activity

Previous studies suggest that cholinergic signaling is not involved in early SNA and only mediated via gap junctions in the zebrafish embryo (Saint-Amant and Drapeau, 2001). However, cholinergic signaling mediates early SNA in several other vertebrates (Chub and O'Donovan, 1998; Hanson and Landmesser, 2003; Blankenship and Feller, 2010). Due to the conservation of transcription factor gradients, homology between different IN types, and the close resemblance of several SNA features across vertebrates, we explored the role of ACh during SNA in zebrafish.

Our results demonstrated that ACh signaling is not necessary for emergence of SNA in the embryonic zebrafish spinal cord, in contrast to other vertebrates (Chub and O'Donovan, 1998; Hanson and Landmesser, 2003). We found no developmental differences between WT and *chat*$^{-/-}$ mutant embryos. The size, heartrate, and percentages of active cells are similar. However, we found that the early rhythmic activity during early SNA in the *chat*$^{-/-}$ embryo is less uniform. The activity in *chat*$^{-/-}$ mutants shows irregularly spaced peaks of activity separated by longer quiescent periods, unlike in the WT siblings where the interval between peaks is small and uniform. Additionally, cholinergic signaling plays a role in the establishment of proper left-right alternation. During rhythmic HF activity in early SNA, WT embryos display consistently alternating activity between the left and right sides, which decreases over the course of development. In the mutants, left-right alternation is not as regular even during early SNA. Furthermore, the number of calcium transients between the left and right sides are less symmetric in mutants than their WT siblings. Our results show that cholinergic signaling modulates early spinal SNA in the embryonic zebrafish spinal cord.

Lack of cholinergic signaling in the *chat*$^{-/-}$ mutant embryos resulted in irregular activity during early SNA. The irregular pattern of activity may be due to the lack- or reduced firing rate of a subset of neurons that maintain the rhythmicity of firing during early development, relying on cholinergic signaling to strengthen its firing rate. Certain channels like the ones producing the persistent Na^+ currents (Rybak et al, 2004) also found in the caudal spinal cord of mammals contribute to sustained depolarizations (Crill, 1996). This was also demonstrated in two zebrafish mutants, whereby a

mutation in the *scn8aa* gene caused lack of sustained motor response upon sensory stimulation (Low et al. 2010). These sodium channels were found in the IC INs during embryonic development and SNA in zebrafish, suggesting that these neurons could act as pacemaker neurons to drive the activity which is independent of any descending inputs or sensory stimulation at that developmental stage (McDearmid et al., 2012). I hypothesize that IC neurons expressing nAChRs play a crucial role in modulating the firing patterns of both excitatory and inhibitory neurons. In the CPG model of simple aquatic vertebrates, glutamatergic neurons project ipsilaterally onto MNs and inhibitory INs, which in turn extend their axons to the contralateral side to inhibit it whenever the side they project their axons from is active (Grillner and El Manira, 2020) **(Figure 2)**. Lack of cholinergic signaling leads to reduced firing of the IC neurons. The IC neurons project onto excitatory INs in the CPG, affecting firing frequency but not contralateral inhibition, as inhibitory INs respond to excitatory INs modulated by the IC neurons. This results in proper contralateral inhibition but disrupts left-right firing balance and rhythmicity in firing frequency.

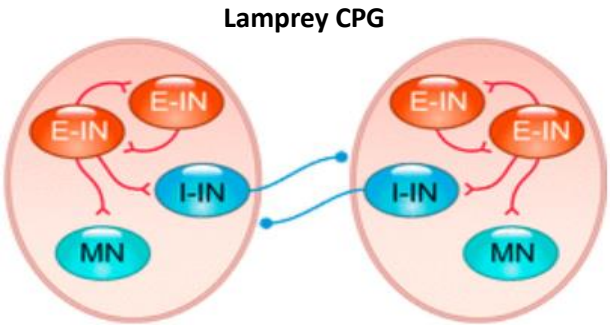

Figure 2. The segmental locomotor network in lamprey. Illustration of cell types forming the central pattern generator (CPG) in lamprey. Excitatory neurons (red) synapse onto ipsilateral MNs and contralaterally projecting inhibitory INs (blue). (Grillner and El Manira, 2020) .

We did not find any INs that express the machinery for ACh synthesis and release as they only expressed receptor subunits (Rima *et al.*, 2020). We only located ACh synthesis machinery in *mnx1*+ cells. Although the *mnx1* line labels VeLD INs in addition to MNs, these INs were shown to be inhibitory (Higashijima, Schaefer and Fetcho, 2004). Additionally, we did not detect any neurons in the brain expressing the machinery responsible for the synthesis and release of ACh. Therefore, we propose that the source of ACh release in the motor circuit is from the MNs. Spontaneous somatic release is a possibility since it was seen in cultured *Xenopus* cells (Young, 1986; Sun and Poo, 1987; Welle *et al.*, 2018). One way to test for the release site of ACh from MNs would be through the expression of an ACh sensor. Briefly, recently

developed ACh sensors are composed of a cholinergic receptor subunit fused to a cpGFP which undergoes conformational changes and increases its fluorescence upon the binding of ACh to the receptor subunit (Jing *et al.*, 2020).

The alternation index in 1-3 MNs per hemisegment *chat*$^{-/-}$ mutant embryos does not resemble that of similarly aged WT siblings but is closer to that of more developed WT embryos. In birds and rodents, glutamatergic signaling replaces cholinergic signaling as the main excitatory drive during later stages of development (Momose-Sato and Sato, 2013). It has been reported that glutamatergic signaling is the main excitatory transmission in the zebrafish spinal cord starting 1.3 dpf (Ali, Buss and Drapeau, 2000). It would be interesting to test if chronic perturbation of the cholinergic system leads to abnormal neuronal specification or to premature emergence of neurotransmitter systems, as has been reported in the embryonic mouse spinal cord (Myers, 2005). These results can be obtained either by immunohistochemistry or *in situ* hybridization experiments to test whether other neurotransmitter systems emerge earlier in the *chat*$^{-/-}$ mutant embryos compared with their WT siblings.

Conversely, could the chronic perturbation of cholinergic signaling lead to differences in cellular properties such as membrane and input resistances in cells expressing nAChRs in the premotor circuit? To study the effect of cholinergic signaling on establishing proper cellular properties, we would need to perform electrophysiological recordings in mutants to determine the membrane and input resistances of the neurons we know are active during early stages of SNA, such as the VeLD, IC, CoPA, and primary MNs.

This study highlights that the disruption of the cholinergic system, either enhancing or reducing its function, leads to effects on neural activity which could be translated into the improper construction of the neural circuit. In the introduction I addressed maternal exposure to nicotine coming from cigarette or vape smoke since they are highly accessible and available to anyone. Yet, there are numerous other substances such as certain pesticides and medications that can affect the cholinergic system and disrupt its activity, subsequently disrupting SNA. Therefore, we shed light on the importance of ensuring a proper environment during the entirety of embryonic

development in which disturbances in neurotransmission and activity may lead to adverse effects.

In conclusion, due to the conservation of transcription factor gradients and homology of several spinal IN types among vertebrates, the zebrafish is a prominent model to study the anomalies that might arise due to the disruption of neurotransmitters and of SNA in vivo. This model can answer some of the questions arising on the impact of disturbances in spontaneous activity caused by genetic, intrinsic factors (inflammation), or extrinsic factors (such as maternal medication or drug abuse) on different activity-dependent processes during the formation of the spinal circuit. Longitudinal studies on this animal model can also shed light on the prolonged effects of these disruptions. These questions remain for future studies.

References

Ali, D.W., Buss, R.R. and Drapeau, P. (2000) 'Properties of Miniature Glutamatergic EPSCs in Neurons of the Locomotor Regions of the Developing Zebrafish', *Journal of Neurophysiology*, 83(1), pp. 181–191. Available at: https://doi.org/10.1152/jn.2000.83.1.181.

Alvarez, F.J. *et al.* (2005) 'Postnatal phenotype and localization of spinal cord V1 derived interneurons', *Journal of Comparative Neurology*, 493(2), pp. 177–192. Available at: https://doi.org/10.1002/cne.20711.

Antinucci, P. *et al.* (2020) 'A calibrated optogenetic toolbox of stable zebrafish opsin lines', *eLife*. Edited by H. Burgess et al., 9, p. e54937. Available at: https://doi.org/10.7554/eLife.54937.

Blankenship, A.G. and Feller, M.B. (2010) 'Mechanisms underlying spontaneous patterned activity in developing neural circuits', *Nature Reviews. Neuroscience*, 11(1), pp. 18–29. Available at: https://doi.org/10.1038/nrn2759.

Chub, N. and O'Donovan, M.J. (1998) 'Blockade and Recovery of Spontaneous Rhythmic Activity after Application of Neurotransmitter Antagonists to Spinal Networks of the Chick Embryo', *Journal of Neuroscience*, 18(1), pp. 294–306. Available at: https://doi.org/10.1523/JNEUROSCI.18-01-00294.1998.

Feller, M.B. (1999) 'Spontaneous Correlated Activity in Developing Neural Circuits', *Neuron*, 22(4), pp. 653–656. Available at: https://doi.org/10.1016/S0896-6273(00)80724-2.

Filosa, A. *et al.* (2016) 'Feeding State Modulates Behavioral Choice and Processing of Prey Stimuli in the Zebrafish Tectum', *Neuron*, 90(3), pp. 596–608. Available at: https://doi.org/10.1016/j.neuron.2016.03.014.

Galli, L. and Maffei, L. (1988) 'Spontaneous Impulse Activity of Rat Retinal Ganglion Cells in Prenatal Life', *Science*, 242(4875), pp. 90–91. Available at: https://doi.org/10.1126/science.3175637.

Gotti, C. *et al.* (2021) 'Nicotinic acetylcholine receptors (nACh) in GtoPdb v.2021.3', *IUPHAR/BPS Guide to Pharmacology CITE*, 2021(3). Available at: https://doi.org/10.2218/gtopdb/F76/2021.3.

Goulding, M. (2009) 'Circuits controlling vertebrate locomotion: moving in a new direction', *Nature Reviews Neuroscience*, 10(7), pp. 507–518. Available at: https://doi.org/10.1038/nrn2608.

Grillner, S. and El Manira, A. (2020) 'Current Principles of Motor Control, with Special Reference to Vertebrate Locomotion', *Physiological Reviews*, 100(1), pp. 271–320. Available at: https://doi.org/10.1152/physrev.00015.2019.

Grillner, S. and Jessell, T.M. (2009) 'Measured motion: searching for simplicity in spinal locomotor networks', *Current Opinion in Neurobiology*, 19(6), pp. 572–586. Available at: https://doi.org/10.1016/j.conb.2009.10.011.

Hamburger, V., Wenger, E. and Oppenheim, R. (1966) 'Motility in the chick embryo in the absence of sensory input', *Journal of Experimental Zoology*, 162(2), pp. 133–159. Available at: https://doi.org/10.1002/jez.1401620202.

Hanson, M.G. and Landmesser, L.T. (2003) 'Characterization of the Circuits That Generate Spontaneous Episodes of Activity in the Early Embryonic Mouse Spinal Cord', *The Journal of Neuroscience*, 23(2), pp. 587–600. Available at: https://doi.org/10.1523/JNEUROSCI.23-02-00587.2003.

Hanson, M.G. and Landmesser, L.T. (2006) 'Increasing the frequency of spontaneous rhythmic activity disrupts pool-specific axon fasciculation and pathfinding of embryonic spinal motoneurons', *The Journal of Neuroscience: The Official Journal of the Society for Neuroscience*, 26(49), pp. 12769–12780. Available at: https://doi.org/10.1523/JNEUROSCI.4170-06.2006.

Higashijima, S. *et al.* (2004) 'Engrailed-1 Expression Marks a Primitive Class of Inhibitory Spinal Interneuron', *The Journal of Neuroscience*, 24(25), pp. 5827–5839. Available at: https://doi.org/10.1523/JNEUROSCI.5342-03.2004.

Higashijima, S.-I., Schaefer, M. and Fetcho, J.R. (2004) 'Neurotransmitter properties of spinal interneurons in embryonic and larval zebrafish', *The Journal of Comparative Neurology*, 480(1), pp. 19–37. Available at: https://doi.org/10.1002/cne.20279.

Hubel, D.H. and Wiesel, T.N. (1970) 'The period of susceptibility to the physiological effects of unilateral eye closure in kittens', *The Journal of Physiology*, 206(2), pp. 419–436. Available at: https://doi.org/10.1113/jphysiol.1970.sp009022.

Jessell, T.M. (2000) 'Neuronal specification in the spinal cord: inductive signals and transcriptional codes', *Nature Reviews Genetics*, 1(1), pp. 20–29. Available at: https://doi.org/10.1038/35049541.

Jing, M. *et al.* (2020) 'An optimized acetylcholine sensor for monitoring in vivo cholinergic activity', *Nature Methods*, 17(11), pp. 1139–1146. Available at: https://doi.org/10.1038/s41592-020-0953-2.

Kastanenka, K.V. and Landmesser, L.T. (2010) 'In vivo activation of channelrhodopsin-2 reveals that normal patterns of spontaneous activity are required for motoneuron guidance and maintenance of guidance molecules', *The Journal of Neuroscience: The Official Journal of the Society for Neuroscience*, 30(31), pp. 10575–10585. Available at: https://doi.org/10.1523/JNEUROSCI.2773-10.2010.

Kimura, Y., Okamura, Y. and Higashijima, S. (2006) 'alx, a Zebrafish Homolog of Chx10, Marks Ipsilateral Descending Excitatory Interneurons That Participate in the Regulation of Spinal Locomotor Circuits', *The Journal of Neuroscience*, 26(21), pp. 5684–5697. Available at: https://doi.org/10.1523/JNEUROSCI.4993-05.2006.

Kinkhabwala, A. and Fetcho, J. (2011) *A structural and functional ground plan for neurons in the hindbrain of zebrafish | PNAS*. Available at: https://www-pnas-org.insb.bib.cnrs.fr/doi/10.1073/pnas.1012185108 (Accessed: 2 August 2023).

Kirkby, L. *et al.* (2013) 'A role for correlated spontaneous activity in the assembly of neural circuits', *Neuron*, 80(5), pp. 1129–1144. Available at: https://doi.org/10.1016/j.neuron.2013.10.030.

Knogler, L.D. *et al.* (2014) 'A Hybrid Electrical/Chemical Circuit in the Spinal Cord Generates a Transient Embryonic Motor Behavior', *Journal of Neuroscience*, 34(29), pp. 9644–9655. Available at: https://doi.org/10.1523/JNEUROSCI.1225-14.2014.

Lewis, K.E. and Eisen, J.S. (2003) 'From cells to circuits: development of the zebrafish spinal cord', *Progress in Neurobiology*, 69(6), pp. 419–449. Available at: https://doi.org/10.1016/S0301-0082(03)00052-2.

McLean, D.L. *et al.* (2007) 'A topographic map of recruitment in spinal cord', *Nature*, 446(7131), pp. 71–75. Available at: https://doi.org/10.1038/nature05588.

McLean, D.L. and Fetcho, J.R. (2009) 'Spinal Interneurons Differentiate Sequentially from Those Driving the Fastest Swimming Movements in Larval Zebrafish to Those Driving the Slowest Ones', *The Journal of Neuroscience*, 29(43), pp. 13566–13577. Available at: https://doi.org/10.1523/JNEUROSCI.3277-09.2009.

Menelaou, E., Kishore, S. and McLean, D.L. (2019) 'Distinct Spinal V2a and V0d Microcircuits Distribute Locomotor Control in Larval Zebrafish'. bioRxiv, p. 559799. Available at: https://doi.org/10.1101/559799.

Milner, L.D. and Landmesser, L.T. (1999) 'Cholinergic and GABAergic Inputs Drive Patterned Spontaneous Motoneuron Activity before Target Contact', *Journal of Neuroscience*, 19(8), pp. 3007–3022. Available at: https://doi.org/10.1523/JNEUROSCI.19-08-03007.1999.

Momose-Sato, Y. and Sato, K. (2013) 'Large-scale synchronized activity in the embryonic brainstem and spinal cord', *Frontiers in Cellular Neuroscience*, 7. Available at: https://www.frontiersin.org/articles/10.3389/fncel.2013.00036 (Accessed: 28 August 2023).

Myers, C. (2005) 'Cholinergic Input Is Required during Embryonic Development to Mediate Proper Assembly of Spinal Locomotor Circuits'. Available at: https://core.ac.uk/reader/82664400 (Accessed: 13 March 2023).

Nishimaru, H. *et al.* (1996) 'Spontaneous motoneuronal activity mediated by glycine and GABA in the spinal cord of rat fetuses in vitro.', *The Journal of Physiology*, 497(1), pp. 131–143. Available at: https://doi.org/10.1113/jphysiol.1996.sp021755.

O'Donovan, M.J. and Landmesser, L. (1987) 'The development of hindlimb motor activity studied in the isolated spinal cord of the chick embryo', *Journal of Neuroscience*, 7(10), pp. 3256–3264. Available at: https://doi.org/10.1523/JNEUROSCI.07-10-03256.1987.

Papke, R.L. *et al.* (2012) 'The nicotinic acetylcholine receptors of zebrafish and an evaluation of pharmacological tools used for their study', *Biochemical Pharmacology*, 84(3), pp. 352–365. Available at: https://doi.org/10.1016/j.bcp.2012.04.022.

Rima, M. *et al.* (2020) 'Dynamic regulation of the cholinergic system in the spinal central nervous system', *Scientific Reports*, 10(1), p. 15338. Available at: https://doi.org/10.1038/s41598-020-72524-3.

Saint-Amant, L. and Drapeau, P. (2000) 'Motoneuron Activity Patterns Related to the Earliest Behavior of the Zebrafish Embryo', *The Journal of Neuroscience*, 20(11), pp. 3964–3972. Available at: https://doi.org/10.1523/JNEUROSCI.20-11-03964.2000.

Saint-Amant, L. and Drapeau, P. (2001) 'Synchronization of an Embryonic Network of Identified Spinal Interneurons Solely by Electrical Coupling', *Neuron*, 31(6), pp. 1035–1046. Available at: https://doi.org/10.1016/S0896-6273(01)00416-0.

Sun, Y.A. and Poo, M.M. (1987) 'Evoked release of acetylcholine from the growing embryonic neuron.', *Proceedings of the National Academy of Sciences of the United States of America*, 84(8), pp. 2540–2544.

Tong, H. and McDearmid, J.R. (2012) 'Pacemaker and Plateau Potentials Shape Output of a Developing Locomotor Network', *Current Biology*, 22(24), pp. 2285–2293. Available at: https://doi.org/10.1016/j.cub.2012.10.025.

Wan, Y. *et al.* (2019) 'Single-Cell Reconstruction of Emerging Population Activity in an Entire Developing Circuit', *Cell*, 179(2), pp. 355-372.e23. Available at: https://doi.org/10.1016/j.cell.2019.08.039.

Warp, E. *et al.* (2012) 'Emergence of patterned activity in the developing zebrafish spinal cord', *Current biology: CB*, 22(2), pp. 93–102. Available at: https://doi.org/10.1016/j.cub.2011.12.002.

Welle, T.M. *et al.* (2018) 'A high spatiotemporal study of somatic exocytosis with scanning electrochemical microscopy and nanoITIES electrodes', *Chemical Science*, 9(22), pp. 4937–4941. Available at: https://doi.org/10.1039/C8SC01131A.

Young, S.H. (1986) 'Spontaneous release of transmitter from the growth cones of Xenopus neurons in vitro: The influence of Ca2+ and Mg2+ ions', *Developmental Biology*, 113(2), pp. 373–380. Available at: https://doi.org/10.1016/0012-1606(86)90172-7.

Zirger, J.M. *et al.* (2003) 'Cloning and expression of zebrafish neuronal nicotinic acetylcholine receptors', *Gene expression patterns: GEP*, 3(6), pp. 747–754. Available at: https://doi.org/10.1016/s1567-133x(03)00126-1.

List of Publications

The work in these publications was conducted at the Sorbonne University (Pierre and Marie Curie Campus at Jussieu) in the department of Neuroscience Paris Seine directed by Dr. Herve Chneiweiss in the team of Formation and Interaction of Neural of Neural Networks (Dr. Elim Hong). This work will result in a total of four scientific publications, with myself being the first and co-first author for two of them.

1- Rima, M., Lattouf, Y.*, **Abi Younes, M.*,** Bullier, E., Legendre, P., Mangin, J.-M., & Hong, E. (2020). Dynamic regulation of the cholinergic system in the Spinal Central Nervous System. Scientific Reports72524-3
(Co-second author)

2- Zaupa, M*., Naini, S. M.*, **Abi Younes, M.,** Bullier, E., Duboué, E. R., Le Corronc, H., Soula, H., Wolf, S., Candelier, R., Legendre, P., Halpern, M. E., Mangin, J.-M., & Hong, E. (2021). Trans-inhibition of axon terminals underlies competition in the habenulo-interpeduncular pathway. Current Biology
(Second author)

3- **Maroun Abi Younes**, Mohamad Rima, Ninon Peysson, Jean-Pierre Coutanceau, Erika Bullier, Jean-Marie Mangin and Elim Hong (manuscript in preparation) Acetylcholine promotes rhythmic motor activity in the zebrafish embryo
(First author)

4- Soumaiya Imarraine, **Maroun Abi Younes**, Herve Le Corronc, Pascal Legendre, Jean-Marie Mangin, Elim Hong (manuscript in preparation for Star Protocols) Whole brain explant preparation for calcium imaging combined with drug perfusion, electrical stimulation or electrophysiology in zebrafish larvae
(Co-author)

Mischief Managed